15:59:50 OCA PAD INITIATION - PROJECT HEADER INFORMATION 09/21/89

Active

Project #: E-25-695 Cost share #: Rev #: 0
Center # : R6822-0A0 Center shr #: OCA file #:
Work type : RES
Contract#: AGMT. DTD. 890912 Mod #: Document : AGR
Prime #: Contract entity: GTRC

Subprojects ? : N
Main project #:

Project unit: ME Unit code: 02.010.126
Project director(s):
SALANT R F ME (404)894-3176

Sponsor/division names: JOHN CRANE, INC / MORTON GROVE, IL
Sponsor/division codes: 209 / 010

Award period: 890915 to 900914 (performance) 900914 (reports)

Sponsor amount	New this change	Total to date
Contract value	82,830.00	82,830.00
Funded	82,830.00	82,830.00
Cost sharing amount		0.00

Does subcontracting plan apply ?: N

Title: MATHEMATICAL MODEL OF HYDROPAD SEALS

PROJECT ADMINISTRATION DATA

OCA contact: Ina R. Lashley 894-4820

Sponsor technical contact

DR TOM W LAI
(312)967-3793

Sponsor issuing office

MR DAVID J BAUMAN, DIRECTOR OF TECH
(312)967-2846
JOHN CRANE INC.
6400 OAKTON STREET
MORTON GROVE, IL 60053

Security class (U,C,S,TS) : U ONR resident rep. is ACO (Y/N): N
Defense priority rating : N/A N/A supplemental sheet
Equipment title vests with: Sponsor GIT
NONE PROPOSED.

Administrative comments -
→ INITIATION OF ONE YEAR PROJECT. NON-DISCLOSURE AGREEMENT APPLIES FOR 24 MOS.
(CONTACT OCA/LEGAL RE: NON-DISCLOSURE AGREEMENT)

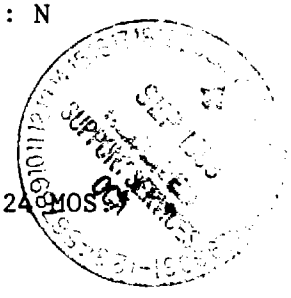

GEORGIA INSTITUTE OF TECHNOLOGY
OFFICE OF CONTRACT ADMINISTRATION

NOTICE OF PROJECT CLOSEOUT

Closeout Notice Date 03/28/91

Project No. E-25-695 Center No. R6822-0A0

Project Director SALANT R F School/Lab MECH ENGR

Sponsor JOHN CRANE, INC/MORTON GROVE, IL

Contract/Grant No. AGMT. DTD. 890912 Contract Entity GTRC

Prime Contract No. _____

Title MATHEMATICAL MODEL OF HYDROPAD SEALS

Effective Completion Date 901231 (Performance) 901231 (Reports)

Closeout Actions Required:	Y/N	Date Submitted
Final Invoice or Copy of Final Invoice	Y	
Final Report of Inventions and/or Subcontracts	Y	
Government Property Inventory & Related Certificate	N	
Classified Material Certificate	N	
Release and Assignment	N	
Other _____	N	

Comments _____

Subproject Under Main Project No. _____

Continues Project No. _____

Distribution Required:

Project Director	Y
Administrative Network Representative	Y
GTRI Accounting/Grants and Contracts	Y
Procurement/Supply Services	Y
Research Property Managment	Y
Research Security Services	N
Reports Coordinator (OCA)	Y
GTRC	Y
Project File	Y
Other _____	N
_____	N

NOTE: Final Patent Questionnaire sent to PDPI.

E-25-695

George W. Woodruff School of Mechanical Engineering
Georgia Institute of Technology
Atlanta, Georgia 30332

MATHEMATICAL MODEL OF HYDROPAD SEALS

Final Report

Contract E25-695

John Crane Inc.

Principal Investigators:

Dr. Richard F. Salant Dr. Itzhak Green

Graduate Student:

Hisham Hegab

March 1991

TABLE OF CONTENTS

LIST OF TABLES

LIST OF FIGURES

NOMENCLATURE

General Notation

A_e	element area
A_f	seal face area
A_{ijkl}	influence coefficient matrix
$A_{P,N,S,E,W}$	diffusion term in finite difference of Reynolds equation
B_{ijkl}	thermal influence coefficient matrix
C_{ij}	sealed pressure influence coefficient matrix
c_f	skin-friction coefficient
d	diameter of O-ring material
D	diameter of O-ring
E	Young's modulus of elasticity
F_c	closing force
$\overline{F}$	normalized spring force
F	cavitation index
ΔF	change in opening force
$F_{k,l}$	force at node k,l
$h(r,\theta)$	film thickness
H_l	local heat generation
H_{kl}	heat generation at node k,l
h_l	local film thickness

h_{ref}	reference film thickness at $h(r_i,0)$
h_{od}	heat transfer coefficient at outer diameter
Δh	change in film thickness
$H(\eta,\theta)$	dimensionless film thickness
$\overline{K}$	normalized spring constant
k	stiffness of seal
$K_{P,N,E,W,S}$	diffusion coefficient
l_g	gap distance between rotating cylinders
m	number of radial nodes in seal face mesh
n	number of circumferential nodes in seal face mesh
n	normal coordinate (for cavitation boundary conditions)
N_b	balance ratio
N_u	Nusselt number
ΔP	seal pressure relative to ambient, P_S-P_A
P	pressure
P_A	ambient pressure
P_S	seal pressure
P_c	cavitation pressure
P_r	Prandtl number
Q	leakage rate
r	radial coordinate
r_i	inner radius
r_o	outer radius
R_e	Reynolds number

S_p	source term in finite difference of Reynolds equation
U_l	local velocity
U_r	velocity at radius r
V_n	normal velocity
x	percent squeeze of O-ring

Greek Letters

α	relaxation factor for ϕ
β	relaxation factor for F
γ	dimensionless parameter in Reynolds equation
$\delta_{i,j}$	deflection at node i,j
η	dimensionless radial coordinate, r/r_i
η_o	dimensionless outer radial coordinate
ρ	density
ρ_c	density in full film
ϕ	dimensionless pressure or density
θ	circumferential coordinate
μ	absolute viscosity
ν	kinematic viscosity
ω	rotational speed

Subscripts

E	east nodal point
e	east boundary surface of control volume
N	north nodal point

n	north boundary surface of control volume
S	south nodal point
s	south boundary surface of control volume
W	west nodal point
ω	west boundary surface of control volume
P	grid point of interest
i	inner boundary
o	outer boundary
new	values of variables obtained in current iteration
old	values of variables obtained in previous iteration
i,j	nodal location (i = 1 to m, j = 1 to n)
k,l	nodal location (k = 1 to m, l = 1 to n)

SUMMARY

A mathematical model of a mechanical seal with deep hydropads is presented. The model is for analyzing prospective seal designs. The model is based on the fact that the hydropads induce the seal face to deform in a circumferential wave pattern, leading to hydrodynamic pressure generation in the fluid film.

There are several physical processes occurring in the seal that are analyzed separately. These include the development of the pressure distribution in the fluid film, the deformation of the seal faces from thermal and mechanical effects, the heat generation in the film from viscous dissipation, and the generation of the opening and closing forces acting on the seal. It is necessary to use an iterative procedure to find an overall solution for the seal since these processes are coupled to each other.

The Reynolds equation is solved for the pressure distribution in the film. It is modified to allow the fluid to cavitate and maintain continuity. A finite difference method is used to solve the equation. The deformations of the seal faces are determined from the pressure distribution and viscous heat generation in the fluid film. An influence coefficient method is used to calculate the deformations.

The influence coefficients are determined from three dimensional finite element analysis of the seal faces.

The work results in a single computer program that can be used to analyze a seal with deep hydropads, given the operating conditions and the influence coefficients for the seal design. The program predicts the pressure distribution, film thickness, leakage rate, and other operating characteristics of the given seal design.

CHAPTER I

INTRODUCTION

Mechanical Seals

Mechanical seals are used to prevent fluid leakage from rotating machines such as pumps and compressors. Figure 1 shows a schematic diagram of a mechanical seal.

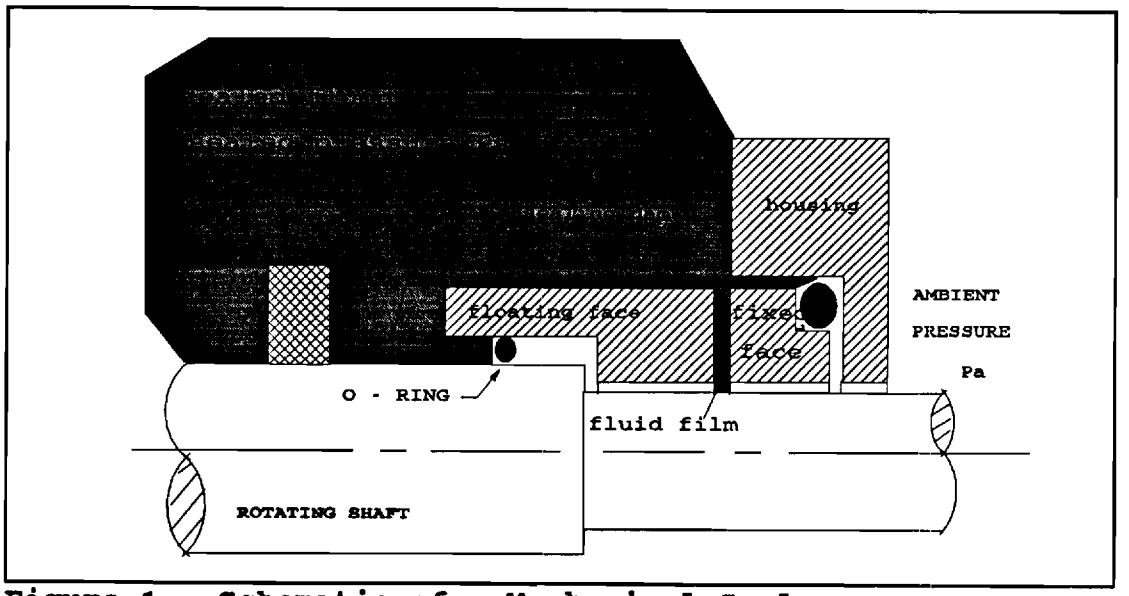

Figure 1. Schematic of a Mechanical Seal

To minimize wear and mechanical damage, most seals

are designed to operate with a thin fluid film separating the seal faces. The thickness of the film is typically on the order of microns and is determined by the position of the floating seal face. The position of the floating seal face is determined by a balance of closing and opening forces acting on it. The closing forces consist of a spring force and a pressure force acting on the backside of the seal. The closing pressure force is determined by the sealed pressure, seal face area, and the balance ratio of the seal. The balance ratio is the ratio of the area of the back side of the floating seal to the area of the seal face. The opening force is produced by the pressure distribution in the fluid film between the seal faces. In order for the seal to operate without contact, high enough pressures must be generated in the fluid film to prevent closing of the clearance between the seal faces.

Problem

In this work, a mechanical seal with deep hydropads is analyzed. A hydropad is a slot or recess placed in one of the seal faces. Hydropads are used to produce hydrodynamic pressures which cause an opening force between the seal faces in the sealing dam [1]. Key, et. al. [1] developed a mathematical model to analyze a seal with deep hydropads which provides results that agree well with experimental data. However, their method is

not practical as a design tool because of the large computational time required for a solution. In their procedure, three dimensional finite element analysis of one of the seal faces is required within an iterative loop. To reduce the computational time without loss in accuracy of the solution, an influence coefficient method can be used to find the seal deformations inside the iterative loop.

Goal of Project

The goal of this project is to develop a mathematical model of a mechanical seal with deep hydropads that could be used for design purposes. This project will result in a computer program to analyze a hydropad mechanical seal, given the operating conditions of the seal and the structural influence coefficients of the seal. The latter may be obtained from a commercial structural analysis program. The program allows the user to predict leakage rates, film thickness, deformations, and other operating characteristics for a given seal design.

CHAPTER II

BACKGROUND

Types of Mechanical Seals

Flat Face Seals

The most basic type of mechanical seal is a flat face seal. In this type of seal the primary mechanism for generating pressures in the film is by hydrostatic load support [2]. In this mechanism the pressure distribution varies radially within the boundaries of the seal face. This pressure distribution is associated with the radial flow across the seal face and is proportional to the pressure drop across the seal face, ΔP. In such a seal, the gap between the faces must converge in the radial direction, from the high pressure side to the low pressure side, for the seal to be stable [3]. This convergence is called coning. The larger the ratio of coning to the average film thickness, the more convex is the pressure distribution, and the larger the opening force.

Hydropad Seals

There are situations where the design of a flat face

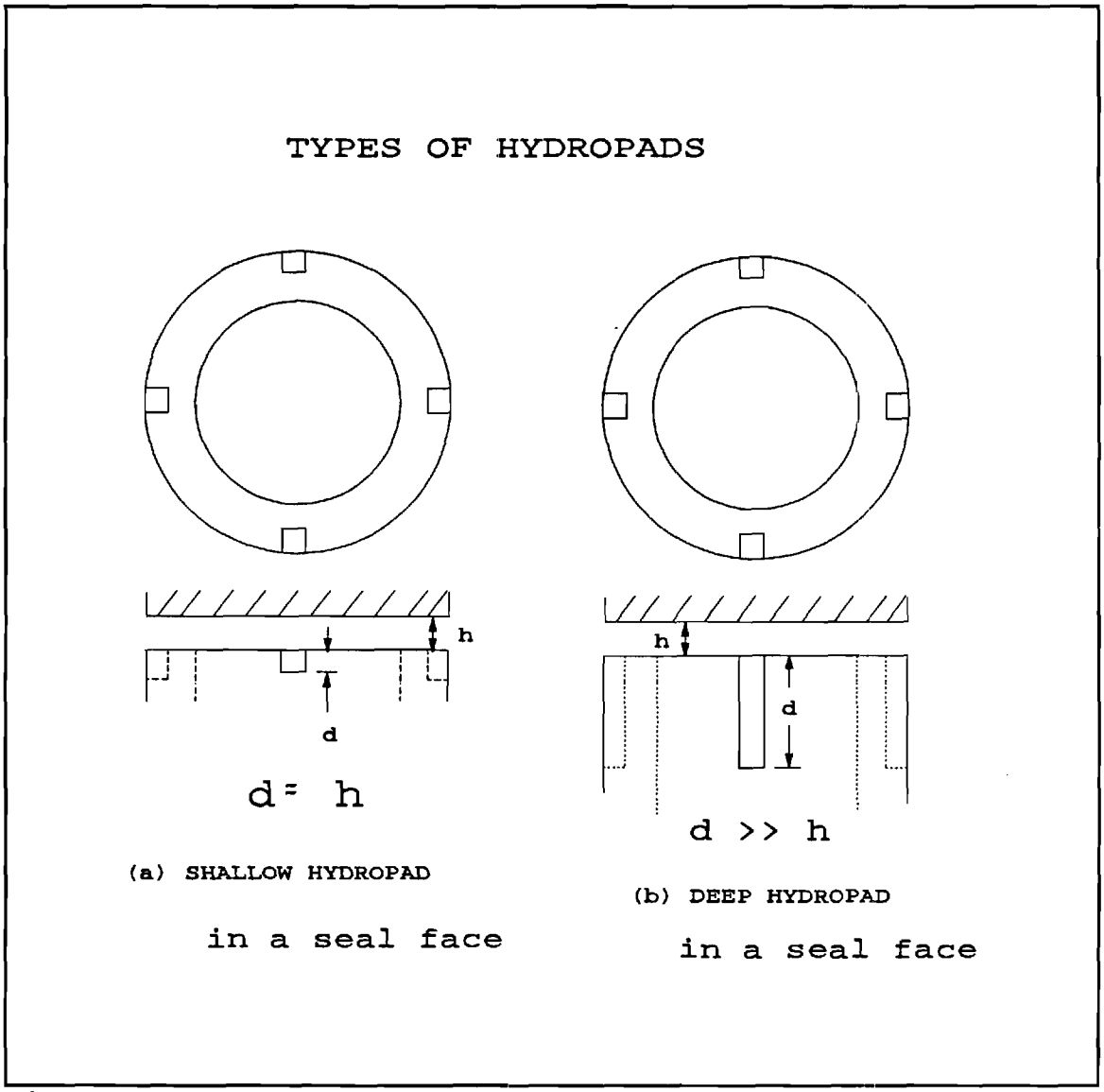

Figure 2. Types of Hydropads.

seal does not produce sufficiently high film pressures to prevent contacting of the seal faces. This may be due to the operating conditions of the seal, such as a very low density fluid, low viscosity, low sealed pressure, or very high temperature [1]. In such cases, it is common to place slots or recesses of various geometries, called hydropads, in one of the seal faces. If designed properly, these

hydropads generate sufficient added pressure to prevent contacting of the seal faces. There are two basic classes of hydropads, as discussed below.

Shallow Hydropads. The first class of hydropads consists of shallow hydropads (figure 2a), where the depths of the slots are on the order of the seal clearance. In seals utilizing such hydropads elevated pressure are generated in the fluid film by a mechanism similar to a Rayleigh step bearing [4,5]. As fluid is dragged by the rotation of one of the seal faces from the hydropad to the narrower gap of the seal, there is an increase in pressure from the sudden convergence in the path of the flow. This is considered a hydrodynamic effect since the pressure increase is proportional to the speed of rotation of the seal face and to the liquid viscosity. The pressure generation is also dependent on the depth of the hydropad. The pressure increase is maximized when the hydropad depth is of the order of the film thickness. It decreases to zero as the ratio of hydropad depth to film thickness becomes very large. Since the depth of shallow hydropads is on the order of microns, they are easily filled with contaminants in the fluid film.

Deep Hydropads. The second class of hydropad seals is the deep hydropad seal (figure 2b). Since the ratio of hydropad depth to film thickness is very large, the mechanism for pressure generation in deep hydropads is

different from that of shallow hydropads.

Key, et. al. [1] provides an analytical model of a mechanical seal with deep hydropads. It is based on two assumptions. The first is that deep hydropads cause the seal face to deform in a circumferential wave pattern that has a wave amplitude on the order of microns. The second is that this wave pattern on the seal face generates higher pressures in the film through the hydrodynamic effect. These elevated pressures provide the increased opening force.

There is evidence to support these hypotheses. It is known that flat face seals deform on the order of microns [2]. This deformation is primarily axisymmetric due to the axisymmetric seal geometry. In a hydropad seal, the geometry has circumferential features so the deformations should vary circumferentially. This deformation results in a circumferential wave pattern on the hydropad seal face.

The circumferential wave pattern is due to both mechanical and thermal deformation of the face. The mechanical deformation contributes to the wave pattern by two effects. First, the presence of the hydropad weakens the seal structurally near the hydropad so that for a uniform load the seal face will deform greatest near the hydropads. Second, since the hydropads are deep, the pressure in the hydropad is approximately the sealed pressure. This produces a boundary condition on the

pressure which results in a circumferentially varying pressure field. Since the pressure field varies circumferentially, the face deformation varies accordingly.

Thermal deformation can also vary circumferentially and contribute to the circumferential wave pattern. Each hydropad provides a boundary condition on temperature, resulting in a circumferentially varying temperature distribution.

The second hypothesis, that the wave pattern on the seal face generates elevated pressures within the film through a hydrodynamic effect, is verified by Iny and Stangham-Batch [6-8]. The flow path in the circumferential direction alternately converges and diverges due to the waviness of the seal face. The converging regions produce elevated pressures (similar to a slider bearing), while the diverging regions produce lower pressures.

For a symmetric wave pattern, the amount of positive pressure generation in the converging regions is equal to the amount of pressure reduction in the diverging regions. Therefore, there is no hydrodynamically generated opening force unless the fluid cavitates in the diverging region. If the fluid cavitates, the negative pressures are eliminated and a net opening force is generated by the positive pressures. On the other hand, it is possible to generate a net opening force without cavitation if the waviness is not symmetric. For an asymmetric wave pattern,

a hydrodynamically generated opening force is produced if the positive contributions of the converging flow regions exceed the negative contributions of the diverging regions [1]. This opening force can be produced without cavitation if the hydrostatic pressure is large enough to prevent the pressures from becoming negative in the diverging regions.

Reynolds Equation

To obtain the solution of the pressure distribution in the fluid film, it is necessary to solve the Reynolds equation [9]. Since the main goal of the present study is to predict leakage rates for the seal, it is necessary to consider cavitation in the seal. Considerable research has been performed in the area of computer algorithms to predict cavitating regions. A method using a cavitation index and a dimensionless density developed by Elrod [10] is used in the previous work by Key, et. al. [1]. In the present work, a similar method, developed by Salant and Payvar [11] is used.

Deformation Analysis

To compute the deformation of the seal faces, through thermal and mechanical effects, an influence coefficient method is used. The finite element method is used to calculate the influence coefficient arrays of the seal faces [12,13].

Main Features of Present Study

As suggested earlier, the main advantage over the previous method of Key, et. al. [1] is the use of an

influence coefficient method to determine the seal deformations. Also to improve the accuracy of the model, three dimensional finite element analysis is used for both seal faces to find mechanical and thermal deformation. In addition, an improved method for solving the cavitating Reynolds equation is used, and the overall solution procedure used by Key, et. al. [1] is changed.

CHAPTER III

ANALYSIS

Seal Configuration

In the present study, a "typical" seal is used as a test case, in order to develop the analytical model. The seal analyzed (figure 3) has a balance ratio of 0.72212. The stator (non-rotating face) is made of silicon carbide. The rotor (rotating face) is made of carbon graphite. The material properties of the seal faces are given in table 1.

The sealed fluid, water, has a viscosity of 1.007×10^{-3} Pa-s (1.46×10^{-7} reyn) at 20 °C (68 °F) [14]. The sealed pressure ranges from 0.345 MPa (50 psig) to 1.035 MPa (150 psig), and the rotational speed varies from 100 rad/s to 400 rad/s.

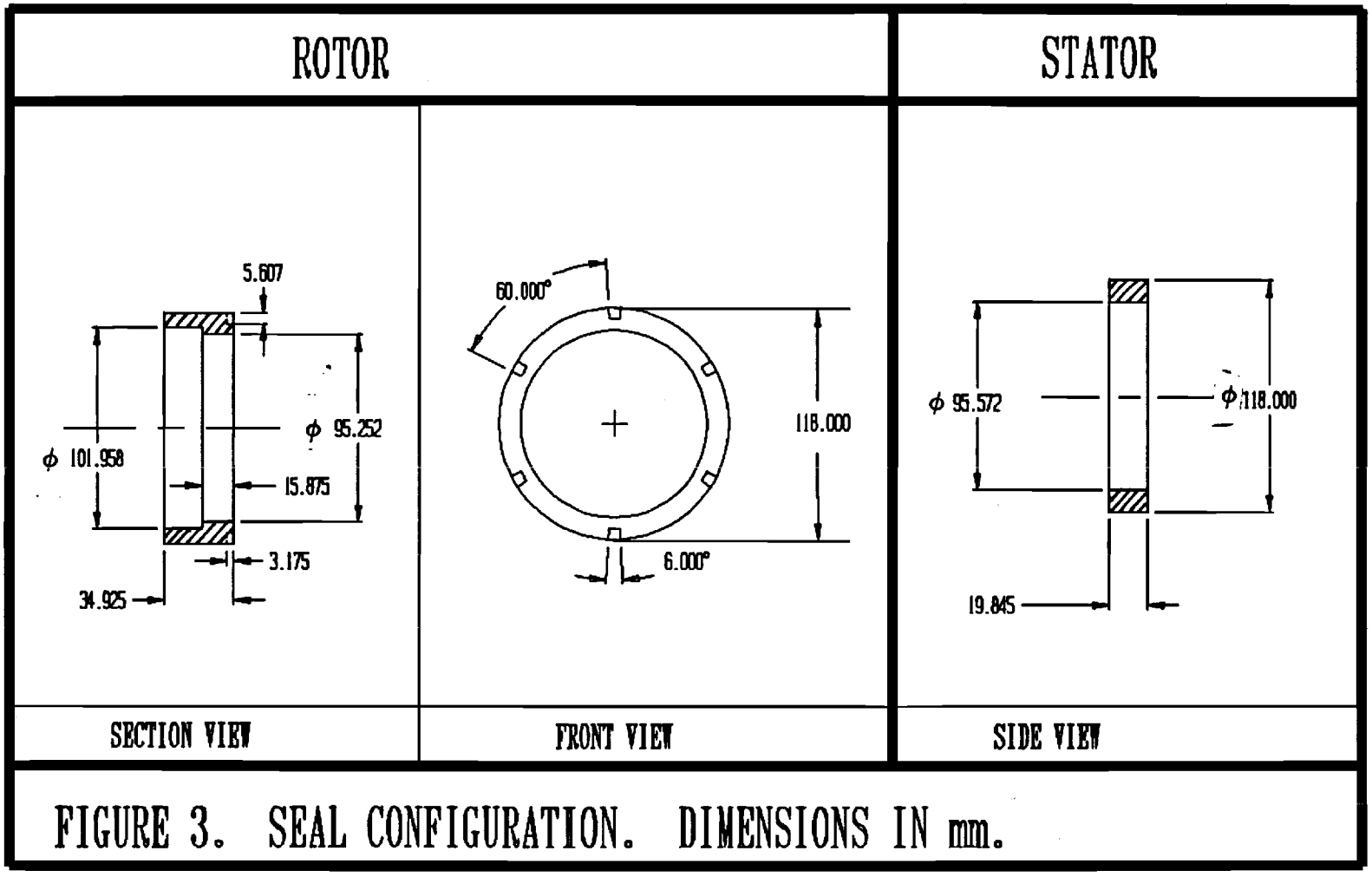

FIGURE 3. SEAL CONFIGURATION. DIMENSIONS IN mm.

Table 1. Material properties of the seal faces.

	ROTOR	STATOR
MATERIAL	CARBON GRAPHITE	SILICON CARBIDE
YOUNG'S MODULUS	22.1 GPa (3.2×10^6 psi)	69 GPa (68×10^6 psi)
THERMAL CONDUCTIVITY	10.0 W/m °K (5.784 Btu/hr ft °F)	42.0 W/m °K (24.276 Btu/hr ft °F)
THERMAL EXPANSION COEFFICIENT	7.635×10^{-5} mm/°K (1.67×10^{-6} in/°F)	11.887×10^{-5} mm /°K (2.6×10^{-6} in/°F)

General Approach

The analysis of the seal must consider both hydrostatic and hydrodynamic load support. Such analysis is difficult since the physical processes in the seal are coupled. The pressure distribution in the film, the deformation of the seal faces, and the heat generation are all interdependent.

The pressure distribution determines the axial position of the floating seal face, thus setting the film thickness. The pressure distribution also affects the mechanical deformation of the seal faces which influences the film thickness distribution. The film thickness in turn affects

the pressure distribution through Reynolds equation. In addition, the film thickness affects the amount of heat generated in the film. The heat generation in turn affects the pressure distribution through thermal deformation of the seal faces.

Since coupled processes occur, the problem is complex to analyze. In light of this complexity, each process is analyzed separately, by numerical means, and then an iterative process is used to account for interactions among the processes.

Reynolds Equation

It is assumed that the hydropads cause the seal to

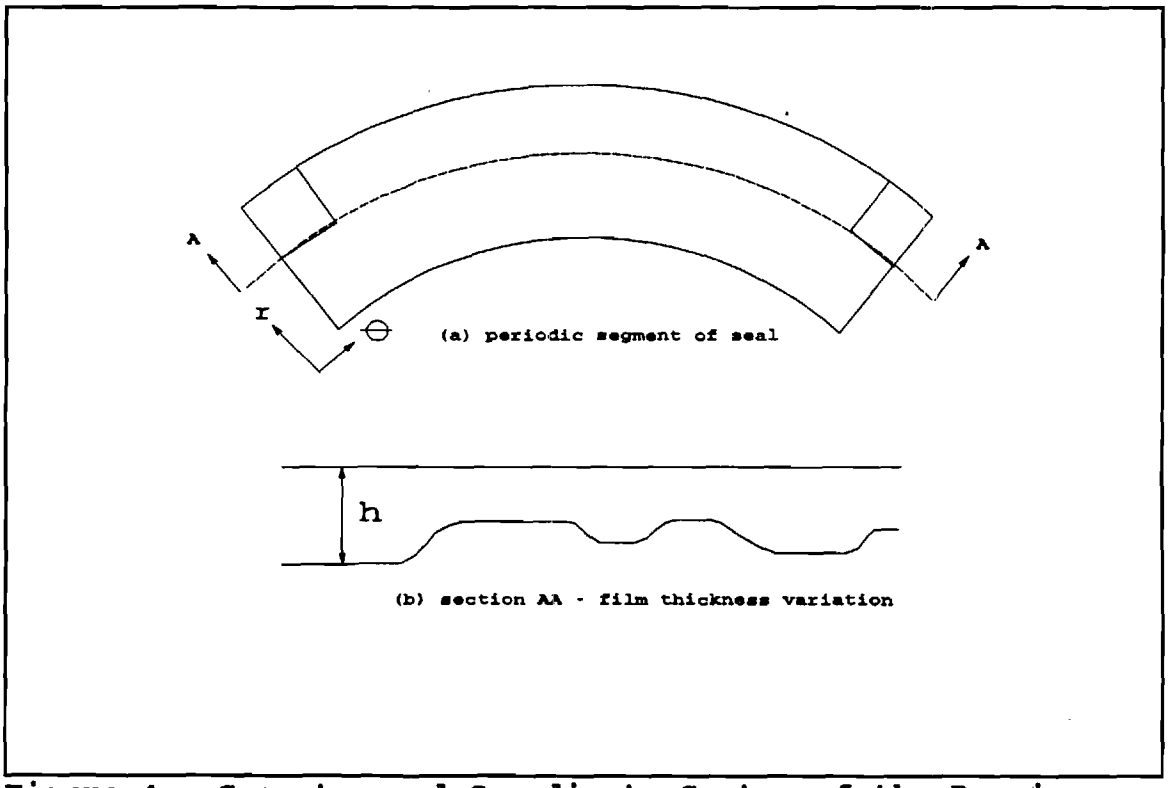

Figure 4. Geometry and Coordinate System of the Domain.

deform in a periodic pattern so it is only necessary to analyze a segment of the seal (figure 4(a)) ranging from one hydropad to an adjacent one.

The segment shown extends from $r=r_i$ to $r=r_o$ and from $\theta=0$ to $\theta=\theta_{max}$ where

$$\theta_{max}=\frac{2\pi}{N}$$

N represents the number of hydropads in the seal. Figure 4(b) shows the fluid film of variable thickness separating the seal faces. The flow field in the seal is governed by Reynolds equation, given in polar coordinates [14]:

$$\frac{1}{r}\frac{\partial}{\partial r}\left(\rho r h^3 \frac{\partial P}{\partial r}\right)+\frac{1}{r}\frac{\partial}{\partial \theta}\left(\frac{\rho h^3}{r}\frac{\partial P}{\partial \theta}\right)=6\mu\omega\frac{\partial(\rho h)}{\partial \theta} \qquad (3.2)$$

with boundary conditions,

$$P = P_A \text{ at } r = r_i$$

$$P = P_S \text{ at } r = r_o \text{ and along the hydropad boundary} \qquad (3.3)$$

In equations (3.2) and (3.3) P represents the pressure, ρ the density, and h the film thickness. All are functions of r and θ. μ is the absolute viscosity of the fluid, and ω is the rotational speed of the seal. P_A is the ambient pressure at the inner radius, r_i, and P_S is the sealed pressure at the outer radius, r_o, and within the hydropad. In regions where equation (3.2) yields pressures below the

cavitation pressure, P_c, the fluid forms striations (figure 5) and both liquid and vapor are present at a uniform pressure, P_c [15]. In these cavitating regions, equation (3.2) reduces to [1],

$$\frac{\partial(\rho h)}{\partial\theta}=0 \qquad (3.4)$$

with boundary conditions [15],

$$\frac{\partial P}{\partial n}=0 \quad \text{at the locus of film rupture} \qquad (3.5)$$

$$\frac{h^2}{12\mu}\frac{\partial P}{\partial n}=\frac{V_n}{2}\left(1-\frac{\rho}{\rho_c}\right) \quad \text{at the locus of film reformation} \qquad (3.6)$$

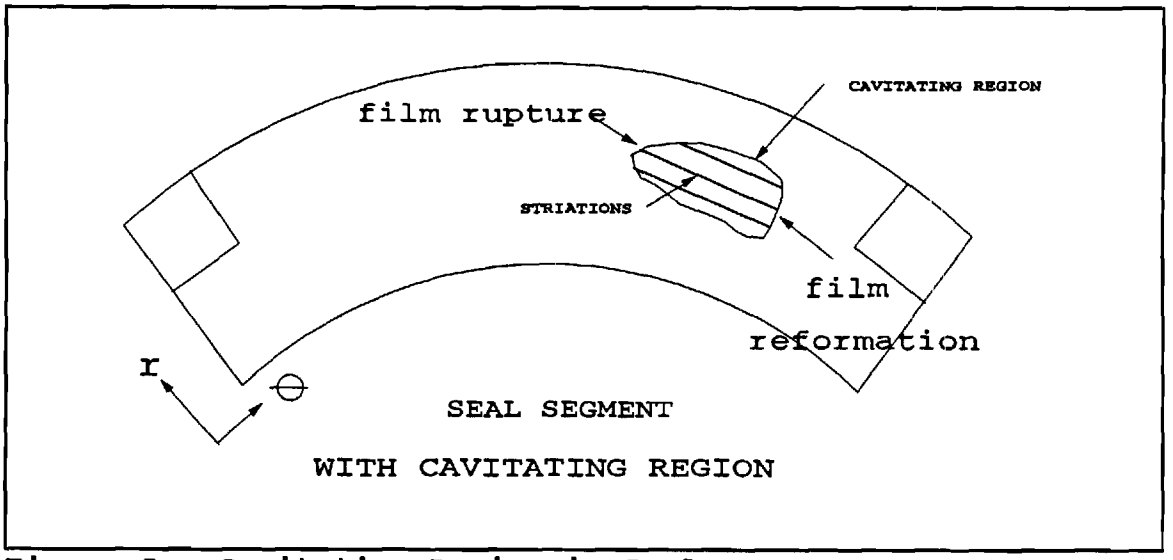

Figure 5. Cavitating Region in Seal.

In the cavitation zone, there is both liquid and vapor present and therefore the value of ρ in equation (3.4) represents the average density of the two phase fluid. Equation (3.5) and (3.6) provide continuity at the boundaries of the cavitating regions and are derived from mass balances by Jakobsson and Floberg [15].

In the liquid regions of the film, where the density is constant at a value ρ_c, equation (3.2) reduces to,

$$\frac{1}{r}\frac{\partial}{\partial r}\left(rh^3\frac{\partial P}{\partial r}\right)+\frac{1}{r}\frac{\partial}{\partial \theta}\left(\frac{h^3}{r}\frac{\partial P}{\partial \theta}\right)=6\mu\omega\frac{\partial h}{\partial \theta} \qquad (3.7)$$

In order to obtain an accurate pressure distribution within the film, the two governing equations, (3.4) and (3.7), are solved simultaneously along with their boundary conditions. To simplify this procedure, a single "universal" differential equation, valid in both the liquid and cavitation regions is established. This is accomplished by introducing a variable, ϕ, which takes on a different meaning in the full film region and the cavitation zone, and by introducing a cavitation index, F, which activates or suppresses terms of the differential equation depending whether the film is cavitating or not. ϕ is defined as follows [10]:

$$F\phi=\frac{P-P_c}{P_s-P_c} \qquad \text{in the liquid film region} \qquad (3.8)$$

$$1+(1-F)\phi=\frac{\rho}{\rho_c} \qquad \text{in the cavitation zone} \qquad (3.9)$$

F is defined by,

$$F(r,\theta)=1 \qquad \text{for } \phi > 0 \qquad (3.10)$$

$$F(r,\theta)=0 \qquad \text{for } \phi < 0 \qquad (3.11)$$

From its definition, it is seen that ϕ is a dimensionless pressure in the full film region and a partial film density in the cavitation zone.

The next step is to normalize the rest of the governing equation. The following dimensionless variables are defined:

$$\eta=\frac{r}{r_i} \qquad (3.12)$$

$$H=\frac{h}{h_{ref}} \qquad (3.13)$$

$$\gamma=\frac{6\mu\omega}{P_s-P_c}\left(\frac{r_i}{h_{ref}}\right)^2 \qquad (3.14)$$

where η is a dimensionless radius. h_{ref} is a reference film thickness at location $r=r_i$ and $\theta=0°$. H is a dimensionless film thickness. γ is a dimensionless parameter for the seal similar to a Sommerfeld number in journal bearings.

Substitution of equation (3.8) through (3.14) into (3.2) yields

$$\frac{1}{\eta}\frac{\partial}{\partial\eta}\left(\eta H^3\frac{\partial(F\phi)}{\partial\eta}\right)+\frac{1}{\eta}\frac{\partial}{\partial\theta}\left(\frac{H^3}{\eta}\frac{\partial(F\phi)}{\partial\theta}\right)=\gamma\frac{\partial[(1+(1-F)\phi)H]}{\partial\theta} \tag{3.15}$$

with boundary conditions,

$$\phi=\frac{P_a-P_c}{P_s-P_c} \qquad \text{at } \eta=1 \tag{3.16}$$

$$\phi=1.0 \qquad \text{at } \eta=\eta_o \tag{3.17}$$

Numerical Method

The finite difference method is used to solve the governing partial differential equation. The specifics of the method are described in Appendix A. The mesh used for the Reynolds solution of the seal (figure 6) consists of 11 by 41 nodes. To solve the algebraic equations resulting from the discretization of equation (3.15), an alternating direction implicit (ADI) method is used.

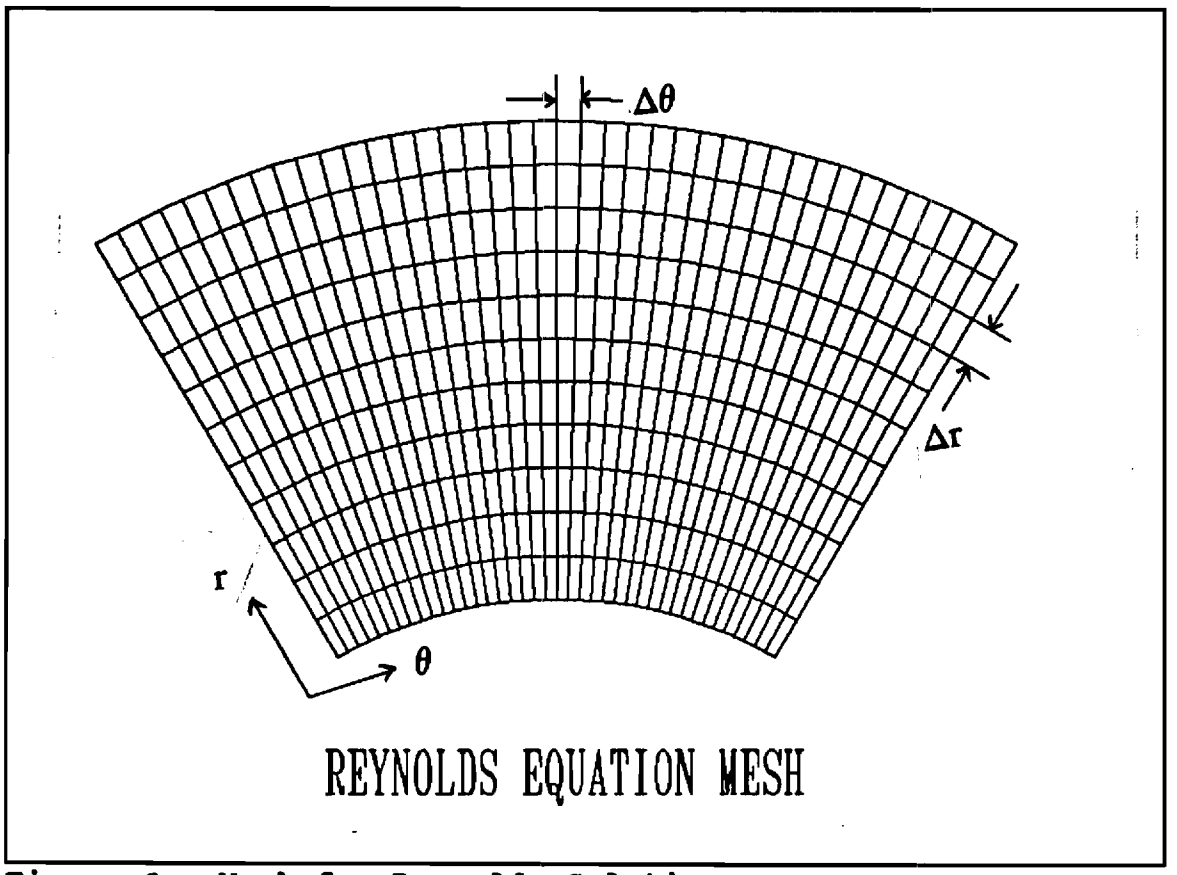

Figure 6. Mesh for Reynolds Solution.

Deformation Analysis

It is necessary to determine the deformation of both seal faces from mechanical and thermal loading. Key, et. al. [1] uses finite element analysis of the carbon seal face to determine deformations from the pressure distribution, and they use an axisymmetric analysis method to deterime the coning of the other face from mechanical and thermal deformation. An influence coefficient method is used to determine all the deformations in this analysis. Figure 7

illustrates the basis of the influence coefficient method. A unit force, F_{kl}, is applied at node (k,l), and the deflections at all the other nodes on the seal face are determined. This process is repeated for each node (i,j) on the seal face. These deflections form the mechanical influence coefficient array, A_{ijkl}. Then the deflection at

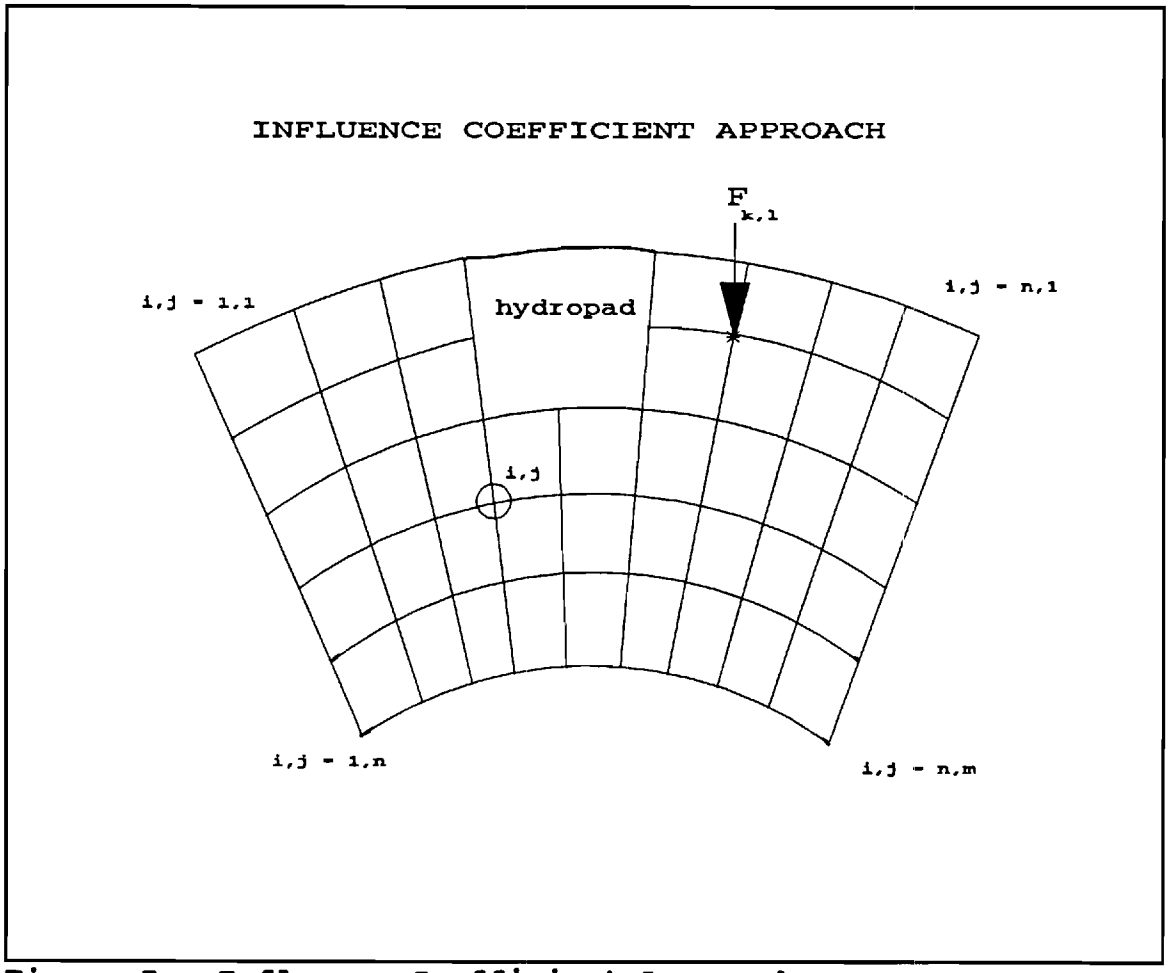

Figure 7. Influence Coefficient Approach.

any node δ_{ij} is given by,

$$\delta_{ij} = \sum_{k=1}^{n} \sum_{l=1}^{m} A_{ijkl} F_{kl} \qquad (3.18)$$

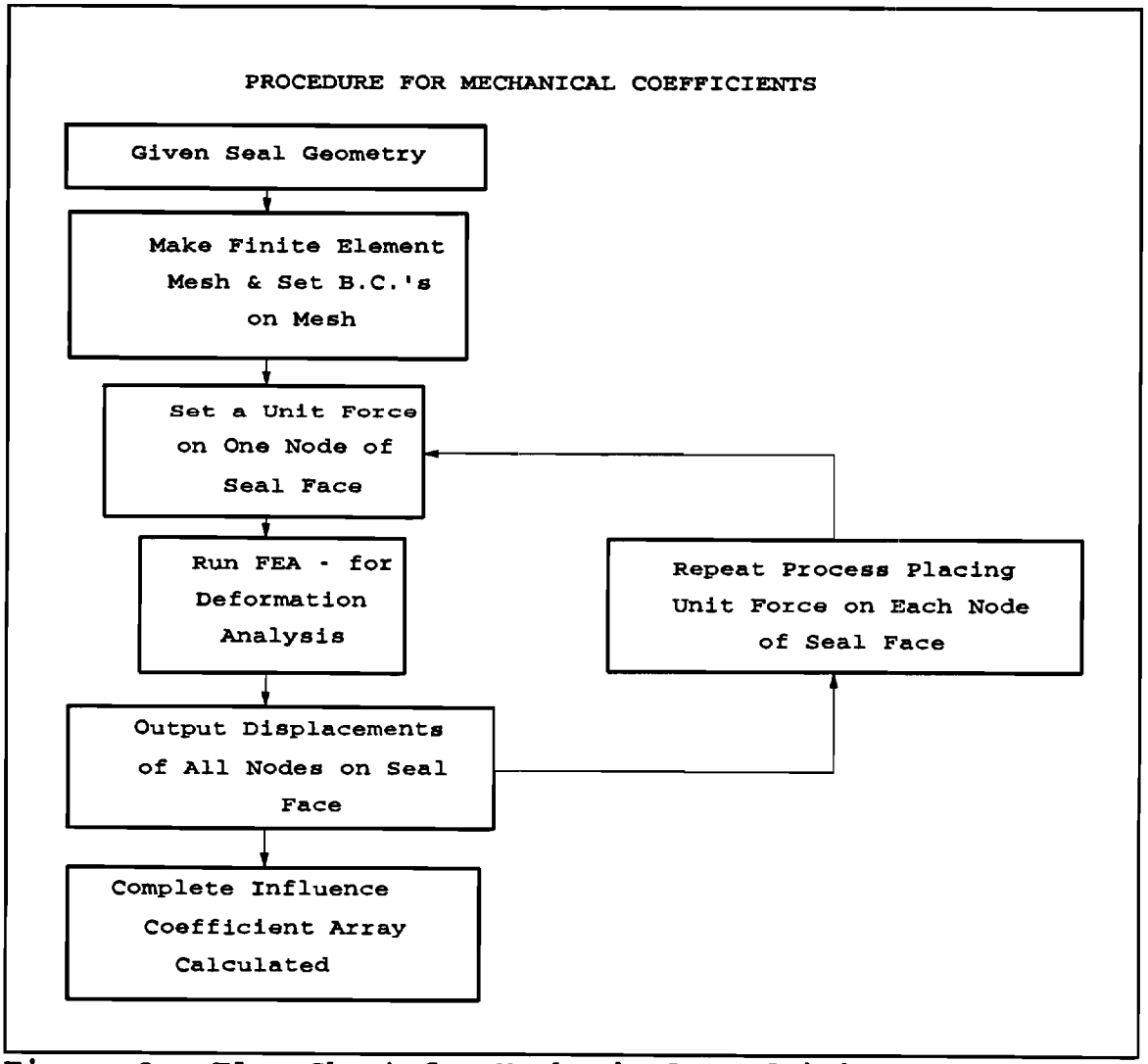

Figure 8. Flow Chart for Mechanical Coefficients.

Since the seal materials respond linearly to pressure and temperature, the influence coefficients are separated into three arrays. The first contains the influence

coefficients for the mechanical deformation. The second contains the thermal influence coefficients, and the third set of influence coefficients accounts for the sealed pressure acting on the back of the floating seal face. Therefore, the deflections at any node on the seal face, δ_{ij}, is

$$\delta_{ij}=\sum_{k=1}^{n}\sum_{l=1}^{m}(A_{ijkl}F_{kl}+B_{ijkl}H_{kl}+C_{ij}P_s) \qquad (3.19)$$

In equation (3.19), A_{ijkl} are the mechanical influence coefficients, B_{ijkl} are the thermal influence coefficients, and C_{ij} are the sealed pressure influence coefficients. F_{kl} is the force due to pressure acting at each node on the seal face, and H_{kl} is the heat generated at each node on the seal face.

Finite element analysis is used to obtain the complete set of influence coefficients. The commercial program ANSYS [16] is used for the finite element analysis of the seal faces. Since the seal analyzed has six hydropads, a 60 degree segment spaning from the center of one hydropad to the center of an adjoining hydropad is considered (figure 3).

Figure 8 shows a flow chart of the procedure used for determining the mechanical coefficients. First a finite element mesh is created from the geometry and material

properties of the seal face. Then a unit force is applied to one node of the seal face. A finite element analysis is performed to find the deformations at each node on the seal face. These deformations are the influence coefficients for the node at which the force is applied. The process is repeated for each node on the seal face. Once it is completed, all the mechanical influence coefficients for the seal face are calculated.

The procedure for determining the thermal coefficients (figure 9) is slightly different. Instead of a unit force input, a unit heat flux input is applied at each node. Then from that heat input, the steady-state temperature distribution in the seal is determined. From the temperature distribution in the seal, the thermal deformations are determined. The format for all of the influence coefficient input files for the computer program is described in appendix G.

It is desirable to have the coarsest mesh size possible since the number of influence coefficients varies with the number of nodes raised to the fourth power. From testing different mesh sizes, it is determined that the finite element mesh is convergent for a mesh of 11 x 21 nodes. Figure 10 shows the grid for the floating seal face, and figure 11 shows the grid for the fixed seal face.

Since the finite element mesh is 11 x 21 nodes and the mesh for the solution of the Reynolds equation is 11 x 41

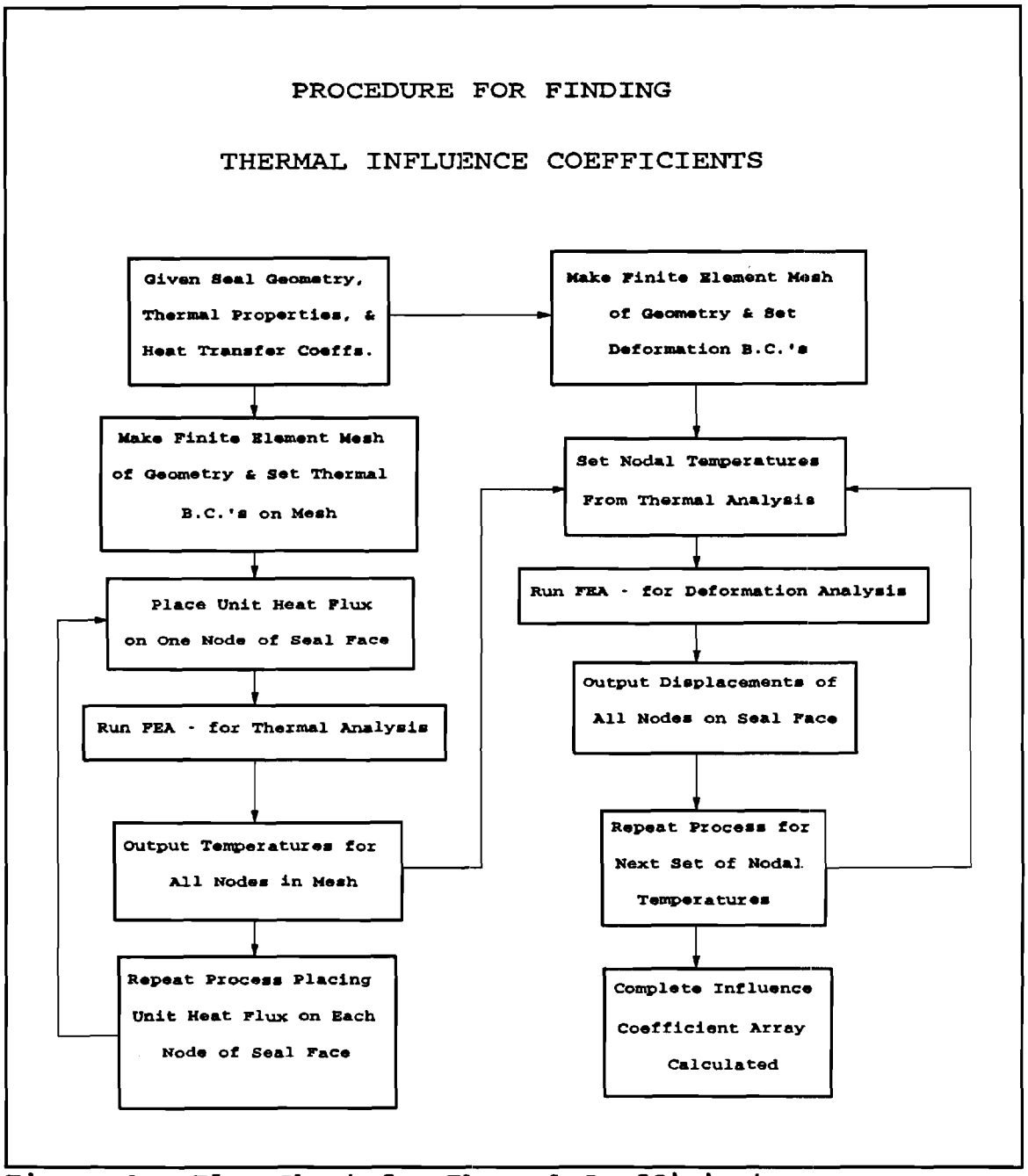

Figure 9. Flow Chart for Thermal Coefficients.

nodes (the coarsest mesh which gives a convergent solution), it is necessary to interpolate for the nodes that do not match up between the two meshes. A Langrangian interpolation is used to determine the deformations at those

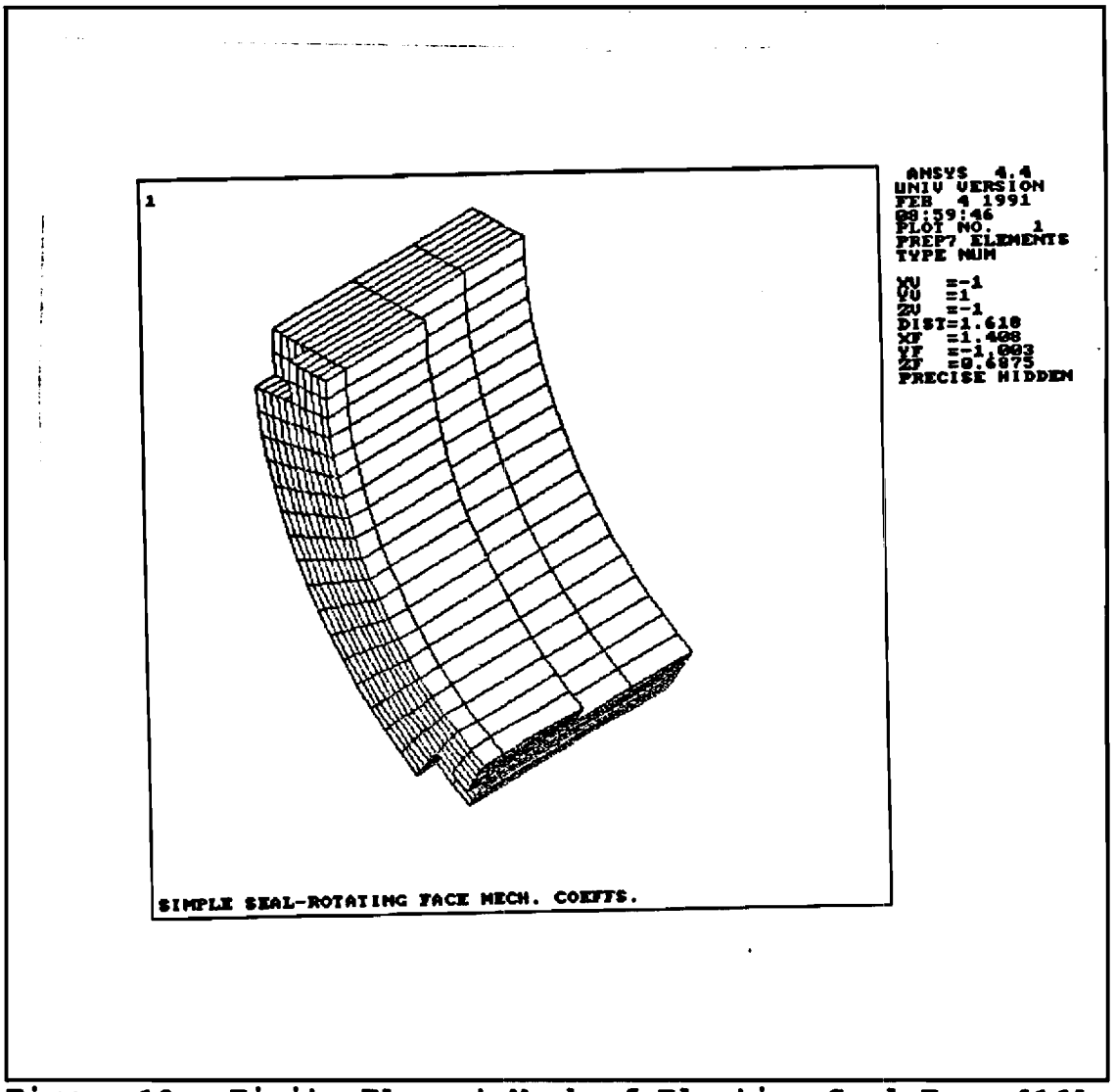

Figure 10. Finite Element Mesh of Floating Seal Face [16].

nodes.

The mesh has symmetric boundary conditions at θ=o° and θ=60° boundaries so there is zero circumferential deformation and matching radial and axial deformations at those nodes. Another boundary condition on the mesh is the O-ring on the floating face. The O-ring is modelled as a spring with a preload acting radially. The spring constant

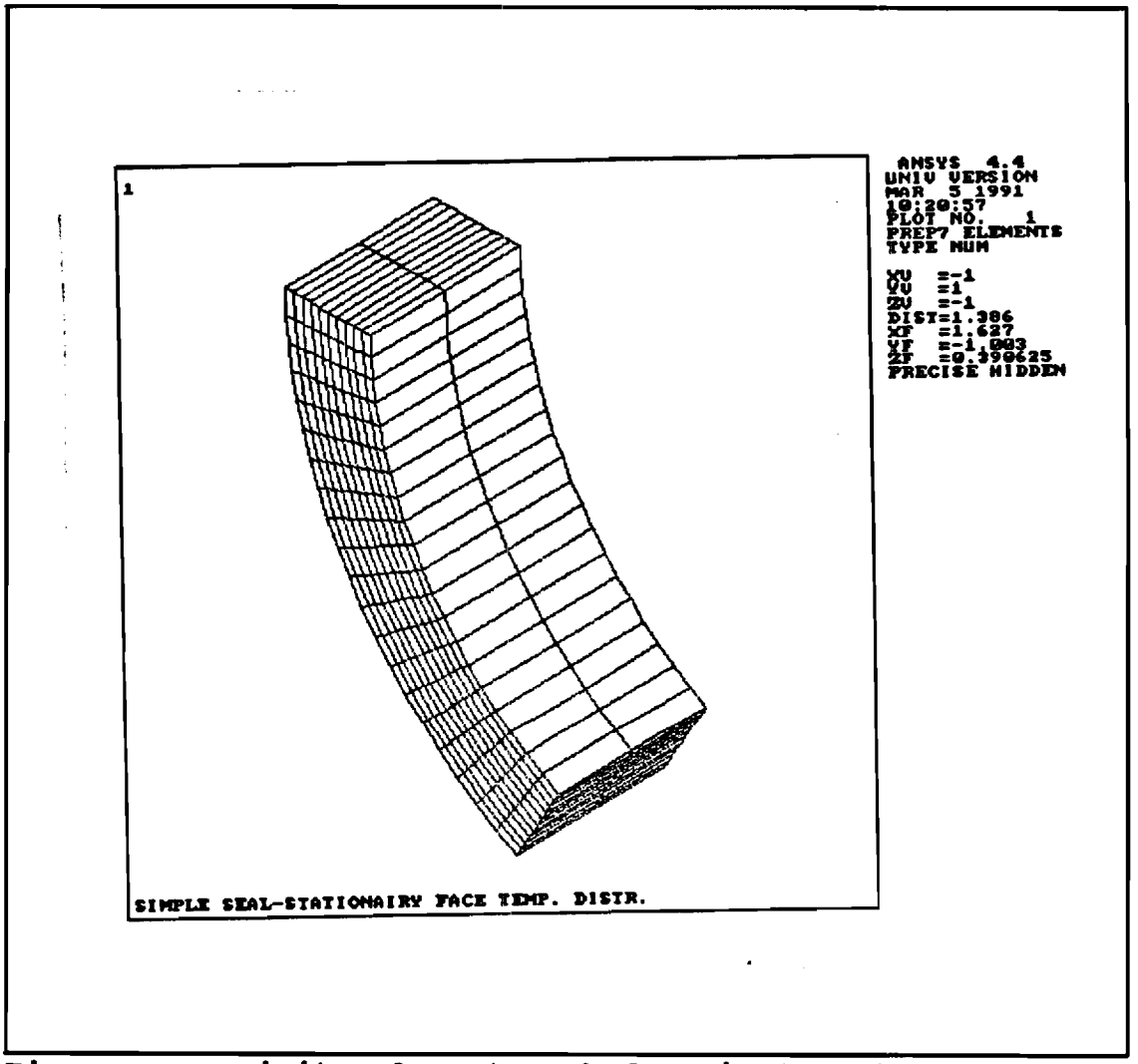

Figure 11. Finite Element Mesh for Fixed Seal Face [16].

for the O-ring boundary condition is 20.1 N/mm per node (114.6 lbf/in per node), and the preload is .778 N per node (0.175 lbf/node). The calculation of these values is described in Appendix B.

For the thermal analysis it is necessary to determine heat transfer coefficients for the outer and back surface of the floating seal face. These values are 34,000 W/m^2 °K and 22,700 W/m^2 °K, respectively. These calculations are

described in Appendix C.

Heat Generation

It is necessary to determine the heat generation in the fluid film in order to determine the thermal loading on the seal faces. The heat generation rate at each node is determined by treating the flow in the film as a Couette flow. The viscous heat generation rate is given by

$$H_L=\mu\frac{U_L^2}{h_L}A_e \qquad (3.20)$$

In this equation, H_L is the local heat generation rate. U_L is the local velocity, and h_L is the film thickness. This gives the heat generation assuming that there is no cavitation. To account for the possibility of cavitation, it is necessary to modify equation (3.20). The following equation is used in the program.

$$H_L=\mu\frac{U_L^2}{h_L}A_e[1+(1-F)\phi] \qquad (3.21)$$

When there is a full film, F = 1 and the equation reduces to equation (3.20), but when there is cavitation, F = 0, the added terms reduce to ϕ which is the partial density of the fluid. This provides a more accurate heat generation rate with or without cavitation in the fluid.

Leakage Rate

Once the final pressure distribution has been determined, the leakage rate of the seal is computed. The leakage flow rate is obtained by integrating the radial flow rate around the circumference of the face at the inner radius. Therefore, the leakage flow rate, Q, is

$$Q=-\int_0^{2\pi}\frac{h^3}{12\mu}\left(\frac{\partial P}{\partial r}\right)_{r=r_i} r_i d\theta \qquad (3.22)$$

Opening & Closing Force

As discussed earlier, the position of the floating seal face is determined by the balance of opening and closing forces acting on it. The closing force consists of a pressure force and a spring force. In the computer program, the spring force is neglected since it is usually insignificant in comparison to the closing pressure force. For a given seal design and operating pressure, the closing force, F_c, is fixed and is given by,

$$F_c=\Delta P A_f N_b \qquad (3.23)$$

where the balance ratio, N_b, is purely a function of the geometry of the seal. ΔP is the difference in pressure

across the seal face, and A_f is the seal face area.

The opening force is obtained by integrating the pressure distribution within the film over the seal face area. That pressure distribution is obtained from the solution of equation (3.15).

Once the opening force is calculated, it is compared to the closing force. If there is agreement within 0.3% between the two, the solution has converged. Otherwise, the reference film thickness, h_{ref}, is adjusted in the proper direction. If the opening force is greater than the closing force, h_{ref} is increased. Conversely, if the opening force is less than the closing force, h_{ref} is decreased.

Iterative Procedure

The individual processes described earlier are combined in an iterative procedure (figure 12) to find the steady state solution for the seal.

First, the seal geometry and operating conditions are input to the program through a data file, given in appendix E. Next an initial reference film thickness, h_{ref}, and a uniform profile is assumed. Then an initial pressure distribution is calculated by solving Reynolds equation, and the distribution of heat generation is also determined. Now the deformation loop is entered. The deformations of the seal faces are calculated using the influence coefficients. The deformations of the seal faces define the film thickness distribution. At this point the new values of the film

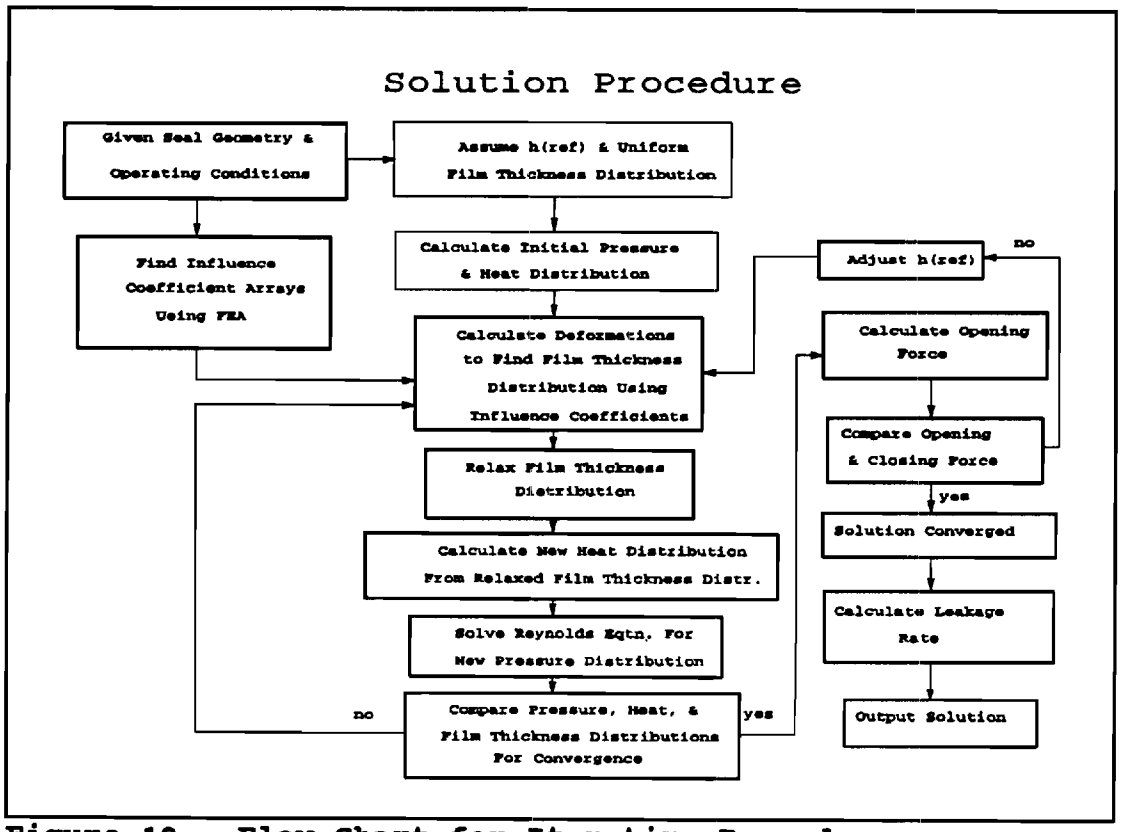

Figure 12. Flow Chart for Iterative Procedure.

thickness are relaxed with the values from the previous iteration in the following manner,

$$H=(1-\alpha)H_{old}+\alpha H_{new} \qquad (3.24)$$

where the relaxation factor, α, is 0.5. This relaxation is necessary to provide stability to the solution procedure. The relaxed values of the film thickness are then used to calculate new values of the pressure distribution and heat flux distribution. Now, the values of film thickness, pressure, and heat generation distributions are compared with the values from the

previous iteration. If the values do not agree within a specified tolerance ($\Delta r \Delta\theta/10$), the deformation-Reynolds loop is entered again. This process is repeated until all of the distributions converge.

After the deformation-Reynolds loop has converged, the opening force is calculated and compared to the closing force. If the two agree within 0.3%, the problem is solved, and the leakage rate is then calculated. If the values do not agree then the value of h_{ref} is adjusted by,

$$h_{ref_{new}} = w\frac{F_o - F_c}{F_c} h_{ref_{old}} + h_{ref_{old}} \qquad (3.25)$$

where w is a weighting factor, and where F_o and F_c are the opening and closing force, respectively. After adjusting h_{ref}, the deformation analysis loop is entered again.

The computer program, given in Appendix D, uses this procedure to find the operating conditions of a seal design given the influence coefficients of the design. Instructions for use of the computer code and arrangement of the influence coefficient arrays are given in appendix E and appendix G, respectively.

CHAPTER IV

RESULTS & DISCUSSION

Film Thickness

Wave Pattern

As discussed in the Analysis section, the deformations for both seal faces are calculated. These deformations are observed in the profiles of the film thickness. Figure 13 shows the circumferential variation in film thickness at various radii in the seal for the case of P_s = 0.345 MPa (50 psig) and ω = 100 rad/s. At this low pressure and speed, there is not a significant wave pattern formed, but it is evident that the deformation is greatest near the hydropads. As the sealed pressure, P_s is increased to 0.690 MPa (100 psig) (figure 14) and 1.035 MPa (150 psig) (figure 15) an asymmetric wave pattern forms. As discussed earlier, this pattern provides hydrodynamic pressure generation that increases the net opening force even without cavitation.

It is also noticed that the deformation at the outer diameter is greater than that at the inner diameter. This is a result of the structural weakening from the presence of the hydropads at the outer diameter.

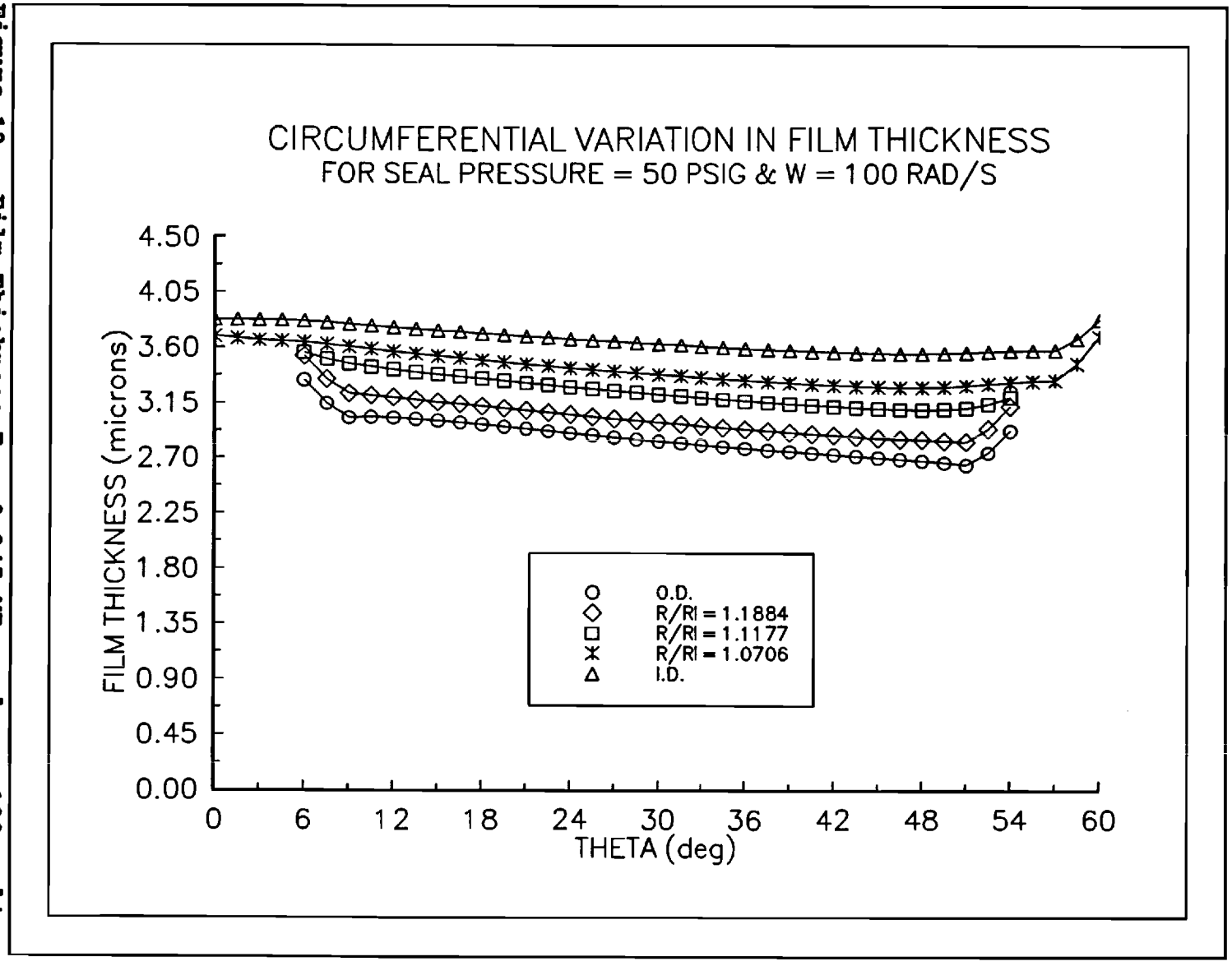

Figure 13. Film Thickness P_s = 0.345 MPa and ω = 100 rad/s.

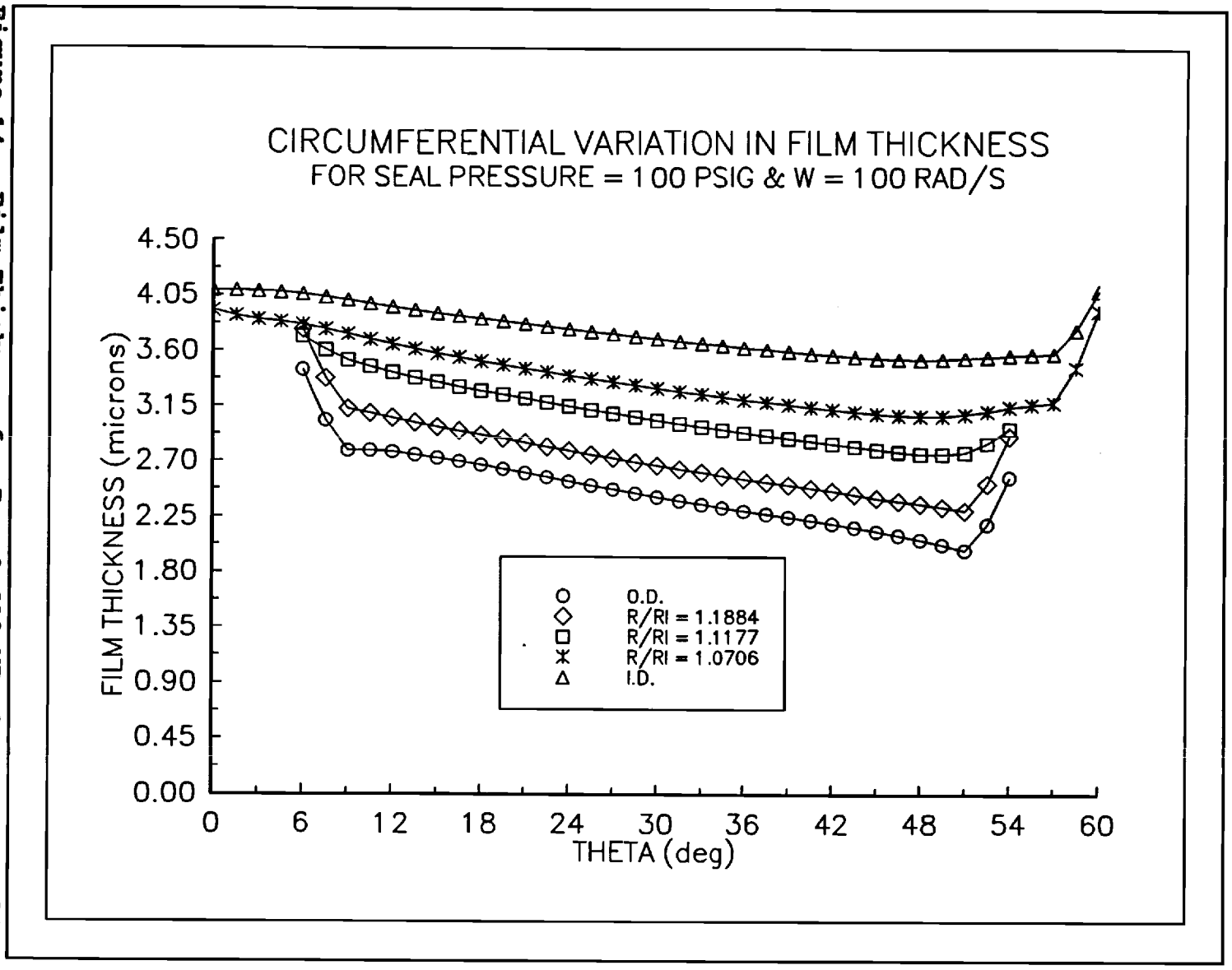

Figure 14. Film Thickness for P_s = 0.690 MPa & ω = 100 rad/s.

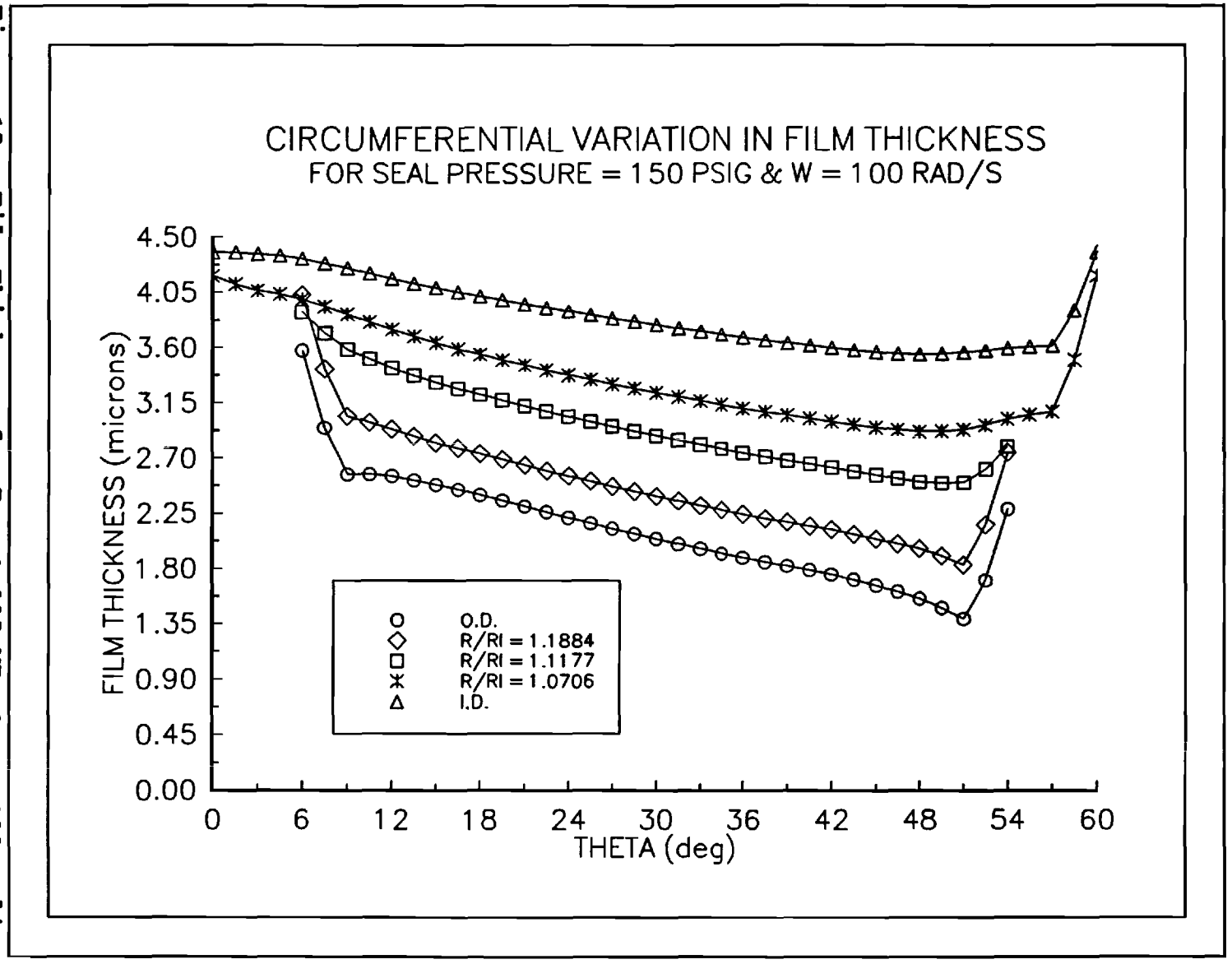

Figure 15. Film thickness for P_i = 1.035 MPa & ω = 100 rad/s.

Coning

Figures 13 through 15 show that the film thickness converges from the inner diameter to the outer diameter. This means the fluid film is diverging in the direction of leakage flow. This is negative coning and is observed by Key, et. al. [1]. Normally, a seal operating in this condition is not stable because the film would have negative stiffness. However, this seal is able to operate under this condition because of the additional hydrodynamic pressure generated by the hydropad configuration.

Effect of Speed

Figures 16 through 18 show the circumferential variation in film thickness for P_s = 1.035 MPa (150 psig) for various values of ω. It is seen that the rotational speed, ω, does not affect the shape of the wave pattern much, but it does increase the average film thickness. This increase is due to increased hydrodynamic pressure generated in the seal. Figure 19 shows the relationship between the reference film thickness, h_{ref}, and the rotational speed. It is observed that the relationship is essentially linear for each sealed pressure and that the reference film thickness increases with the sealed pressure.

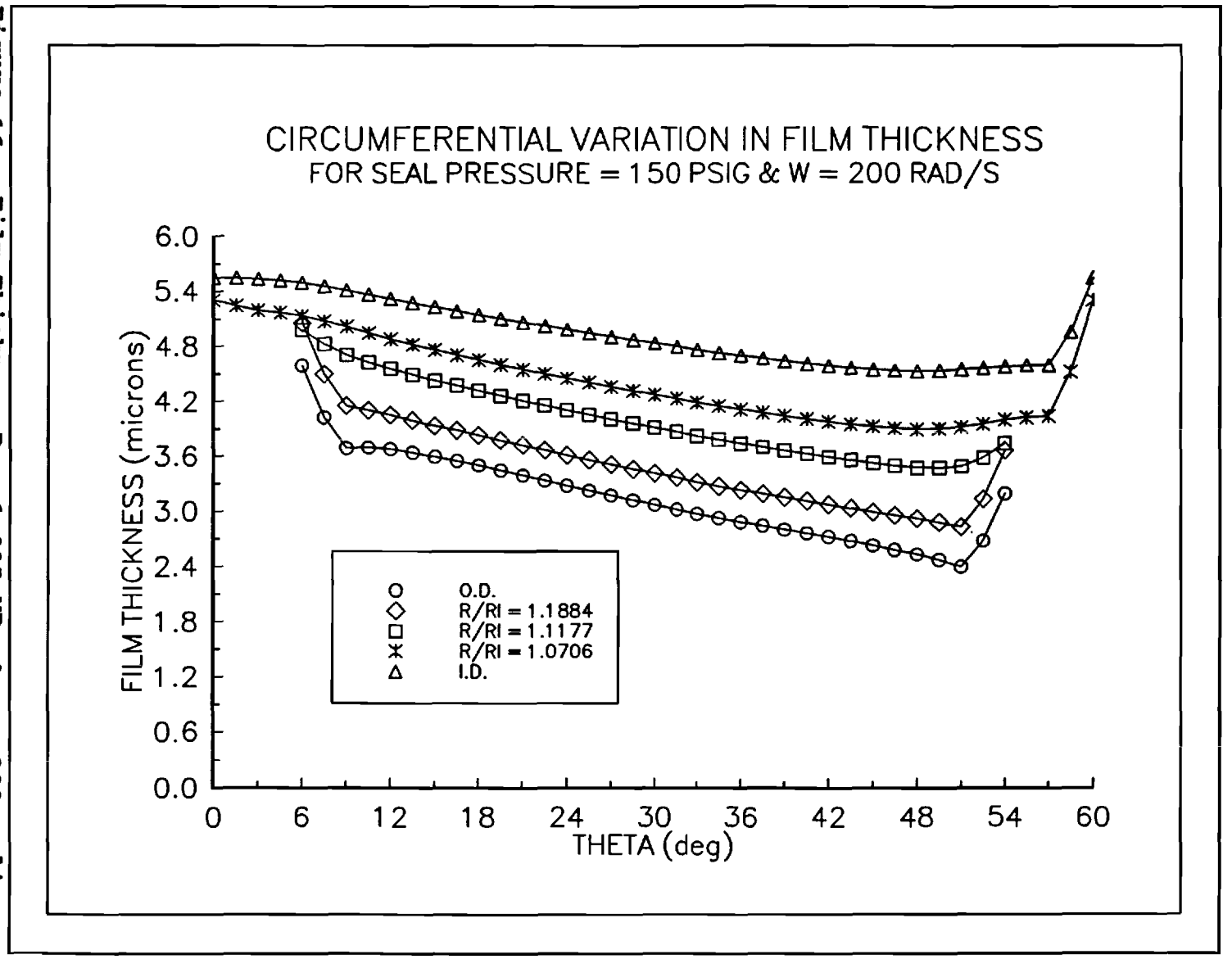

Figure 16. Film Thickness P, = 1.035 MPa & ω = 200 rad/s.

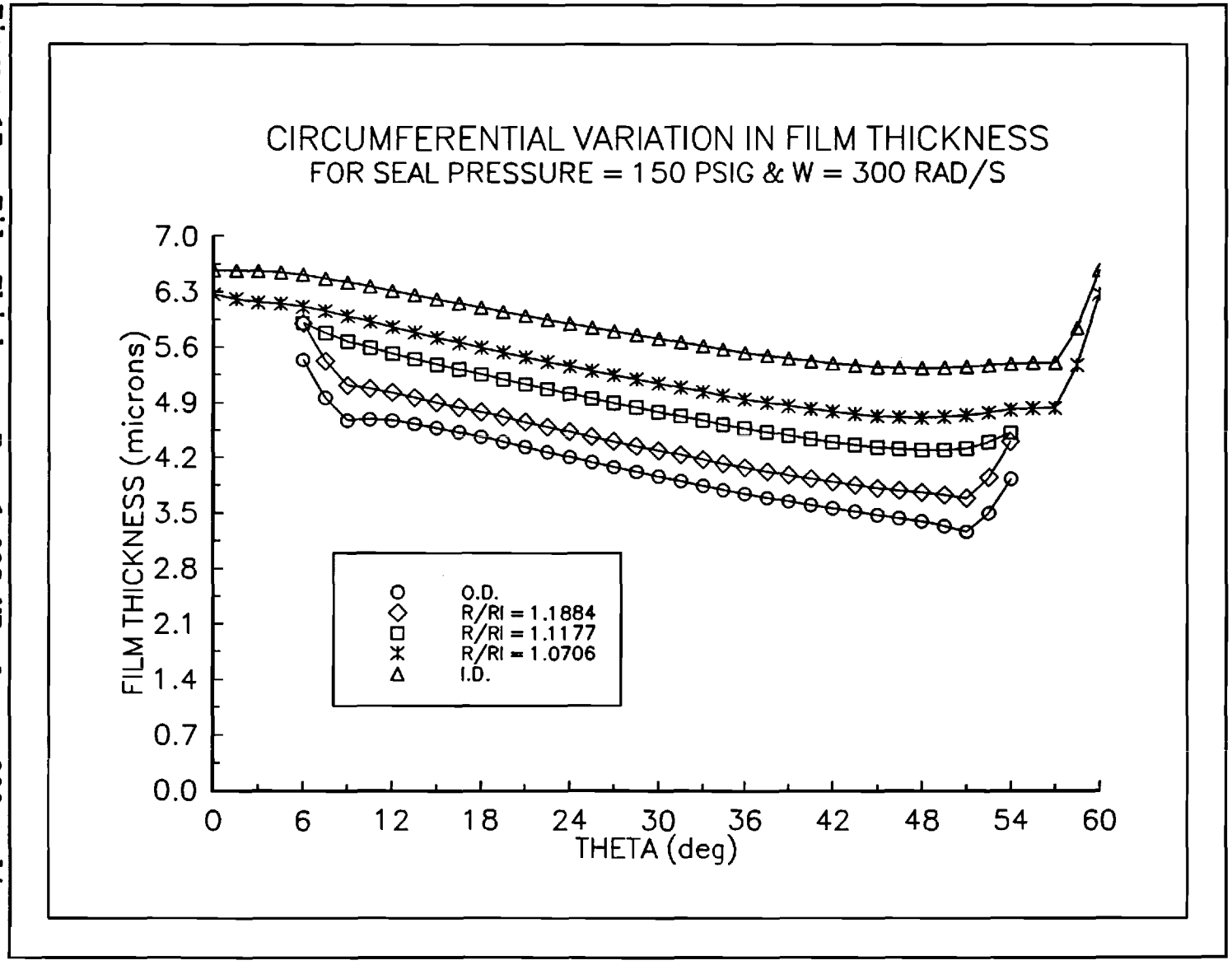

Figure 17. Film Thickness P, = 1.035 MPa & ω = 300 rad/s.

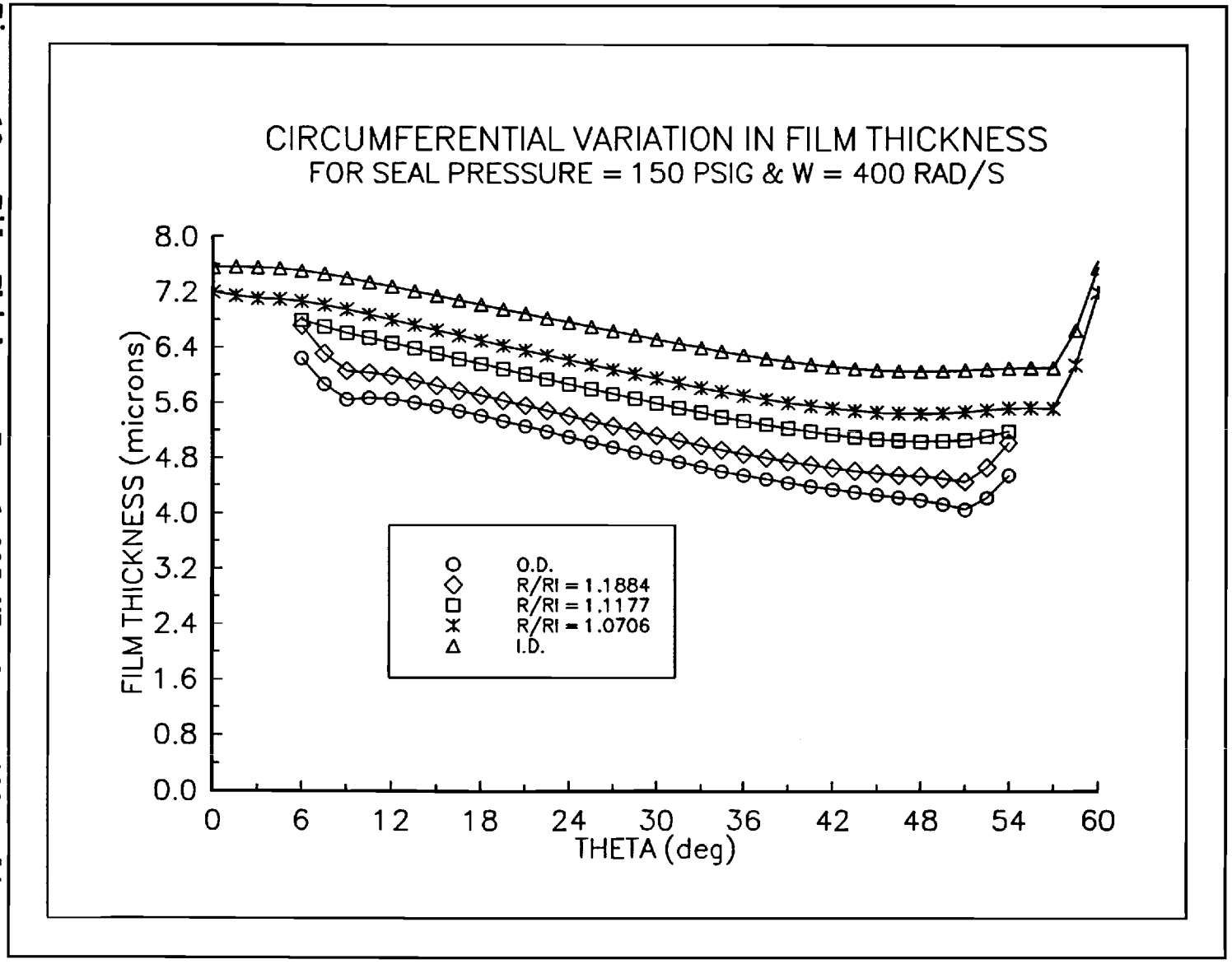

Figure 18. Film Thickness P_s = 1.035 MPa & ω = 400 rad/s.

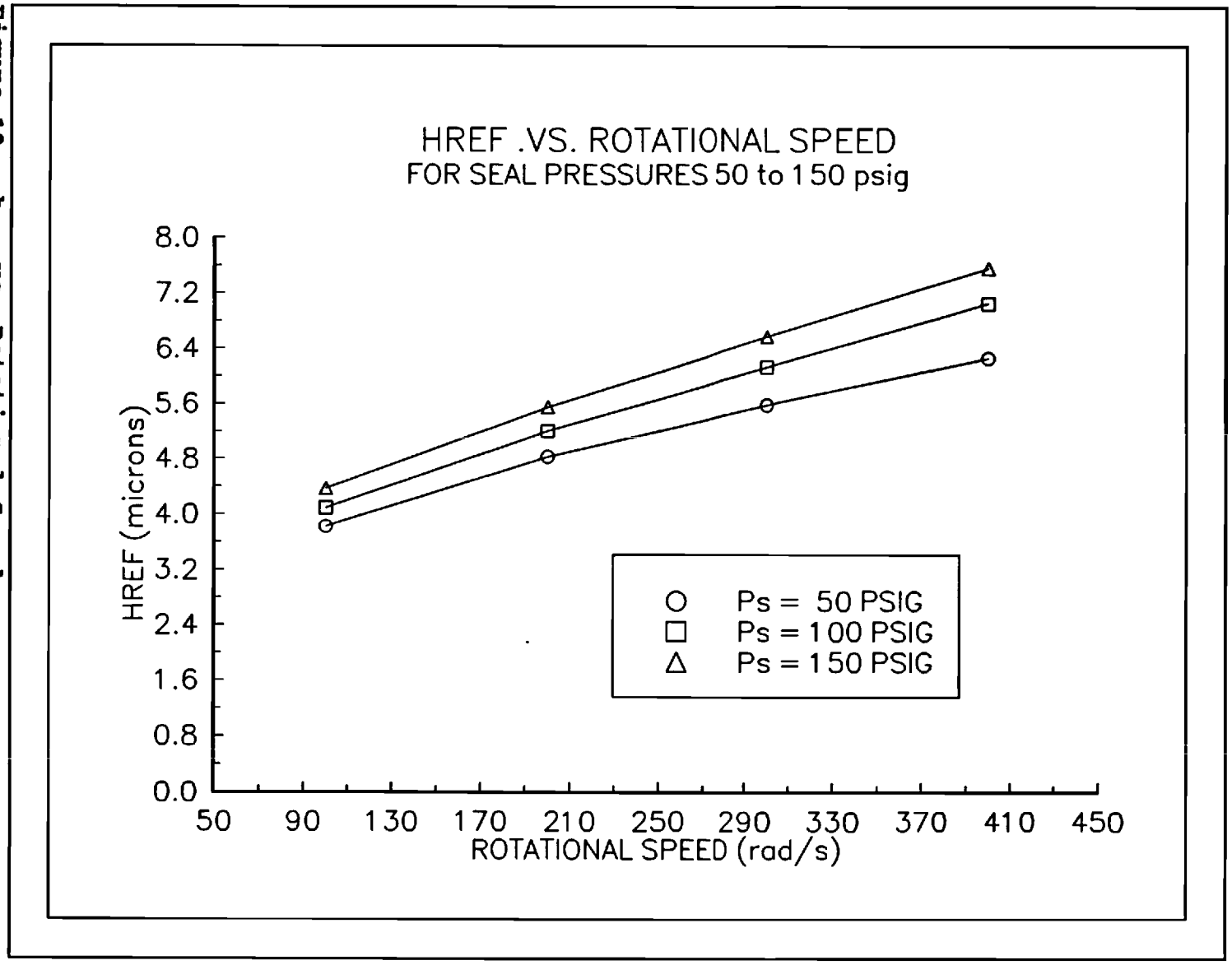

Figure 19. h_{ref} .vs. Rotational speed.

Minimum Film Thickness

In figure 20, a similar relationship with speed is shown for the minimum film thickness. However, it should be noted that the minimum film thickness decreases with increasing seal pressure.

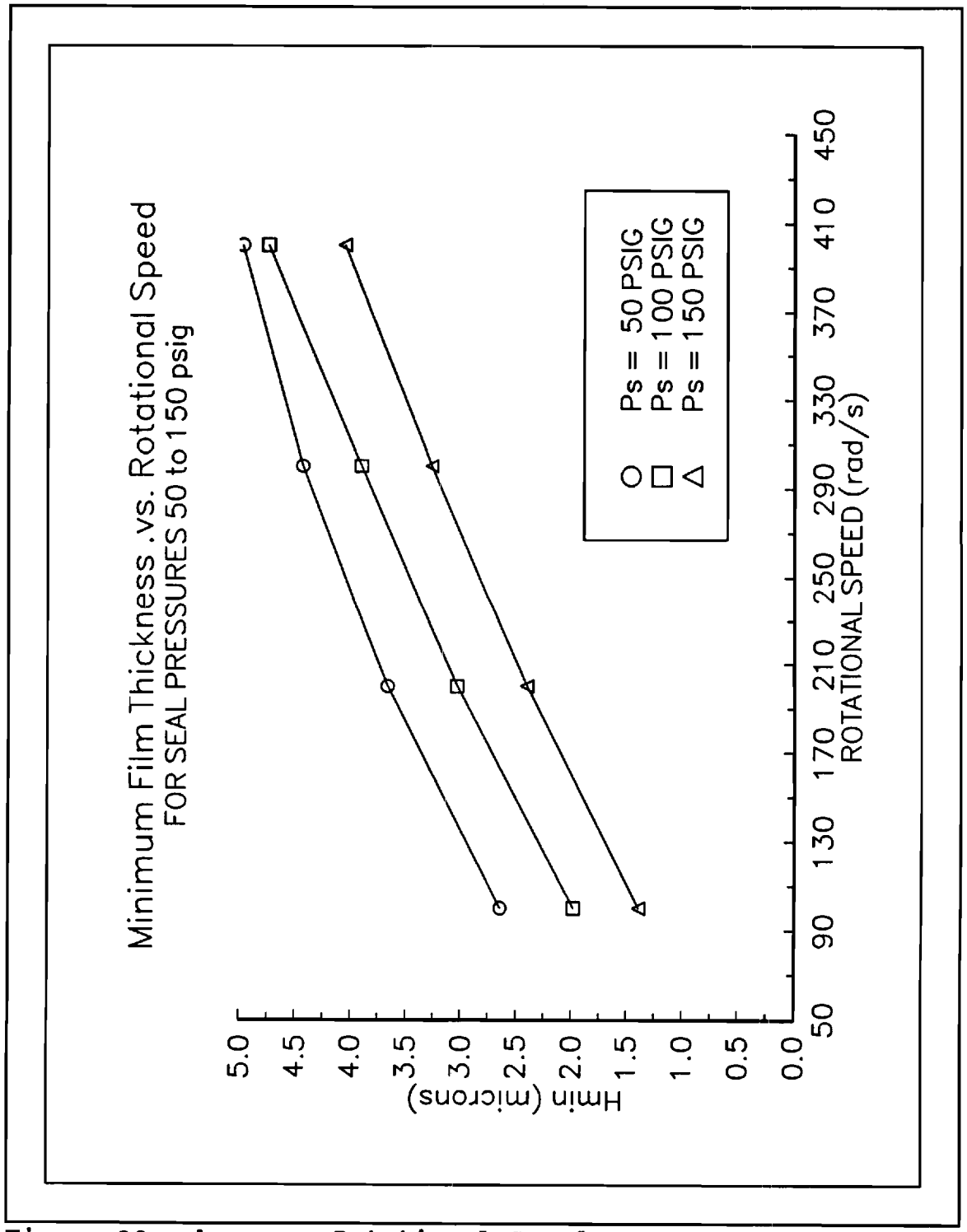

Figure 20. h_{min} .vs. Rotational Speed.

Pressure Distribution

The pressure distributions for cases P_s = 0.345 MPa (50 psig), 0.690 MPa (100 psig), and 1.035 MPa (150 psig) are shown in three dimensional plots in figures 21, 22, and 23. There is a distinct wave pattern in the pressure distribution. By comparing each distribution with its corresponding plot of variation in film thickness, it is observed that the elevated pressures are produced in regions where the circumferential flow is converging, meaning the film thickness is decreasing as θ increases. Conversely, it is also noticed that the low pressure regions correspond to locations where the circumferential flow is diverging.

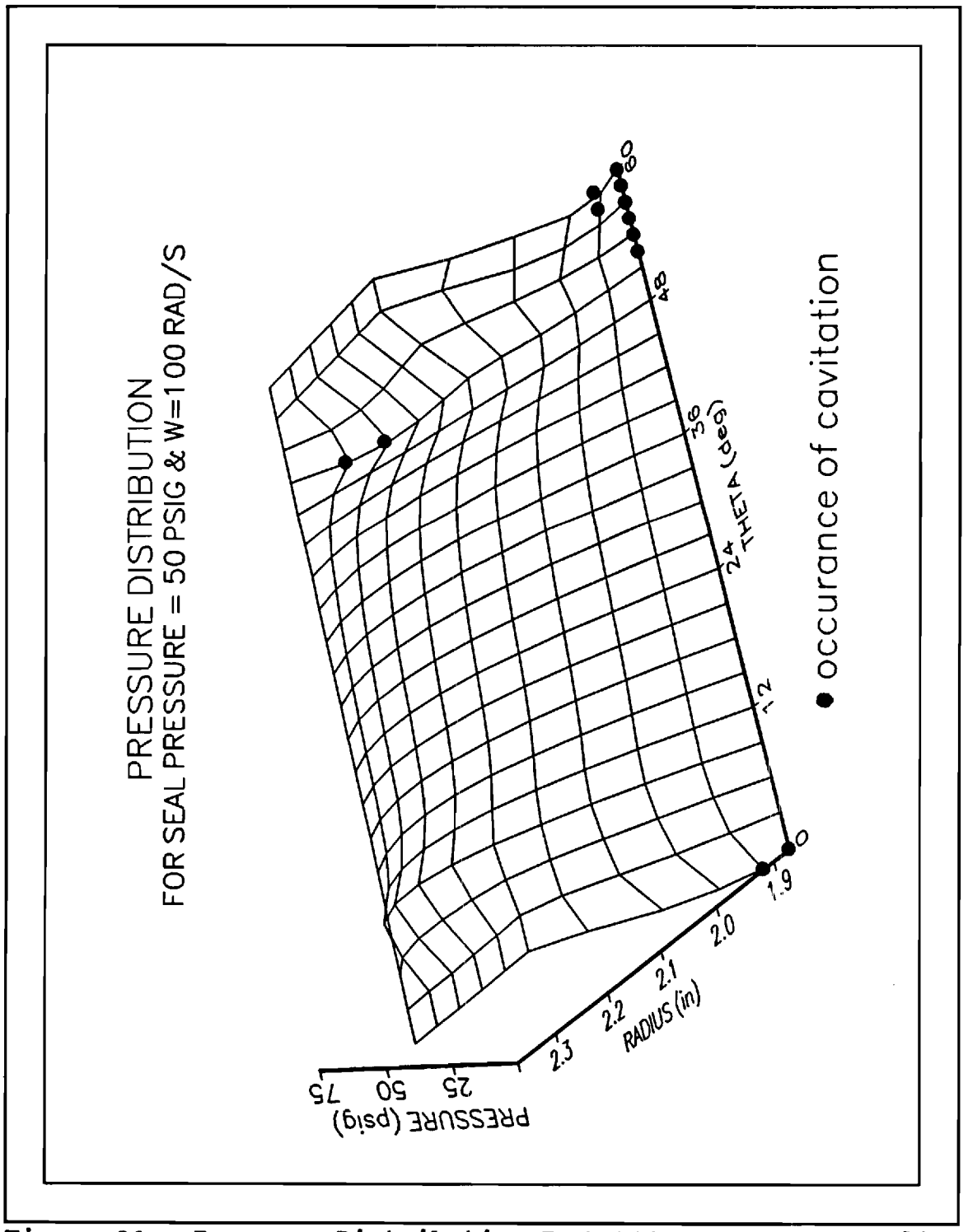

Figure 21. Pressure Distribution P_s=0.345 MPa & ω=100 rad/s.

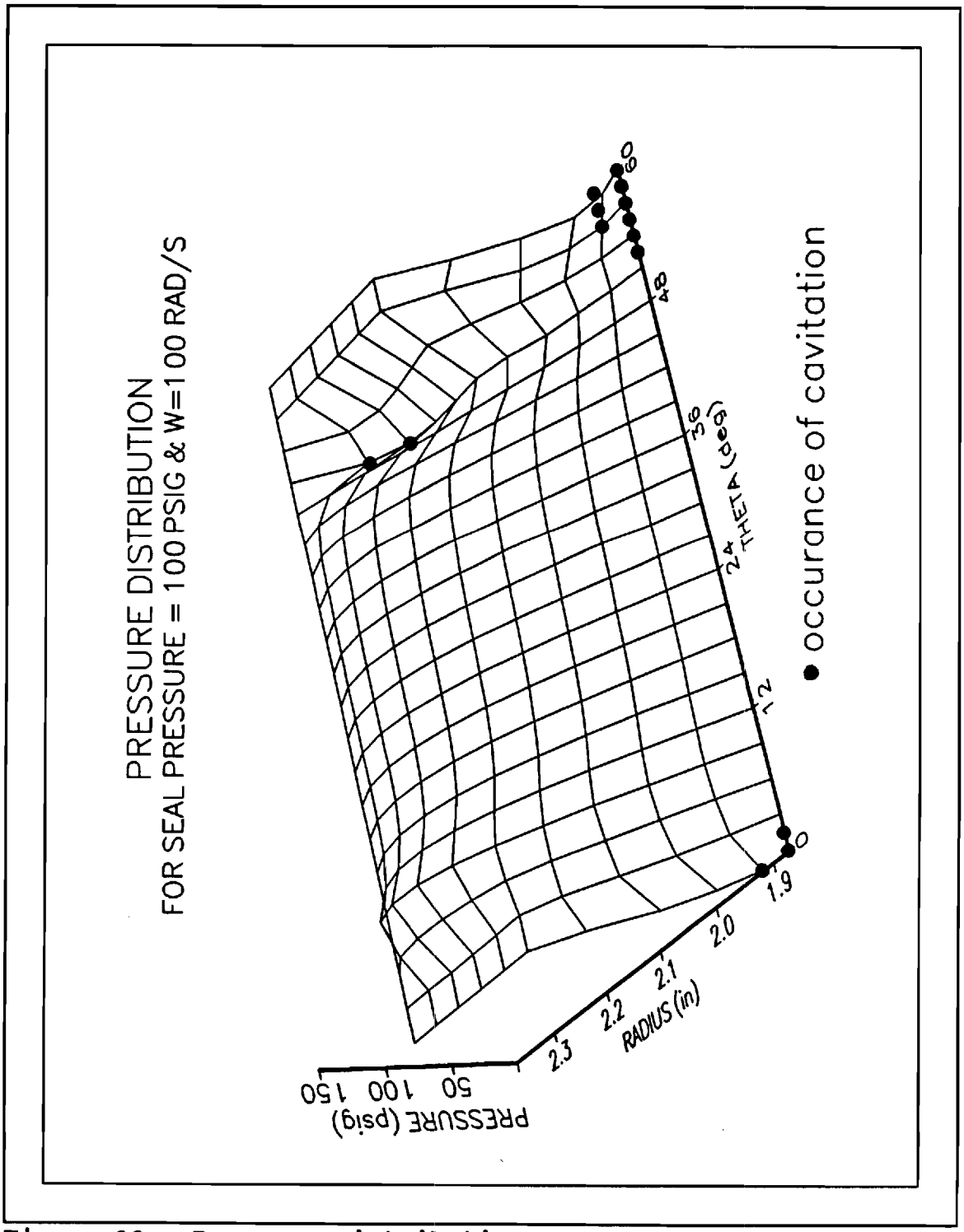

Figure 22. Pressure Distribution P_s=0.690 MPa & ω=100 rad/s.

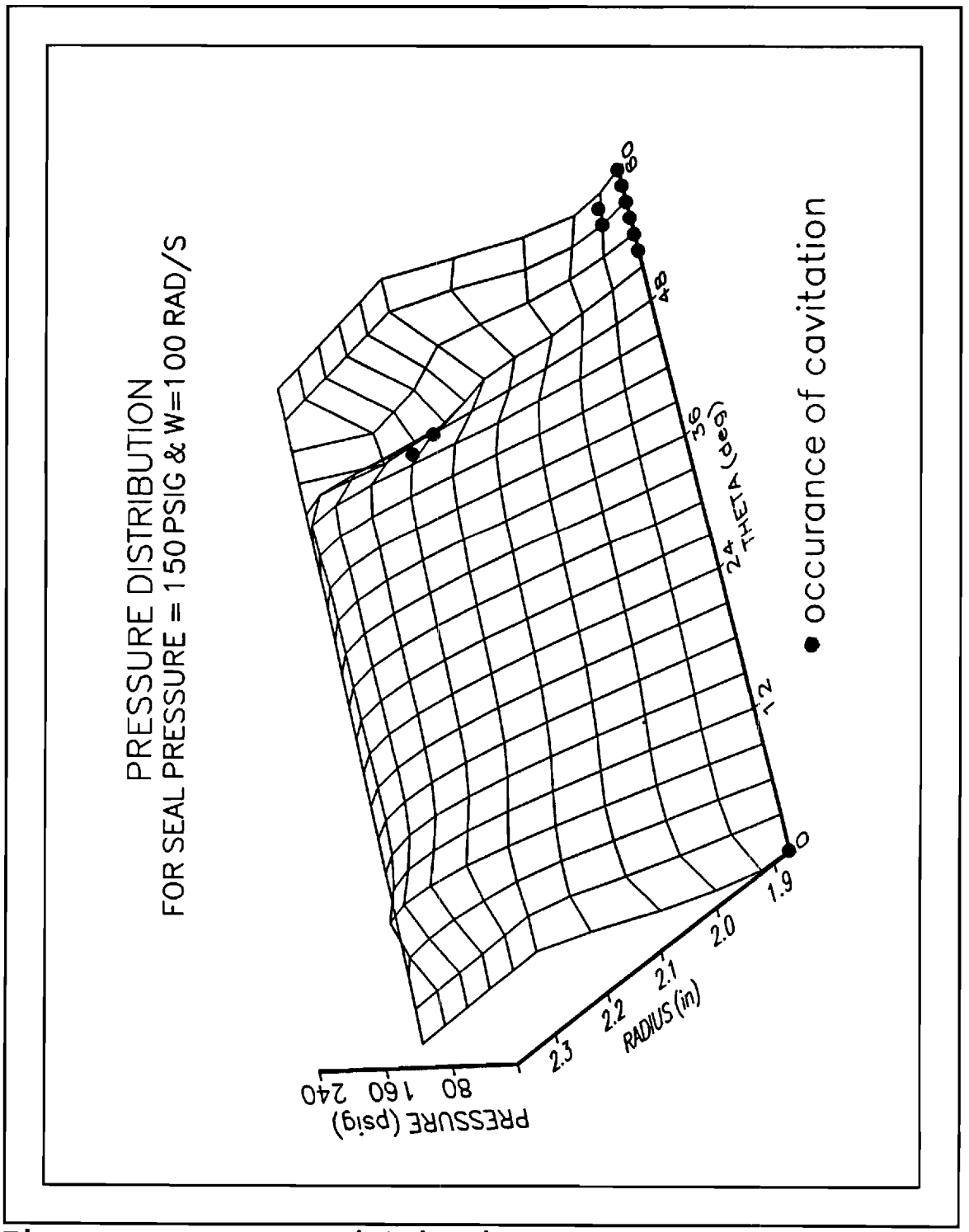

Figure 23. Pressure Distribution P_s=1.035 MPa & ω=100 rad/s.

Effect of Speed

Figures 24, 25, and 26 show the pressure distributions for ω = 200 rad/s, 300 rad/s, and 400 rad/s in the case of P_s = 1.035 MPa (150 psig). It is noted that the amplitude of the wave pattern in the distributions seems to decrease with ω. From looking at figures 13 through 15, it is seen that this is reasonable since the converging and diverging regions near the hydropads are much steeper and the reference film thickness, h_{ref}, is smaller at the lower speeds than at the higher ones.

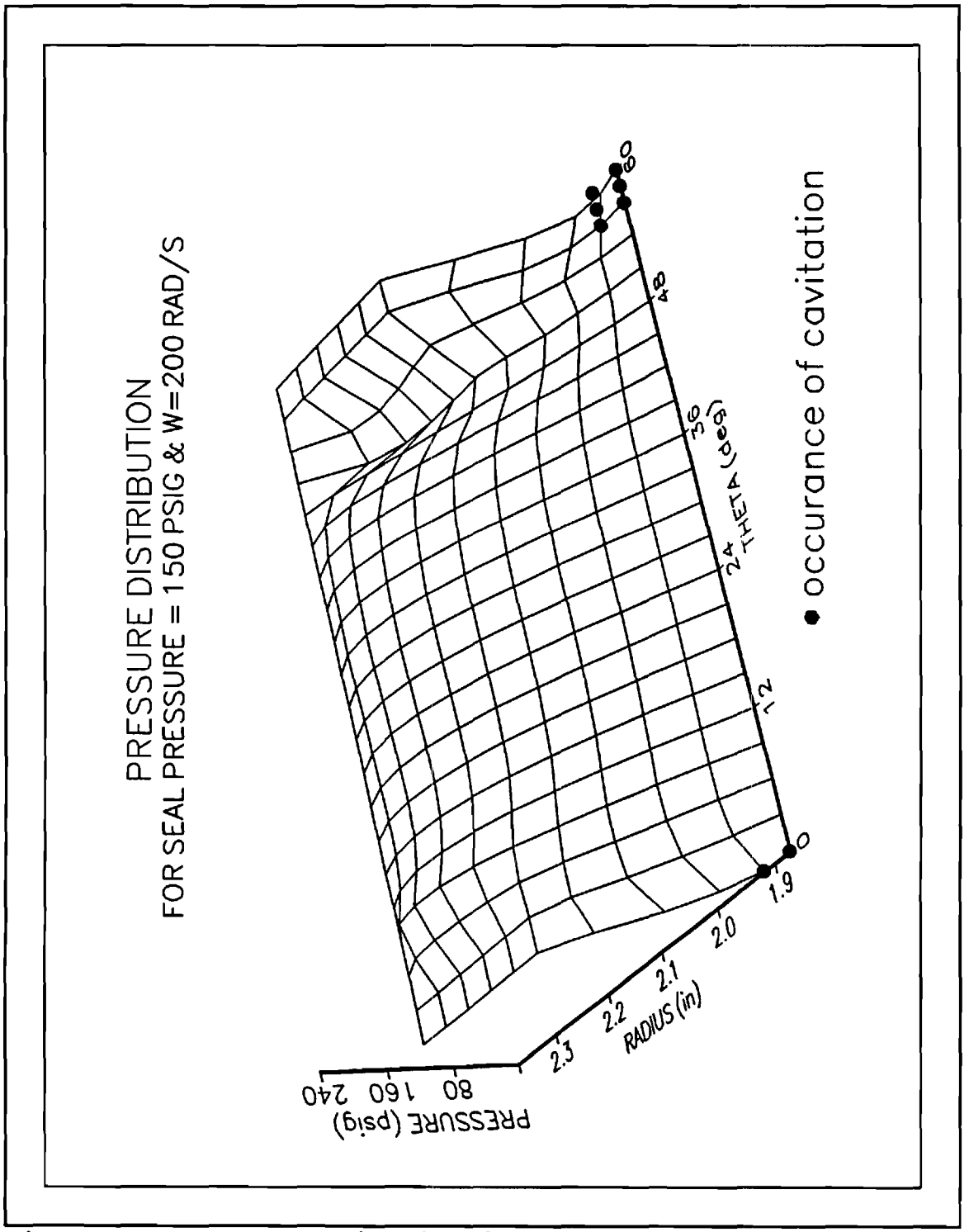

Figure 24. Pressure Distribution P_s=1.035 MPa & ω=200 rad/s.

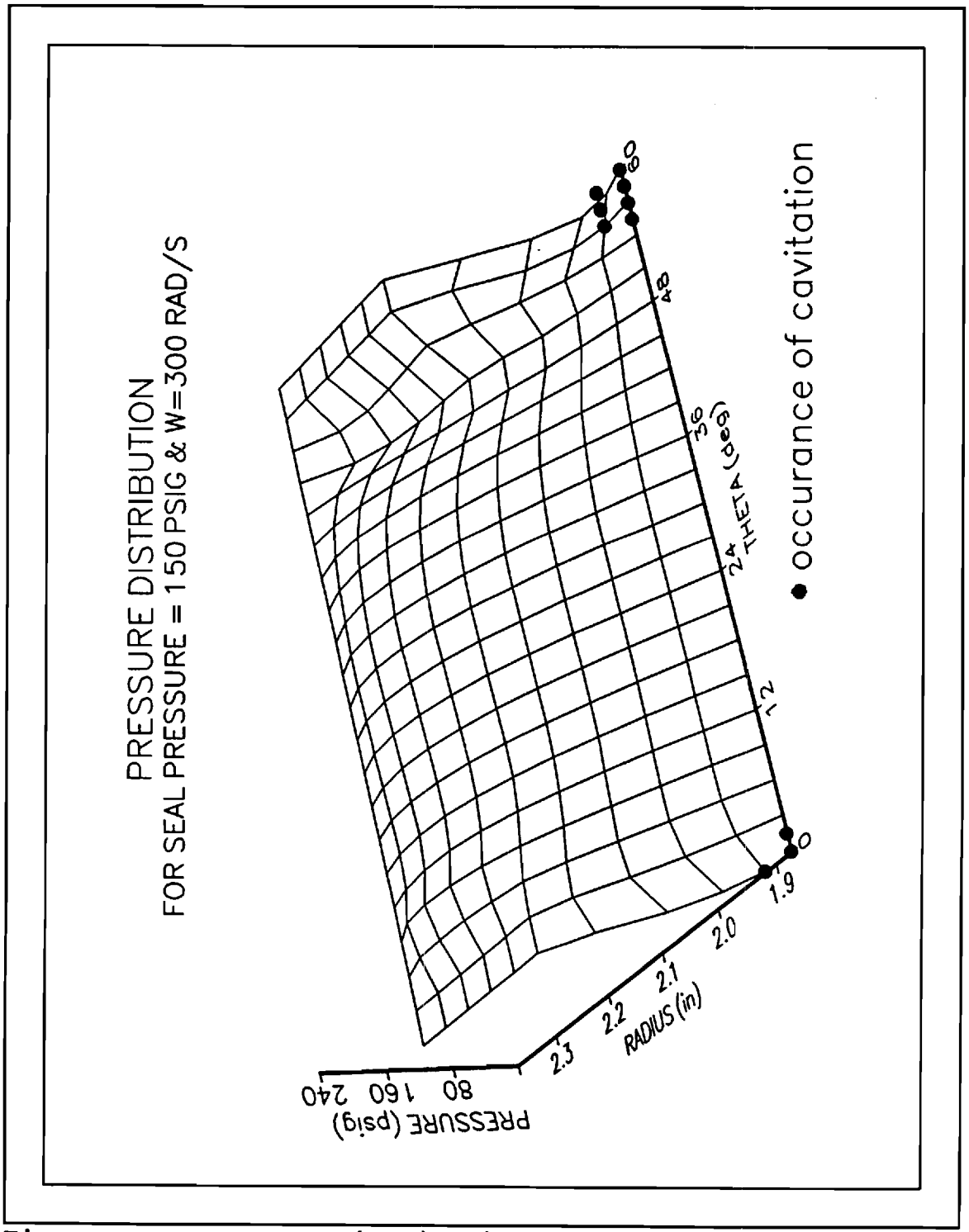

Figure 25. Pressure Distribution P_s=1.035 MPa & ω=300 rad/s.

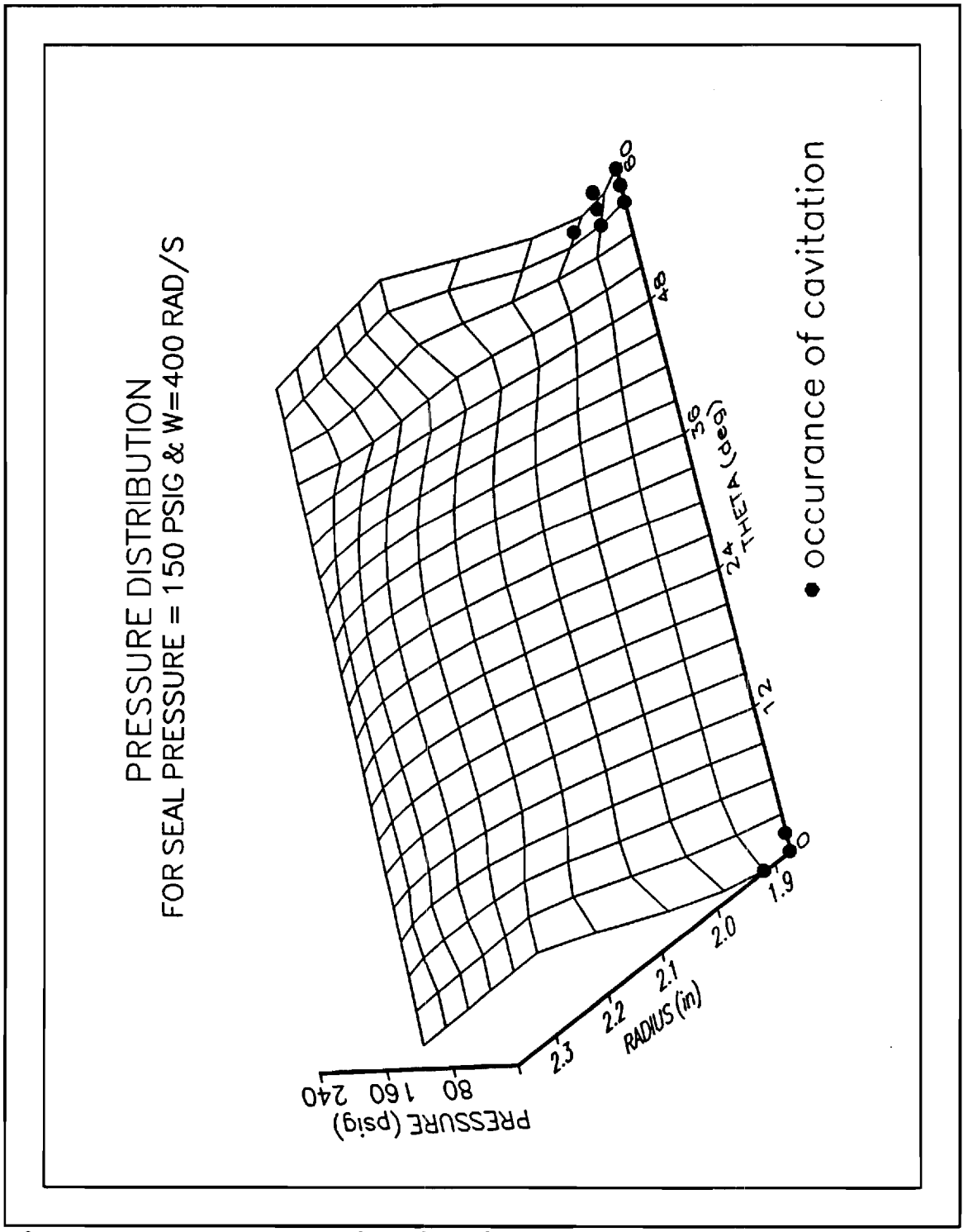

Figure 26. Pressure Distribution P_s=1.035 MPa & ω=400 rad/s.

Cavitation

In figures 21 to 26, locations of cavitating nodes are noted by the black circles. From the figures, it is seen that there are two cavitation regions. The first is a small region near the outer diameter, immediately upstream of the hydropad. The second is located at the inner radius beneath the location of the hydropad. These cavitation regions were present in the cases of ω = 100 rad/s, but the cavitation upstream from the hydropad was not present at higher speeds.

Leakage Rate

Figure 27 shows the leakage flow rates for all the cases analyzed. It is evident that the leakage rate increases with the seal pressure, and that it increases rapidly with increasing speed.

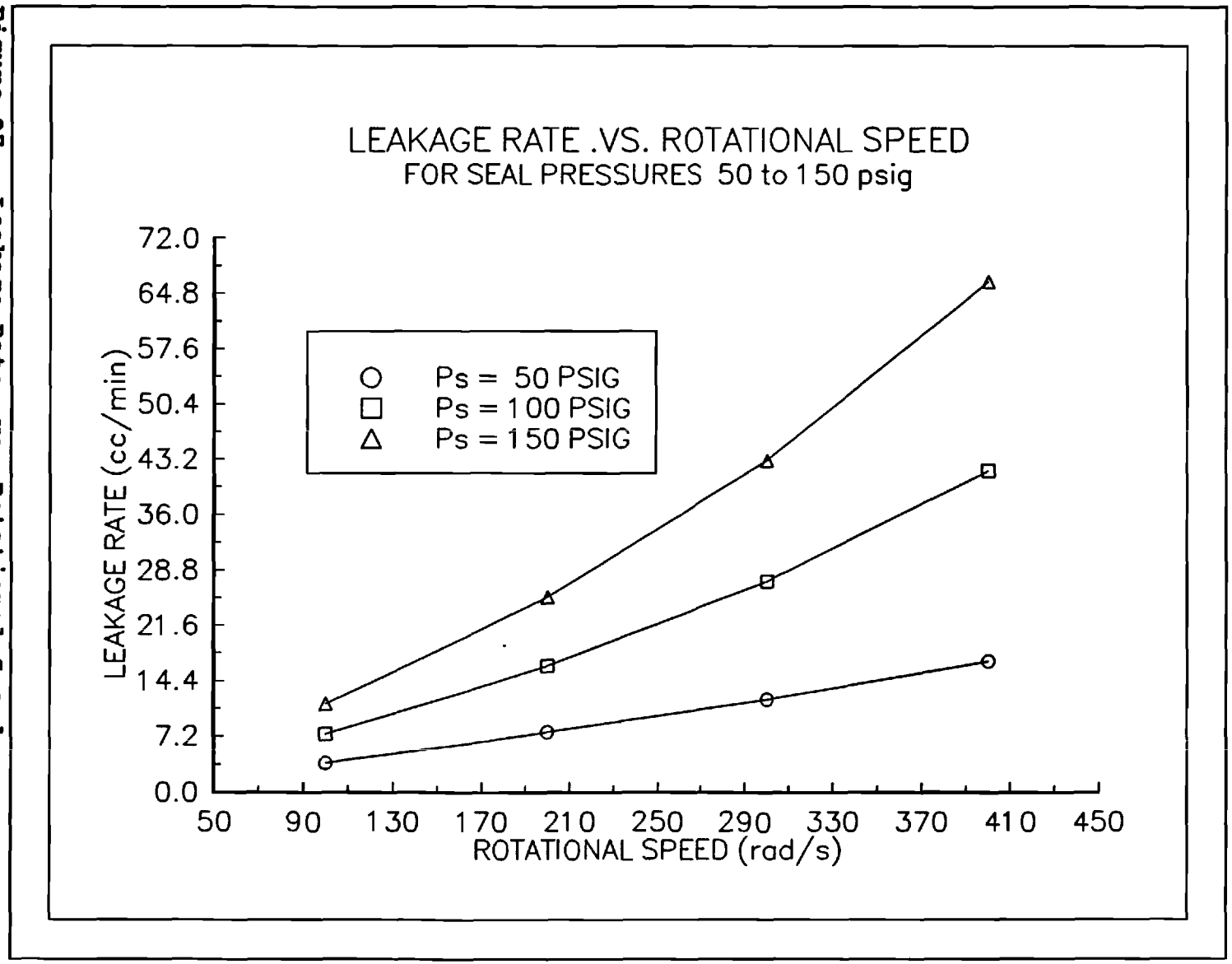

Figure 27. Leakage Rate .vs. Rotational Speed.

Stiffness

Since negative coning is observed in this seal design, it is interesting to examine the stiffness of the seal. The stiffness, k, is defined by,

$$k = -\frac{\Delta F_o}{\Delta h}$$

where ΔF_o is the change in the opening force and Δh is the change in the film thickness. Figure 28 and figure 29 show relationship between the opening force and the reference film thickness for several of the cases analyzed. The corresponding values of stiffness are also shown. It is seen in these graphs that the stiffness is positive for all the cases even though the film gap diverges.

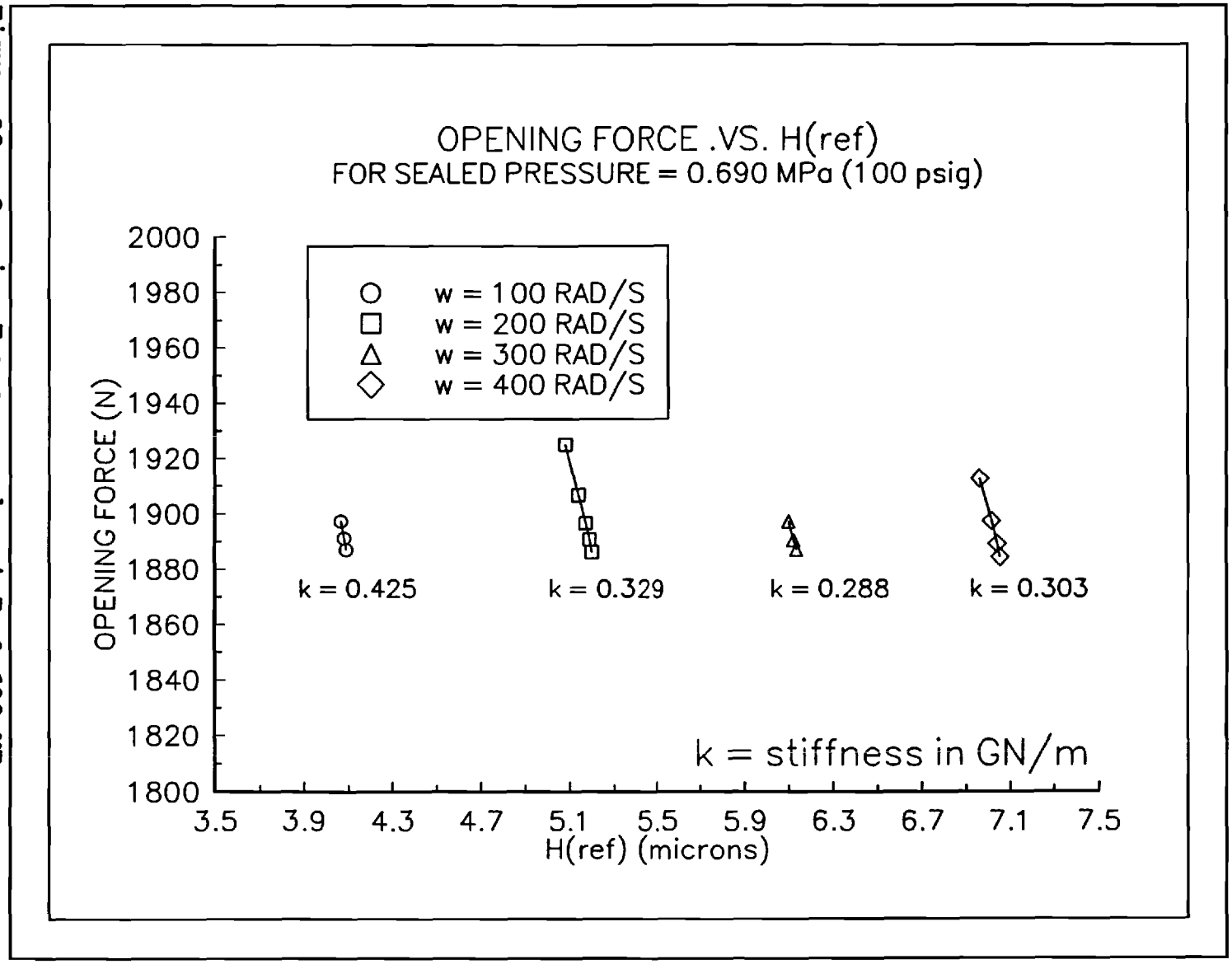

Figure 28. Opening Force .vs. h_{ref} at P_s=0.690 MPa

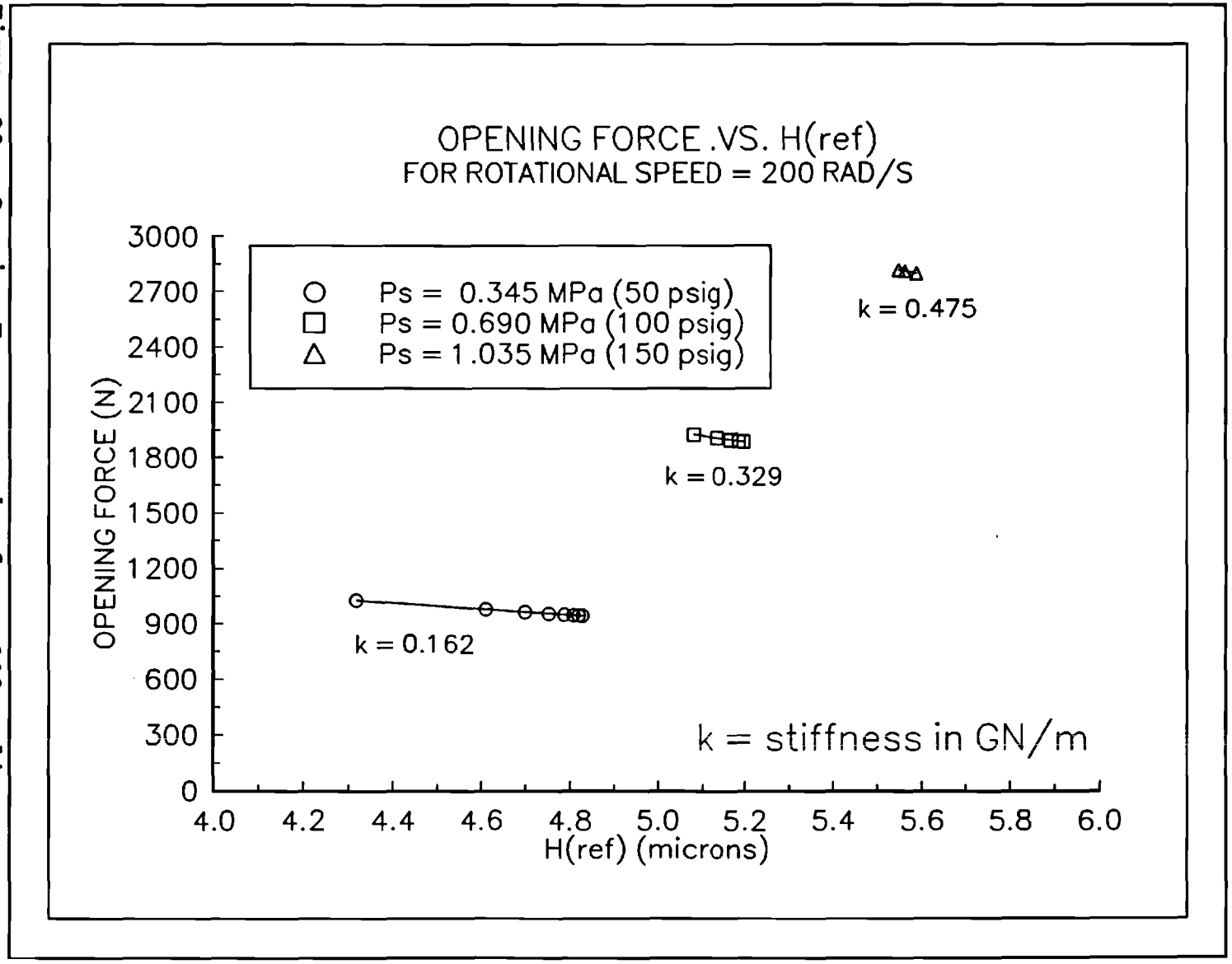

Figure 29. Opening Force .vs. h_{ref} for ω=200 rad/s.

Computational Efficiency

All of the cases are analyzed using a Northgate 486/25 MHz computer. In general each case converges on a solution within one hour of cpu time. The longest running case requires two hours of cpu time. The amount of cpu time required can vary substantially depending on the seal design being analyzed. It is very dependent on the size of the mesh required to analyze the seal design. It is also important to note that this computing time does not include the computation of the influence coefficients. For the seal analyzed, 365 finite element analyses are performed on each seal face in order to determine the entire set of mechanical and thermal influence coefficients.

CHAPTER V

CONCLUSIONS

The work presented in this paper offers an analysis of a deep hydropad seal design and a prediciton of performance, including leakage rate. The procedure does require a fair amount of computational effort, but once the structural influence coefficients are found for a new hydropad seal design, steady state operating solutions can be found in a reasonable amount of time. The work also provides support to the work of Key, et. al. [1] which suggests that deep hydropads provide load support by inducing the face of the seal to deform in a circumferential wave pattern, which provides hydrodynamic pressure generation to increase load support.

In developing the computer program, several convergence problems are encountered. The first is with the Reynolds solution for the pressure distribution. It is found that for the method used it is necessary for the aspect ratio of the grid to be very close to one, or the method could lead to convergence problems. The second convergence problem

encountered is with deformation-Reynolds iterative loop. In the work of Key, et. al. [1], the pressure distribution is relaxed between iterations to provide stability to the problem. In analyzing the prospective seal design, it is found that this loop would not converge for high pressures and the high speed of ω=400 rad/s. Through experimentation it is found that by relaxing the film thickness distribution instead of the pressure distribution these cases would converge. It is also found that the program converges on a solution faster by this method.

Cavitation effects do not appear significant in the cases analyzed because of the hydrostatic pressure drop which suppresses the creation of cavitation. Analyzing cases for a zero pressure drop across the seal face reveals that the computer program will not converge on a steady state solution.

Recommendations

The analysis method presented in this paper only allows for hydropads that are essentially square radial grooves in the seal face. This is an approximation since in practice the hydropads are not machined exactly in that shape. It would be preferable to allow for curved hydropad surface to provide a more precise solution as well as allow for analyzing unusually shaped hydropad configurations. Since a finite difference scheme is used for the Reynolds solution of the flow field, it is difficult to analyze unusual

configurations because the finite difference method requires a uniform grid. One possible solution to this is to use a finite element method to solve the Reynolds equation. This would allow for the grid to be nonuniform. It would also simplify the solution process. It would eliminate the need to have different mesh sizes for the finite element deformation analysis and Reynolds solution analysis.

APPENDIX A

FINITE DIFFERENCE SOLUTION OF REYNOLDS EQUATION

The normalized "universal" governing equation is

$$\frac{1}{\eta}\frac{\partial}{\partial\eta}\left(\eta H^3\frac{\partial(F\phi)}{\partial\eta}\right)+\frac{1}{\eta}\frac{\partial}{\partial\theta}\left(\frac{H^3}{\eta}\frac{\partial(F\phi)}{\partial\theta}\right)=\gamma\frac{\partial[(1+(1-F)\phi)H]}{\partial\theta} \qquad \text{(A.1)}$$

with boundary conditions,

$$\phi=1.0 \qquad \text{at } \eta=\eta_o \qquad \text{(A.2)}$$

$$\phi=\frac{P_a-P_c}{P_s-P_c} \qquad \text{at } \eta=1 \qquad \text{(A.3)}$$

To obtain the algebraic equations for the mesh, equation (A.1) is integrated over an element area in the flow field extending from θ_w to θ_e and from r_s to r_n [17]. This element area is shown in figure 29 with the node of interest denoted by P. Multiplying equation (A.1) by $\eta d\eta d\theta$

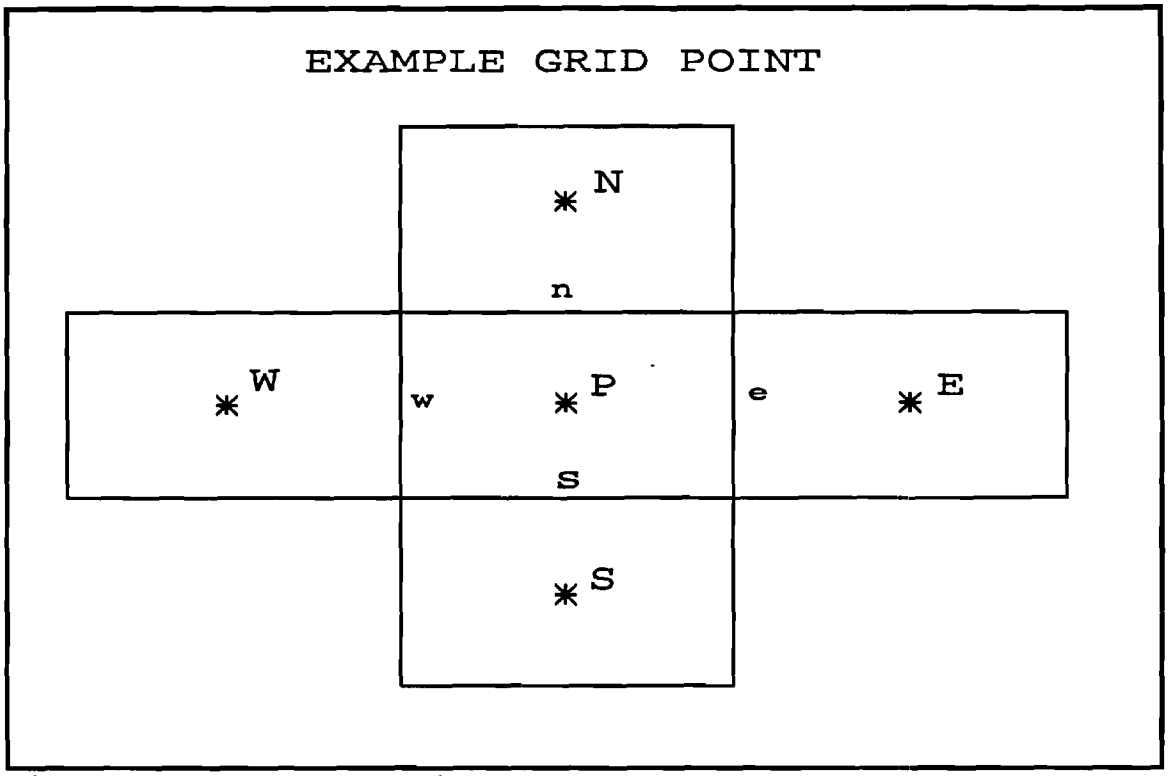

Figure 30. Example Grid for Reynolds Mesh

and integrating $\theta=\theta_w$ to $\theta=\theta_e$ and $r=r_s$ to $r=r_n$ yields

$$[\eta H^3 \frac{\partial(F\phi)}{\partial\eta}]_n \Delta\theta - [\eta H^3 \frac{\partial(F\phi)}{\partial\eta}]_s \Delta\theta + [\frac{H^3}{\eta} \frac{\partial(F\phi)}{\partial\theta}]_e \Delta\eta - \quad \textbf{(A.4)}$$

$$[\frac{H^3}{\eta} \frac{\partial(F\phi)}{\partial\theta}]_w \Delta\eta = \gamma [\{1+(1-F)\phi\}H]_e \eta \Delta\eta - \gamma [\{1+(1-F)\phi\}H]_w \eta \Delta\eta$$

The accuracy of Patankar's finite differene method [17] is established by mesh refinement calculations. Equation (A.4) has the characteristics of a diffusion equation with variable diffusion coefficients and a source term.

Therefore, we define a conductivity, K, as

$$K=\eta H^3 \tag{A.5}$$

and use a central difference to expand the terms in equation (A.4) to obtain:

$$\frac{K_n\Delta\theta}{\Delta\eta}(F_N\phi_N-F_P\phi_P)-\frac{K_s\Delta\theta}{\Delta\eta}(F_P\phi_P-F_S\phi_S)+$$

$$\frac{K_e\Delta\eta}{\eta_P^2\Delta\theta}(F_E\phi_E-F_P\phi_P)-\frac{K_w\Delta\eta}{\eta_P^2\Delta\theta}(F_P\phi_P-F_W\phi_W)$$

$$=\gamma\eta_P\Delta\eta\,[\{1+(1-F_P)\phi_P\}H_e-\{1+(1-F_W)\phi_W\}H_w] \tag{A.6}$$

In equation (A.6), F_P and ϕ_P are used for the Couette flow term at the east boundary since the flow is in the positive θ direction so fluid crossing the east boundary originates from point P. In the formulation of the finite difference scheme, mass balance is maintained at the boundaries of every node including those at the cavitating boundaries. Therefore, the universal equation (A.1) with its boundary conditons, (A.2) and (A.3), and the cavitating boundary conditions (3.5) and (3.6) are all satisfied [11]. Due to the nature of the flow, the diffusion coefficients K_n, K_s, K_e, and K_w are calculated by taking the harmonic mean of the conductivities at the nodes adjacent to the boundary of

interest [17]. For example:

$$K_e = \frac{2K_P K_E}{K_P + K_E} \tag{A.7}$$

H_e and H_w are taken as the mean values between neighboring nodes to provide an approximation of the film thickness at the boundaries.

$$H_e = \frac{(H_P + H_E)}{2} \tag{A.8}$$

$$H_w = \frac{(H_P + H_W)}{2} \tag{A.9}$$

The following definitions are introduced for simplicity:

$$A_n = \frac{K_n \Delta\theta}{\Delta\eta} \tag{A.10}$$

$$A_s = \frac{K_s \Delta\theta}{\Delta\eta} \tag{A.11}$$

$$A_e = \frac{K_e \Delta\eta}{\eta_P^2 \Delta\theta} \tag{A.12}$$

$$A_w = \frac{K_w \Delta\eta}{\eta_P^2 \Delta\theta} \tag{A.13}$$

$$A_P = A_n + A_s + A_e + A_w + \gamma\eta_P (1 - F_P) H_e \Delta\eta \tag{A.14}$$

$$S_P=\gamma\eta_P\Delta\eta\,[H_e-\{1+(1-F_W)\phi_W\}H_W] \qquad \text{(A.15)}$$

The final algebraic equation becomes:

$$A_PF_P\phi_P=A_nF_N\phi_N+A_sF_S\phi_S+A_eF_E\phi_E+A_wF_W\phi_W+S_P \qquad \text{(A.16)}$$

For each node P, an equation of this form with appropriate values of coefficients $A_{P,N,E,S,W}$ and cavitation indexes $F_{P,N,E,S,W}$ can be written.

It is worthwhile to examine the boundary conditions. At the outer radius, $\eta=\eta_o$, and along the hydropad boundary, there is a fixed value of $\phi = 1$. In this model the high pressure P_S is at the outer radius, and the nodes along the outer radius do not cavitate.

At the inner boundary, in most seal applications, the pressure is maintained at atmospheric. If the cavitation pressure P_c is greater than the atmospheric pressure P_A, then there is two phase flow in the radial direction and an accompanying pressure change. The method presented will no longer be valid if pressure changes occur in the two phase region. Therefore, it is necessary for the cavitation pressure P_c to be less than or equal to the atmospheric pressure P_A for this method to be valid [11].

If P_c is less than P_A, then the cavitation zone is confined between the inner and outer radius of the seal boundaries. In the case that P_c equals P_A, it is possible

$$S_P=\gamma\eta_P\Delta\eta\,[H_e-\{1+(1-F_W)\phi_W\}H_W] \qquad \text{(A.15)}$$

The final algebraic equation becomes:

$$A_PF_P\phi_P=A_nF_N\phi_N+A_sF_S\phi_S+A_eF_E\phi_E+A_wF_W\phi_W+S_P \qquad \text{(A.16)}$$

For each node P, an equation of this form with appropriate values of coefficients $A_{P,N,E,S,W}$ and cavitation indexes $F_{P,N,E,S,W}$ can be written.

It is worthwhile to examine the boundary conditions. At the outer radius, $\eta=\eta_o$, and along the hydropad boundary, there is a fixed value of $\phi = 1$. In this model the high pressure P_S is at the outer radius, and the nodes along the outer radius do not cavitate.

At the inner boundary, in most seal applications, the pressure is maintained at atmospheric. If the cavitation pressure P_c is greater than the atmospheric pressure P_A, then there is two phase flow in the radial direction and an accompanying pressure change. The method presented will no longer be valid if pressure changes occur in the two phase region. Therefore, it is necessary for the cavitation pressure P_c to be less than or equal to the atmospheric pressure P_A for this method to be valid [11].

If P_c is less than P_A, then the cavitation zone is confined between the inner and outer radius of the seal boundaries. In the case that P_c equals P_A, it is possible

for nodes along the inner radius to cavitate. In order to predict this case, the boundary condition at the inner radius may be written more generally as,

$$(1-F)\frac{\partial(\phi H)}{\partial\theta}+F(\phi-\frac{P_a-P_c}{P_s-P_c})=0 \qquad \textbf{(A.17)}$$

If the node along the boundary is in the full film region, F = 1, then equation (A.17) reduces to equation (A.3). If the node is in the cavitating region, F = 0, the equation reduces to the general governing equation for cavitating regions.

$$\frac{\partial(\phi H)}{\partial\theta}=0 \qquad \textbf{(A.18)}$$

The set of equations resulting from this method is solved using an alternating direction implicit method. A tridiagonal matrix algorithm is used for the column by column solution of the system of equations. It is necessary to use both a circular tridiagonal matrix algorithm and a tridiagonal matrix algorithm for the row by row solution of the equations. For the rows below the hydropads a circular tridiagonal matrix algorithm is needed, since the nodes at θ=0° and θ=60° are at the same pressure.

After the solution of each column or row of equations, the values of ϕ and F are relaxed with the values from the

previous iteration by coefficients α and β,

$$\phi=\alpha\phi_{new}+(1-\alpha)\phi_{old} \qquad \text{(A.19)}$$

$$F=\beta F_{new}+(1-\beta)F_{old} \qquad \text{(A.20)}$$

For the method to be stable, it is necessary to use a very small value of β=0.01, and a small value of α=0.2. For cases where there is no cavitation in the flow field, this method converges rapidly (usually within 300 iterations). For cases of cavitation the number of iterations varies with the size of the cavitating region (ranges from 700-1500 iterations). In the cases of significant presence of cavitating regions, the method requires approximately five minutes of cpu time on a 486/25 MHz personal computer to arrive at a pressure distribution solution.

APPENDIX B

CALCULATION OF O-RING SPRING CONSTANT & PRELOAD

The O-ring at the inner radius of the floating seal face is modelled as a spring with a preload. This is done according to the work of Green and English [18]. In their work they developed correlations for the spring constant and preload based on the amount of compression in the O-ring, using finite element analysis. For this seal, the squeeze, x, in the O-ring is assumed to be 10%. The normalized force, $\overline{F}$, in the O-ring is

$$\overline{F}=ax^{b}+cx^{d} \qquad \text{(B.1)}$$

where,

$$\overline{F}=\frac{F}{\pi dDE} \qquad \text{(B.2)}$$

and coefficients a,b,c, and d are,

$$\begin{aligned} a&=1.03792 \\ b&=1.28710 \\ c&=7.77994 \\ d&=3.53400 \end{aligned} \qquad \text{(B.3)}$$

Similarly, the normalized spring stiffness, $\bar{K}$, is defined by the derivative of the force equation.

$$\bar{K}=abx^{b-1}+cdx^{d-1} \qquad \text{(B.4)}$$

where,

$$\bar{K}=\frac{k}{\pi DE} \qquad \text{(B.5)}$$

The O-ring is made of a Viton-70 elastomer, which has a modulus of 7.2 MPa (1,040 psi). From these equations the preload in the O-ring is 191.3 N (43 lbf). This is equivalent to 0.778 N per node (0.175 lbf/node) in the finite element mesh. The spring constant for the O-ring is 823 N/mm (4,700 lbf/in) or 20.1 N/mm per node (114.6 lbf/in node).

APPENDIX C

CALCULATION OF HEAT TRANSFER COEFFICIENTS

It is necessary to determine two heat transfer coefficients for the floating seal face in order to perform the thermal finite element analysis of the face. The first coefficient is for the surface at the outer radius of the seal. The method for determining this coefficient is based on work by Gazley [19] on heat transfer between rotating cylinders. The Reynolds number, R_e, for this case is defined by:

$$R_e = \frac{l_G U_R}{\nu} \qquad \text{(C.1)}$$

where l_G is the distance between the cylinders, U_R is the velocity of the rotating cylinder, and ν is the kinematic viscosity of the fluid. It is necessary to choose an operating speed to determine the Reynolds number. Since this method provides only an approximation for the heat transfer coefficient the operating speed of 400 rad/s is

chosen. This results in a Reynolds number of approximately 100,000. The skin-friction coefficient, c_f, is related to

the Reynolds number by the following expression:

$$\frac{1}{\sqrt{c_f}} = 2.04 + 1.768 \ln R_e \sqrt{c_f} \qquad \text{(C.2)}$$

$$c_f \sim 0.003 \qquad \text{(C.3)}$$

From the skin-friction coefficient, the Reynolds number, and the Prandtl number, Grazley [19] gives a correlation to find the Nusselt number, N_u. The Prandlt number, P_r, for water is approximately 8.

$$N_u = \frac{P_r R_e (c_f/2)^{1/2}}{5\left[P_r + \ln(1+5P_r) + \frac{1}{2}\ln\frac{R_e}{120}(c_f/2)^{1/2}\right]} \qquad \text{(C.4)}$$

From this expression the Nusselt number is approximately 520. The Nusselt number is related to the heat transfer coefficient by:

$$N_u = \frac{2 h_{od} l_g}{k} \qquad \text{(C.5)}$$

From this expression the value of h_{od} is found to be approximately 34,000 W/ m^2 °K (6,000 Btu/ hr ft^2 °F). This

value varies with rotational speed, but since it is an approximation it is used in analyzing all of the cases.

The second heat transfer coefficient is along the backside of the floating seal face. The heat transfer coefficient for this case is determined from the work of Kreith [20] on heat transfer from rotating disks. In this case the Reynolds number is

$$R_e = \frac{\omega r}{\nu} \tag{C.6}$$

Again, the rotational speed of 400 rad/s is chosen for ω. For the seal analyzed, the Reynolds number is approximately 1×10^6. The Nusselt number is determined from a graph (figure 30) given in Kreith [20]. From this graph the Nusselt number is determined to be 900, but this is for air as the fluid.

To determine the Nusselt number for water as the fluid, the following analogy is used.

$$N_u \propto P_r^{\frac{1}{3}} \tag{C.7}$$

$$\frac{N_{u_{water}}}{N_{u_{air}}} = \left(\frac{P_{r_{water}}}{P_{r_{air}}}\right)^{\frac{1}{3}} \tag{C.8}$$

From this analogy, the Nusselt number for water as the fluid

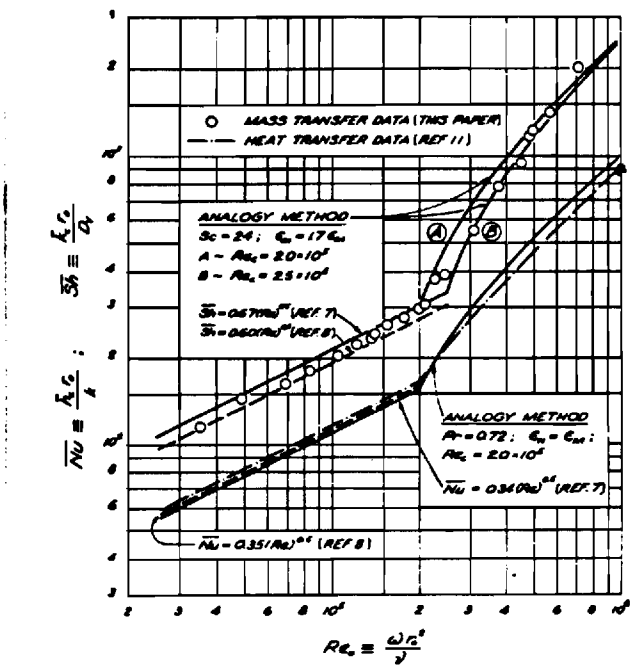

Fig. 3 Average Sherwood number and average Nusselt number as a function of rotational Reynolds number for a disk rotating in an infinite environment

Figure 31. Reynolds Number .vs. Nusselt Number for Rotating Disk [20].

is approximately 2,000, and the heat transfer coefficient is almost 22,700 W/ m^2 °K (4,000 Btu / hr ft^2 °F).

APPENDIX D

COMPUTER PROGRAM

```
************************************************
*
*     HISHAM HEGAB
*     3/11/91
*     PROGRAM FOR SOLUTION OF PRESSURE DISTRIBUTION
*     IN SEAL WITH HYDROPADS USING INFLUENCE
*     COEFFICIENTS FOR MECHANICAL & THERMAL
*     DEFORMATION - RELAX THICKNESS DISTRIBUTION
*
************************************************
*
*     VARIABLE LIST
*
*     A1() ---- MECHANICAL INFLUENCE COEFFICIENT MATRIX FOR
*               FACE 1
*     A2() ---- THERMAL INFLUENCE COEFFICIENT MATRIX FOR
*               FACE 1
*     A3() ---- MECHANICAL INFLUENCE COEFFICIENT MATRIX FOR
*               FACE 2
*     A4() ---- THERMAL INFLUENCE COEFFICIENT MATRIX FOR
*               FACE 2
*     ALPHA1 -- RELAXATION FACTOR FOR F
*     ALPHA2 -- RELAXATION FACTOR FOR PHI
*     AN ------ TERM IN REYNOLD'S GOVERNING EQT.
*     AS ------ TERM IN REYNOLD'S GOVERNING EQT.
*     AW ------ TERM IN REYNOLD'S GOVERNING EQT.
*     AE ------ TERM IN REYNOLD'S GOVERNING EQT.
*     ANG() --- ANGULAR POSITION OF NODES
*     CONV1 --- CONVERGENCE FOR PRESSURE FOR DEFORMATION
*               LOOP
*     CONV2 --- CONVERGENCE FOR OPENING & CLOSING FORCE
*     CONV ---- CONVERGENCE FOR PHI
*     COUNT --- # OF ITERATIONS OF REYNOLD'S EQT.
*     COUNT1 -- # OF ITERATIONS OF DEFORMATION LOOP
*     COUNT2 -- # OF ITERATIONS OF ADJUSTING HREF
*     DEPTH --- DEPTH OF HYDROPAD
*     DIF ----- CURRENT DIFFERENCE BETWEEN PHI & PHITEM
*     DIFF ---- CURRENT DIFFERENCE BETWEEN F & FTEM
```

```
*      DQIN ---- FLOW IN AT SINGLE NODE
*      DQOUT --- FLOW OUT AT SINGLE NODE
*      DR ------ DIFFERENTIAL RADIUS
*      DT ------ DIFFERENTIAL THETA
*      F() ----- CAVITATIN INDEX
*      FC ------ CLOSING FORCE
*      FO ------ OPENING FORCE
*      FLAG ---- FLAG FOR REYNOLD'S EQT. EXCEEDING MAX. # OF
*                ITERATIONS
*      FLAG2 --- FLAG FOR FILM THICKNESS GOING TO ZERO
*      FNEW() -- NEW VALUES FOR F()
*      FTEM() -- TEMPORARY VALUES FOR F()
*      GAMMA --- NONDIMENSIONAL PARAMETER IN GOVERNING EQT.
*      H() ----- DIMENSIONLESS FILM THICKNESS DISTRIBUTION
*      HDIF ---- MAXIMUM DIFFERENCE IN ITERATION FOR PHI
*      HDIFF --- MAXIMUM DIFFERENCE IN ITERATION FOR F
*      HREF ---- REFERENCE FILM THICKNESS
*      HTNEW() - HEAT GENERATION DISTRIBUTION
*      I ------- NODE # FOR CURRENT THETA LOCATION
*      J ------- NODE # FOR CURRENT RADIAL LOCATION
*      K() ----- CONDUCTIVITY DISTRIBUTION (R*H^3)
*      KE ------ TERM IN GOVERNING EQT.
*      KW ------ TERM IN GOVERNING EQT.
*      KS ------ TERM IN GOVERNING EQT.
*      KN ------ TERM IN GOVERNING EQT.
*      KSB ----- CONDUCTIVITY FOR FLOW AT INNER RADIUS
*      KNB ----- CONDUCTIVITY FOR FLOW AT OUTER RADIUS
*      L ------- DO LOOP VARIABLE FOR READING INFL. COEF.
*                MATRICES
*      LEAK ---- LEAKAGE RATE (DIMENSIONAL)
*      MAXIT --- MAXIMUM NUMBER ITERATION ALLOWED
*      MU ------ VISCOSITY
*      NR------- # OF NODES IN RADIAL DIRECTION
*      NT ------ # OF NODES IN THETA DIRECTION
*      NTD ----- NODE NUMBER OF THETA POSITION OF HYDROPAD
*      NRD ----- NODE NUMBER OF RADIAL POSITION OF HYDROPAD
*      NW------- # OF WAVES IN SEAL FACE
*      OMEGA --- ROTATIONAL SPEED OF SEAL
*      P() ----- CURRENT PRESSURE DISTRIBUTION (DIMENSIONAL)
*      PA ------ AMBIENT PRESSURE
*      PC ------ CAVITATION PRESSURE
*      PS ------ SEAL PRESSURE
*      PERC ---- PERCENT ERROR BETWEEN OPENING & CLOSING
*                FORCE
*      PHI() --- DIMENSIONLESS PRESSURE
*      PHITEM()- TEMPORARY VALUES FOR PHI()
*      PHINEW()- NEW VALUES FOR PHI()
*      PHII ---- PHI VALUE AT R=RI
*      PHIP ---- PHI VALUE USED IN DETERMINING FLOW
*      PHIN ---- PHI VALUE USED IN DETERMINING FLOW
*      PHIS ---- PHI VALUE USED IN DETERMINING FLOW
*      POLD()--- PREVIOUS PRESSURE DISTRIBUTION (DIMENSIONAL)
```

```
*      QIN ----- DIMENSIONLESS FLOW INTO SEAL
*      QOUT ---- DIMENSIONLESS FLOW OUT OF SEAL
*      R() ----- DIMENSIONLESS RADIUS AT RADIAL NODES
*      RI------- INNER RADIUS
*      RO------- OUTTER RADIUS
*      RELAX --- RELAXATION FACTOR ON PRESSURE FOR
*                DEFORMATION LOOP
*      SP ------ TERM IN GOVERNING EQT.
*      TEST ---- MAXIMUM DIFFERENCE IN PHI BETWEEN DEFORM.
*                ITERATIONS
*      TESTH --- MAXIMUM DIFFERENCE IN DIMENSIONLESS FILM
*                THICKNESS
*      TESTHT--- MAXIMUM DIFFERENCE IN DIMENSIONLESS HEAT
*                GENERATION
*      A() ---
*      B() ----- COEFFICIENTS USED FOR TDMA & CTDMA
*      C() ----- SUBROUTINES
*      D() ---
*
**************************************************
*
       IMPLICIT DOUBLE PRECISION (A-H,O-Z)
       DOUBLE PRECISION NB,MU,NW,MU2
       INTEGER COUNT,COUNT1,FLAG,COUNT2,FLAG2,START
       CHARACTER*12 NFIL
       DIMENSION H(41,11),P(41,11),A1(21,11,21,11),
     C A2(21,11,21,11),A3(21,11,21,11),A4(21,11,21,11),
     C PHI(41,11),R(11),ANG(41),F(41,11),HTNEW(41,11),
     C POLD(41,11),PS1(21,11),SP(21,11),
     C HOLD(41,11),HTOLD(41,11)
       OPEN(UNIT=10,FILE='CONV.DAT')
*
*      SET GOVERNING PARAMETERS FOR SEAL ANALYSIS
*
       COUNT1 = 0
       COUNT2 = 0
       CONV2 = 0.003D0
       PI = 3.14159
       MAXIT=2200
       FLAG = 0
       FLAG2 = 0
*
*      READ IN SEAL OPERATING CONDITIONS & GEOMETRY DATA
*
       CALL INDAT(NB,PS,PA,PC,OMEGA,MU2,RI,RO,NW,NR,NT,
     C NTD,NRD,HREF,NFIL,RELAX1,DEPTH,MAXIT2,START)
       MU = MU2 * 144.D0 * 32.2D0
*
*      DETERMINE DIMENSIONLESS PARAMETERS FROM GIVEN SEAL
*      CONDITIONS
*
       DR = (RO/RI - 1.D0)/DBLE(NR-1)
```

```
      DT = (2.0D0*PI/NW)/DBLE(NT-1)
      CONV1 = DT*DR/10.D0
      GAMMA=6.0D0*MU*OMEGA/(PS-PC)*RI**2.D0
     C /HREF**2./32.2D0/144.D0
      PHII = (PA-PC)/(PS-PC)
*
*     READ IN INFLUENCE COEFFICIENTS
*
      CALL INA(NT,NR,A1,A2,A3,A4,PS1,SP)
      WRITE(*,101)
101   FORMAT(' READ IN INFLUENCE COEFFICIENTS')
      IF (START.EQ.1) THEN
         CALL RESTART(NT,NR,P,PHI,H,F,PS,PC)
      ELSE
*
*     INITIALIZE PHI VALUES & SET BOUNDARY VALUES
*
      CALL PHIIN(NR,NT,PHI,PHII,NRD,NTD)
*
*     INITILIZE F VALUES
*
      CALL FINIT(F,NT,NR)
*
*     ASSUME INITIAL RIGID PROFILE FOR FILM THICKNESS
*     & ASSUME INITIAL HREF
*
      CALL HINIT (H,NT,NR,HREF,NRD,NTD,R,ANG,RI,RO,DT,DEPTH)
      WRITE(*,102)
102   FORMAT(' INITIALIZED FILM THICKNESS')
*
*     CALCULATE PRESSURE DISTRIBUTION USING REYNOLD'S EQT.
*
      WRITE(*,109) HREF,GAMMA
      WRITE(10,109) HREF,GAMMA
      CALL REYN(H,NT,NR,P,GAMMA,COUNT,CONV,ALPHA1,ALPHA2,
     C PS,PC,HDIF,HDIFF,R,F,PHI,QIN,QOUT,DT,DR,PHII,
     C NTD,NRD,MAXIT,FLAG)
      WRITE(*,103)
103   FORMAT(' SOLVED REYNOLDS EQUATION FOR INITIAL'
     C 'PRESSURE DISTRIBUTION')
      WRITE(*,113) COUNT
      WRITE(10,113) COUNT
      ENDIF
*
*     CALCULATE HEAT GENERATION FOR GIVEN FILM THICKNESS
*
      CALL HEAT(HTNEW,NT,NR,DT,DR,H,HREF,R,F,PHI)
      WRITE(*,104)
104   FORMAT(' CALCULATED HEAT DISTRIBUTION')
*
*     CALCULATE FILM THICKNESS USING INFLUENCE COEFFICIENTS
*
```

```
2       COUNT2 = COUNT2 + 1
3       DO 14 I=1,NT
        DO 14 J=1,NR
        HTOLD(I,J) = HTNEW(I,J)
14      HOLD(I,J) = H(I,J)
        TEST = 0.D0
        TESTH = 0.D0
        TESTHT = 0.D0
        CALL HINIT (H,NT,NR,HREF,NRD,NTD,R,ANG,RI,RO,DT,DEPTH)
        FLAG = 0
        FLAG2 = 0
        CALL DEFORM(P,NT,NR,HTNEW,HREF,H,A1,A2,A3,A4,R,RI,
     C DR,DT,FLAG2,PS1,PS,SP,NTD,NRD,MU,OMEGA)
        DO 50 I=1,NT
        DO 50 J=1,NR
        H(I,J) = RELAX1*H(I,J) + (1.D0-RELAX1)*HOLD(I,J)
        IF (H(I,J).LT.0) THEN
           WRITE(*,131)
           WRITE(10,131)
131        FORMAT(' SEALS ARE CONTACTING ')
           GOTO 200
        ENDIF
50      CONTINUE
*
*       STORE PRESSURE DISTRIBUTION FOR COMPARISON
*
        COUNT1 = COUNT1 + 1
        DO 12 I=1,NT
        DO 12 J=1,NR
12      POLD(I,J)=PHI(I,J)
*
*       CALCULATE HEAT GENERATION FOR NEW FILM THICKNESS
*
        CALL HEAT(HTNEW,NT,NR,DT,DR,H,HREF,R,F,PHI)
*
*       CALCULATE NEW PRESSURE DISTRIBUTION USING REYNOLDS
*           EQUATION
*
        CALL REYN(H,NT,NR,P,GAMMA,COUNT,CONV,ALPHA1,ALPHA2,
     C PS,PC,HDIF,HDIFF,R,F,PHI,QIN,QOUT,DT,DR,PHII,NTD,
     C NRD,MAXIT,FLAG)
        WRITE(*,113) COUNT
        WRITE(10,113) COUNT
113     FORMAT(' # OF ITERATIONS FOR CONVERGENCE REYN"S EQT.='
     C ,I4)
        IF (FLAG.EQ.1) WRITE(*,116)
116     FORMAT(' REYNOLD"S EQUATION EXCEEDED MAXIMUM # OF'
     C 'ITERATIONS')
        IF (FLAG.EQ.1) GOTO 200
*
*       COMPARE NEW & OLD PRESSURE IF NOT EQUAL RELAX PRESSURE
*       & RECALCULATE NEW FILM THICKNESS
```

```
*
      DO 40 I=1,NT-1
      DO 40 J=1,NR
      DIF = DABS(PHI(I,J)-POLD(I,J))
      DIFH = DABS(H(I,J)-HOLD(I,J))
      DIFHT = DABS(HTNEW(I,J)-HTOLD(I,J))
      IF (DIF.GT.TEST) TEST = DIF
      IF (DIFH.GT.TESTH) TESTH = DIFH
      IF (DIFHT.GT.TESTHT) TESTHT = DIFHT
40    CONTINUE
      WRITE(*,1200) COUNT1,TEST
      WRITE(*,1201) TESTH,TESTHT
      WRITE(10,1200) COUNT1,TEST
      WRITE(10,1201) TESTH,TESTHT
1200  FORMAT(' ITERATION # ',I3,' MAX. DIFFERENCE PHI='
     C ,E15.8)
1201  FORMAT(' MAX. DIFFERENCE H = ',E15.8,' MAX.
     C ' DIFFERENCE HT = ',E15.8)
      IF (COUNT1.GT.1000) GOTO 200
      IF (TEST.GT.CONV1.OR.TESTH.GT.CONV1.OR.
     C TESTHT.GT.CONV1) THEN
         GOTO 3
      ENDIF
*
*     CALCULATE OPENING FORCE
*
157   FO = 0.D0
      DO 10 I=1,NT-1
      DO 10 J=2,NR-1
10    FO = FO + P(I,J)*R(J)*DR*DT*RI**2.D0
      DO 20 I=1,NT-1
      FO = FO+ P(I,NR)*(R(NR)+R(NR-1))*DR*DT*RI**2.D0*0.25D0
20    FO = FO + P(I,1)*(R(1)+R(2))*DR*DT*RI**2.D0*0.25D0
      FO = FO * NW
      FC = NB*(PS-PA)*PI*(RO**2.D0-RI**2.D0)
      WRITE(*,107) FO,FC
      WRITE(10,107) FO,FC
      WRITE(*,108) COUNT2
      WRITE(10,108) COUNT2
107   FORMAT(' OPENING FORCE = ',E15.8,5X,'CLOSING FORCE ='
     C ,E15.8)
108   FORMAT(' ITERATION # FOR ADJUSTING HREF ',I3)
*
*     COMPARE OPENING & CLOSING FORCE
*     IF NOT EQUAL ADJUST HREF & CALCULATE NEW FILM
*     THICKNESS
*
      PERC = ABS(FO-FC)/FC
      IF (PERC.LT.CONV2) GOTO 200
      IF (COUNT2.GT.MAXIT2) GOTO 200
      IF (PERC.LT.0.04D0) THEN
         HREF = HREF + 0.50D0*(FO-FC)/FC*HREF
```

```
      ELSEIF (PERC.LT.0.10D0) THEN
         HREF = HREF + 0.75D0*(FO-FC)/FC*HREF
      ELSEIF (PERC.LT.0.25D0) THEN
         HREF = HREF + 0.85D0*(FO-FC)/FC*HREF
      ELSEIF (PERC.LT.0.5D0) THEN
         HREF = HREF + 1.00D0*(FO-FC)/FC*HREF
      ELSE
         HREF = HREF + 1.25D0*(FO-FC)/FC*HREF
      ENDIF
      GAMMA = 6.0D0*MU*OMEGA/(PS-PC)*RI**2.D0
     C /HREF**2.D0/144.D0/32.2D0
      WRITE(*,109) HREF,GAMMA
      WRITE(10,109) HREF,GAMMA
109   FORMAT(' NEW HREF = ',E15.8,5X,'NEW GAMMA = ',E14.8)
      COUNT1 = 0
      GOTO 2
*
*     OUTPUT SOLUTION
*
200   CALL HVAL(NR,NT,H,HMIN,HAVE,NRD,NTD,HAVERI)
      CALL OUTDAT(COUNT,CONV,ALPHA1,ALPHA2,NR,NT,HDIF,HDIFF,
     C GAMMA,RI,RO,ANG,R,H,F,PHI,PC,PS,QIN,QOUT,NFIL,
     C COUNT1,FO,FC,HREF,TEST,COUNT2,OMEGA,MU2,PA,NW,
     C NB,RELAX1,P,HMIN,HAVE,HAVERI,MU,TESTHT,TESTH,HTNEW)
      END
*
*
*     SUBROUTINES
*
*
      SUBROUTINE REYN(H,NT,NR,P,GAMMA,COUNT,CONV,ALPHA1,
     C ALPHA2,PS,PC,HDIF,HDIFF,R,F,PHI,QIN,QOUT,DT,DR,
     C PHII,NTD,NRD,MAXIT,FLAG)
      IMPLICIT DOUBLE PRECISION (A-H,O-Z)
      DOUBLE PRECISION KE,KN,KW,KS,K(41,11)
      INTEGER COUNT,FLAG
      DIMENSION PHI(41,11),H(41,11),F(41,11),R(11),P(41,11),
     C PHITEM(41,11),A(41),B(41),C(41),D(41),FTEM(41,11),
     C FNEW(41,11),PHINEW(41,11)
*
*     SET GOVERNING PARAMETERS FOR SEAL
*
      ALPHA1 = 0.01D0
      ALPHA2 = 0.2D0
      CONV = DT*DR/10.D0
      COUNT = 0
*
*     SET FILM THICKNESS
*
      CALL HK(NT,NR,K,H,R)
*
*     START LOOP FOR SOLVE PRESSURE DISTRIBUTION USING ADI
```

```
*
5       HDIF = 0.D0
        HDIFF = 0.D0
        COUNT = COUNT + 1
*
*       ENTER LOOP TO COVER GRID, 1 COLUMN AT A TIME
*
        DO 10 I=1,NT-1
*
*       SET COEFFICIENTS FOR TDMA AT INNER & OUTTER RADIUS
*
        A(1) = 0.D0
        B(1) = 1.D0
        C(1) = 0.D0
        D(1) = 1.D0
        A(NR) = 0.D0
        B(NR) = 1.D0
        C(NR) = 0.D0
        IF (I.EQ.1) THEN
        D(NR)=((1.D0-F(I,NR-1))*((PHI(NT-1,NR)+1.D0)
      C *H(NT-1,NR)/R(NR)/DT-H(I,NR)/R(NR)/DT) +
      C  F(I,NR-1)*PHII)/((1.D0-F(I,NR-1))*H(I,NR)/
      C R(NR)/DT + F(I,NR-1))
        ELSE
        D(NR)=((1.D0-F(I,NR-1))*((PHI(I-1,NR)+1.D0)*
      C H(I-1,NR)/R(NR)/DT-H(I,NR)/R(NR)/DT) +
      C F(I,NR-1)*PHII)/((1.D0-F(I,NR-1))*H(I,NR)/
      C R(NR)/DT + F(I,NR-1))
        ENDIF
*
*       START LOOP TO DETERMINE COEFFICIENT FOR TDMA FOR
*       INTERIOR NODES
*
        DO 20 J=2,NR-1
*
*       DETERMINE TERMS IN GOVERNING NODAL EQUATIONS
*
          KE = 2.D0*K(I+1,J)*K(I,J)/(K(I+1,J)+K(I,J))
          HE = .5D0*(H(I,J)+H(I+1,J))
          IF (I.EQ.1) THEN
            KW = 2.D0*K(NT-1,J)*K(I,J)/(K(NT-1,J)+K(I,J))
            HW = .5D0*(H(I,J)+H(NT-1,J))
            SP = -GAMMA*R(J)*DR*(HE-(1.D0+(1.D0-F(NT-1,J))
      C          *PHI(NT-1,J))*HW)
          ELSE
            KW = 2.D0*K(I-1,J)*K(I,J)/(K(I-1,J)+K(I,J))
            HW = .5D0*(H(I,J)+H(I-1,J))
            SP =-GAMMA*R(J)*DR*(HE-(1.D0+(1.D0-F(I-1,J))
      C         *PHI(I-1,J))*HW)
          ENDIF
          KS = 2.D0*K(I,J+1)*K(I,J)/(K(I,J+1)+K(I,J))
          KN = 2.D0*K(I,J-1)*K(I,J)/(K(I,J-1)+K(I,J))
```

```
         AN = KN*DT/DR
         AS = KS*DT/DR
         AW = KW*DR/DT/R(J)**2.D0
         AE = KE*DR/DT/R(J)**2.D0
*
*       SET COEFFICIENTS FOR TDMA
*
         A(J) = -AN*F(I,J-1)
         B(J) = F(I,J)*(AN+AS+AE+AW)+
     C          GAMMA*R(J)*(1.D0-F(I,J))*HE*DR
         C(J) = -AS*F(I,J+1)
         IF (I.EQ.1) THEN
           D(J) = AE*F(I+1,J)*PHI(I+1,J)+AW*F(NT-1,J)
     C            *PHI(NT-1,J)+SP
         ELSE
           D(J) = AE*F(I+1,J)*PHI(I+1,J)+AW*F(I-1,J)*
     C            PHI(I-1,J) + SP
         ENDIF
20     CONTINUE
       IF (I.LE.NTD.OR.I.GE.NT-NTD+1) THEN
          DO 19 J=2,NRD
            A(J) = 0.D0
            B(J) = 1.D0
            C(J) = 0.D0
            D(J) = 1.D0
19        CONTINUE
       ENDIF
*
*      CALL TRIDIAGONAL MATRIX SOLVER
*
       CALL TDMA(I,NR,A,B,C,D,PHITEM)
*
*      DETERMINE TEMPORARY VALUES OF F FOR VALUES OF PHI FROM
*      TDMA
*
       DO 30 J=2,NR
         IF (PHITEM(I,J).GE.0.D0) THEN
            FTEM(I,J)=1.D0
         ELSE
            FTEM(I,J)=0.D0
         ENDIF
30     CONTINUE
*
*      RELAX PHI & F AND CHECK FOR MAXIMUM DIFFERENCE FOR
*      ITERATION
*
       DO 40 J=2,NR
         PHINEW(I,J)=ALPHA2*PHITEM(I,J)+
     C               (1.D0-ALPHA2)*PHI(I,J)
         FNEW(I,J)=ALPHA1*FTEM(I,J)+(1.D0-ALPHA1)*F(I,J)
         DIF = DABS(PHINEW(I,J)-PHI(I,J))
         IF (DIF.GT.HDIF) HDIF = DIF
```

```
          DIFF = DABS(FNEW(I,J)-F(I,J))
          IF (DIFF.GT.HDIFF) HDIFF=DIFF
          PHI(I,J)=PHINEW(I,J)
          F(I,J)=FNEW(I,J)
40      CONTINUE
10      CONTINUE
*
*       SET PHI & F VALUES AT NODES ON THETA (MAX) EQUAL
*       TO NODES AT THETA EQUAL ZERO DEGREES
*
        DO 11 J=1,NR
        PHI(NT,J)=PHI(1,J)
11      F(NT,J)=F(1,J)
*
*       ENTER LOOP TO COVER GRID, 1 ROW AT A TIME
*
        DO 50 J=2,NR-1
*
*       START LOOP TO DETERMINE COEFFICIENTS FOR CTDMA
*
          DO 60 I=1,NT-1
*
*       DETERMINE TERMS IN GOVERNING NODAL EQUATIONS FOR CTDMA
*
          KE = 2.D0*K(I+1,J)*K(I,J)/(K(I+1,J)+K(I,J))
          IF (I.EQ.1) THEN
             KW = 2.D0*K(NT-1,J)*K(I,J)/(K(NT-1,J)+K(I,J))
          ELSE
             KW = 2.D0*K(I-1,J)*K(I,J)/(K(I-1,J)+K(I,J))
          ENDIF
          KS = 2.D0*K(I,J+1)*K(I,J)/(K(I,J+1)+K(I,J))
          KN = 2.D0*K(I,J-1)*K(I,J)/(K(I,J-1)+K(I,J))
          AN = KN*DT/DR
          AS = KS*DT/DR
          AW = KW*DR/DT/R(J)**2.D0
          AE = KE*DR/DT/R(J)**2.D0
          HE = .5D0*(H(I,J)+H(I+1,J))
          IF (I.EQ.1) THEN
            HW = 0.5D0*(H(I,J)+H(NT-1,J))
          ELSE
            HW = .5D0*(H(I,J)+H(I-1,J))
          ENDIF
          SP = -GAMMA*R(J)*DR*(HE-HW)
*
*         SET COEFFICIENTS FOR CTDMA
*
          IF (J.GT.NRD) THEN
            A(I) = F(I,J)*(AN+AW+AS+AE)+
     C             GAMMA*R(J)*(1.D0-F(I,J))*HE*DR
            B(I) = AE*F(I+1,J)
             IF (I.EQ.1) THEN
            C(I) = AW*F(NT-1,J)+GAMMA*R(J)*DR*
```

```
C            (1.D0-F(NT-1,J))*HW
          ELSE
            C(I) = AW*F(I-1,J)+GAMMA*R(J)*DR*
C            (1.D0-F(I-1,J))*HW
          ENDIF
            D(I) = SP + AS*F(I,J+1)*PHI(I,J+1) +
C            AN*F(I,J-1)*PHI(I,J-1)
        ELSE
          IF (I.LE.NTD.OR.I.GE.NT-NTD+1) THEN
             A(I) = 0.D0
             B(I) = 1.D0
             C(I) = 0.D0
             D(I) = 1.D0
             A(NT) = 0.D0
             B(NT) = 1.D0
             C(NT) = 0.D0
             D(NT) = 1.D0
          ELSE
            A(I) = -AW*F(I-1,J)-GAMMA*R(J)*DR*
C              (1.D0-F(I-1,J))*HW
            B(I) = F(I,J)*(AN+AW+AS+AE)+GAMMA*
C              R(J)*(1.D0-F(I,J))*HE*DR
            C(I) = -AE*F(I+1,J)
            D(I) = AN*F(I,J-1)*PHI(I,J-1) +
C              AS*F(I,J+1)*PHI(I,J+1)+ SP
          ENDIF
        ENDIF
60      CONTINUE
*
*       CALL CIRCULAR TRIDIAGONAL MATRIX SOLVER
*
        IF (J.GT.NRD) THEN
           CALL CTDMA(J,NT,A,B,C,D,PHITEM)
        ELSE
           CALL TDMA2(J,NT,A,B,C,D,PHITEM)
           PHITEM(NT,J)=1.D0
        ENDIF
*
*       DETERMINE TEMPORARY VALUES OF F BASED ON PHI VALUES
*       FROM CTDMA
*
        DO 70 I=1,NT
          IF (PHITEM(I,J).GE.0.D0) THEN
             FTEM(I,J)=1.D0
          ELSE
             FTEM(I,J)=0.D0
          ENDIF
70      CONTINUE
*
*       RELAX PHI & F AND CHECK FOR MAXIMUM DIFFERENCE FOR
*       ITERATION
*
```

```
         DO 80 I=1,NT
           PHINEW(I,J)=ALPHA2*PHITEM(I,J)+
     C                 (1.D0-ALPHA2)*PHI(I,J)
           FNEW(I,J)=ALPHA1*FTEM(I,J)+(1.D0-ALPHA1)*F(I,J)
           DIF = DABS(PHINEW(I,J)-PHI(I,J))
           IF (DIF.GT.HDIF) HDIF=DIF
           DIFF = DABS(FNEW(I,J)-F(I,J))
           IF (DIFF.GT.HDIFF) HDIFF=DIF
           PHI(I,J) = PHINEW(I,J)
           F(I,J)=FNEW(I,J)
80       CONTINUE
50     CONTINUE
*
*      CHECK FOR CONVERGENCE OF SOLUTION
*
       IF (COUNT.GT.MAXIT) THEN
          IF (HDIF.GT.CONV.OR.HDIFF.GT.0.01D0) FLAG = 1
          GOTO 7
       ENDIF
       IF (HDIF.GT.CONV.OR.HDIFF.GT.CONV) GOTO 5
7      CALL Q(K,PHI,NT,NR,QIN,QOUT,DT,DR,NRD)
       DO 160 I=1,NT
       DO 160 J=1,NR
       IF (PHI(I,J).GT.0) THEN
          P(I,J) = PHI(I,J)*(PS-PC) + PC
       ELSE
          P(I,J) = PC
       ENDIF
160    CONTINUE
999    FORMAT(E15.8,3X,E15.8)
       END
       SUBROUTINE OUTDAT(COUNT,CONV,ALPHA1,ALPHA2,NR,NT,HDIF,
     C HDIFF,GAMMA,RI,RO,ANG,R,H,F,PHI,PC,PS,QIN,QOUT,
     C NFIL,COUNT1,FO,FC,HREF,TEST,COUNT2,OMEGA,MU2,PA,NW,
     C NB,RELAX1,P,HMIN,HAVE,HAVERI,MU,TESTHT,TESTH,HTNEW)
       IMPLICIT DOUBLE PRECISION (A-H,O-Z)
       INTEGER COUNT,COUNT1,COUNT2
       DOUBLE PRECISION MU2,LEAK,NB,NW,MU
       CHARACTER*12 NFIL
       DIMENSION PHI(41,11),F(41,11),R(11),ANG(41),H(41,11),
     C P(41,11),HTNEW(41,11)
       OPEN(UNIT=7,FILE=NFIL)
       OPEN(UNIT=8,FILE='PLOTP.FIL')
       OPEN(UNIT=9,FILE='PLOTHT.FIL')
       OPEN(UNIT=11,FILE='PLOTF.FIL')
       OPEN(UNIT=12,FILE='PLOTHR.FIL')
       OPEN(UNIT=13,FILE='PLOTH.FIL')
       OPEN(UNIT=14,FILE='RESTART.FIL')
       OPEN(UNIT=15,FILE='HTGEN.FIL')
       DO 3 I=1,NT
       DO 3 J=1,NR
       WRITE(14,996) PHI(I,J)
```

```
      WRITE(14,996) H(I,J)
3     WRITE(14,996) F(I,J)
996   FORMAT(E15.8)
*
*     OUTPUT SOLUTION
*
      WRITE(7,1000)
1000  FORMAT(10X,'SOLUTION OF PRESSURE FIELD IN RADIAL
     C SEAL')
      WRITE(7,1010)
1010  FORMAT('')
      WRITE(7,1019) NB
      WRITE(7,1021) PS
      WRITE(7,1022) PA
      WRITE(7,1023) PC
      WRITE(7,1030) COUNT
      WRITE(7,1040) CONV
      WRITE(7,1050) ALPHA1
      WRITE(7,1055) ALPHA2
      WRITE(7,1056) RELAX1
      WRITE(7,1060) NR,NT
      WRITE(7,1080) HDIF,HDIFF
      WRITE(7,1090) GAMMA
      WRITE(7,1092) MU2
      WRITE(7,1091) OMEGA
      WRITE(7,1200) RI
      WRITE(7,1210) RO
      WRITE(7,1490) QIN
      WRITE(7,1495) QOUT
      LEAK = (PS-PC)*HREF**3.D0/12.D0/MU*32.2D0*
     C 144.D0*60.D0*NW*QOUT*2.54D0**3.D0
      WRITE(7,1496) LEAK
      WRITE(7,1510) FO
      WRITE(7,1520) FC
      WRITE(7,1525) HREF
      WRITE(7,1529) HREF*2.54D0*1.D06/100.D0
      WRITE(7,1526) HMIN*HREF*2.54D0*1.D06/100.D0
      WRITE(7,1527) HAVE*HREF*2.54D0*1.D06/100.D0
      WRITE(7,1528) HAVERI*HREF*2.54D0*1.D06/100.D0
      WRITE(7,1530) COUNT1
      WRITE(7,1540) TEST
      WRITE(7,1541) TESTHT
      WRITE(7,1542) TESTH
      WRITE(7,1550) COUNT2
1019  FORMAT('BALANCE RATIO = ',F7.5)
1496  FORMAT('LEAKAGE RATE = ',E15.8,' CM^3/MIN')
1021  FORMAT('SEAL PRESSURE = ',F9.4,' PSI')
1022  FORMAT('AMBIENT PRESSURE = ',F9.4,' PSI')
1023  FORMAT('CAVITATION PRESSURE = ',F9.4,' PSI')
1550  FORMAT('# OF ITERATIONS OF ADJUSTING HREF = ',I3)
1540  FORMAT('MAXIMUM DIFFERENCE IN PHI BETWEEN DEFORMATION'
     C ' ANAL. = ',E15.8)
```

```
1541  FORMAT('MAXIMUM DIFFERENCE IN HT BETWEEN DEFORMATION'
     C ' ANAL. = ',E15.8)
1542  FORMAT('MAXIMUM DIFFERENCE IN H BETWEEN DEFORMATION'
     C ' ANAL. = ',E15.8)
1510  FORMAT('OPENING FORCE = ',E15.8,' LBF')
1520  FORMAT('CLOSING FORCE = ',E15.8,' LBF')
1525  FORMAT('HREF = ',E15.8,' IN')
1526  FORMAT('HMIN = ',E15.8,' 10^-6 METERS')
1527  FORMAT('HAVE = ',E15.8,' 10^-6 METERS')
1529  FORMAT('HREF = ',E15.8,' 10^-6 METERS')
1528  FORMAT('HAVE @ RI = ',E15.8,' 10^-6 METERS')
1530  FORMAT('NUMBER OF ITERATIONS OF DEFORMATION ANALYSIS =
     C ',I3)
1490  FORMAT('QIN = ',E15.8)
1495  FORMAT('QOUT = ',E15.8)
1200  FORMAT('INNER RADIUS = ',F7.4,' IN    ')
1210  FORMAT('OUTER RADIUS = ',F7.4,' IN  ')
1030  FORMAT('NUMBER OF ITERATIONS IN REYNOLD"S EQT. = ',I4)
1040  FORMAT('CONVERGENCE FOR REYNOLD"S EQT. = ',E8.2)
1050  FORMAT('RELAXATION FACTOR FOR F = ',F4.2)
1055  FORMAT('RELAXATION FACTOR FOR PHI = ',F4.2)
1056  FORMAT('RELAXATION FACTOR ON FILM THICKNESS = ',F4.2)
1060  FORMAT('# RADIAL NODES = ',I2,10X,' # OF THETA NODES =
     C ',I2)
1080  FORMAT('MAXIMUM DIFFERENCE IN PHI = ',E10.4,10X,' IN F
     C = ',E10.4)
1090  FORMAT('GAMMA = ',E15.8)
1091  FORMAT('ROTATIONAL SPEED = ',F9.3,' RAD/S')
1092  FORMAT('VISCOSITY = ',E10.4,' REYN')
      WRITE(7,1010)
      WRITE(7,1300)
      WRITE(7,1010)
1300  FORMAT(10X,'DIMENSIONLESS FILM THICKNESS')
      WRITE(7,1010)
      DO 210 I=1,NT-1,4
      IF (I+1.GT.NT) THEN
         WRITE(7,1100) ANG(I)
      ELSEIF (I+2.GT.NT) THEN
         WRITE(7,1100) ANG(I),ANG(I+1)
      ELSEIF (I+3.GT.NT) THEN
         WRITE(7,1100) ANG(I),ANG(I+1),ANG(I+2)
      ELSE
         WRITE(7,1100) ANG(I),ANG(I+1),ANG(I+2),ANG(I+3)
      ENDIF
      WRITE(7,1010)
      DO 220 J=1,NR,1
      IF (I+1.GT.NT) THEN
         WRITE(7,1110) R(J),H(I,J)
      ELSEIF (I+2.GT.NT) THEN
         WRITE(7,1110) R(J),H(I,J),H(I+1,J)
      ELSEIF (I+3.GT.NT) THEN
         WRITE(7,1110) R(J),H(I,J),H(I+1,J),H(I+2,J)
```

```
      ELSE
        WRITE(7,1110) R(J),H(I,J),H(I+1,J),H(I+2,J),H(I+3,J)
      ENDIF
220   CONTINUE
      WRITE(7,1010)
210   CONTINUE
      WRITE(7,1010)
      WRITE(7,1020)
1020  FORMAT(10X,'DIMENSIONLESS PHI VALUES')
      WRITE(7,1010)
      DO 110 I=1,NT-1,4
      IF (I+1.GT.NT) THEN
         WRITE(7,1100) ANG(I)
      ELSEIF (I+2.GT.NT) THEN
         WRITE(7,1100) ANG(I),ANG(I+1)
      ELSEIF (I+3.GT.NT) THEN
         WRITE(7,1100) ANG(I),ANG(I+1),ANG(I+2)
      ELSE
         WRITE(7,1100) ANG(I),ANG(I+1),ANG(I+2),ANG(I+3)
      ENDIF
1100  FORMAT('RADIUS',6X,4(F5.2,13X))
1101  FORMAT('0',4(',',F5.2))
      WRITE(7,1010)
      DO 120 J=1,NR,1
      IF (I+1.GT.NT) THEN
         WRITE(7,1110) R(J),PHI(I,J)
      ELSEIF (I+2.GT.NT) THEN
         WRITE(7,1110) R(J),PHI(I,J),PHI(I+1,J)
      ELSEIF (I+3.GT.NT) THEN
         WRITE(7,1110) R(J),PHI(I,J),PHI(I+1,J),PHI(I+2,J)
      ELSE
         WRITE(7,1110) R(J),PHI(I,J),PHI(I+1,J),
     C                 PHI(I+2,J),PHI(I+3,J)
      ENDIF
1110  FORMAT(F6.4,1X,4(E15.8,3X))
120   CONTINUE
      WRITE(7,1010)
110   CONTINUE
      WRITE(7,1010)
      WRITE(7,1120)
1120  FORMAT(10X,'VALUES FOR F')
      WRITE(7,1010)
      DO 130 I=1,NT-1,4
      IF (I+1.GT.NT) THEN
         WRITE(7,1100) ANG(I)
      ELSEIF (I+2.GT.NT) THEN
         WRITE(7,1100) ANG(I),ANG(I+1)
      ELSEIF (I+3.GT.NT) THEN
         WRITE(7,1100) ANG(I),ANG(I+1),ANG(I+2)
      ELSE
         WRITE(7,1100) ANG(I),ANG(I+1),ANG(I+2),ANG(I+3)
      ENDIF
```

```
      WRITE(7,1010)
      DO 140 J=1,NR,1
      IF (I+1.GT.NT) THEN
         WRITE(7,1130) R(J),F(I,J)
      ELSEIF (I+2.GT.NT) THEN
         WRITE(7,1130) R(J),F(I,J),F(I+1,J)
      ELSEIF (I+3.GT.NT) THEN
         WRITE(7,1130) R(J),F(I,J),F(I+1,J),F(I+2,J)
      ELSE
        WRITE(7,1130) R(J),F(I,J),F(I+1,J),F(I+2,J),F(I+3,J)
      ENDIF
1130  FORMAT(F6.4,4X,4(F8.4,10X))
140   CONTINUE
      WRITE(7,1010)
130   CONTINUE
      WRITE(7,1230)
1230  FORMAT(10X,'VALUES FOR P IN psia')
      WRITE(7,1010)
      DO 150 I=1,NT-1,4
        IF (I+1.GT.NT) THEN
           WRITE(7,1100) ANG(I)
        ELSEIF (I+2.GT.NT) THEN
           WRITE(7,1100) ANG(I),ANG(I+1)
        ELSEIF (I+3.GT.NT) THEN
           WRITE(7,1100) ANG(I),ANG(I+1),ANG(I+2)
        ELSE
           WRITE(7,1100) ANG(I),ANG(I+1),ANG(I+2),ANG(I+3)
        ENDIF
        WRITE(7,1010)
        DO 160 J=1,NR,1
        IF (I+1.GT.NT) THEN
           WRITE(7,1110) R(J),P(I,J)
        ELSEIF (I+2.GT.NT) THEN
           WRITE(7,1110) R(J),P(I,J),P(I+1,J)
        ELSEIF (I+3.GT.NT) THEN
           WRITE(7,1110) R(J),P(I,J),P(I+1,J),P(I+2,J)
        ELSE
           WRITE(7,1110) R(J),P(I,J),P(I+1,J),
     C                   P(I+2,J),P(I+3,J)
        ENDIF
1111    FORMAT(F6.4,',',4(E15.8,','))
160     CONTINUE
      WRITE(7,1010)
150   CONTINUE
      HREF3 = HREF * 1.D06 * 2.54 / 100.D0
      DO 351 I=1,NT
      WRITE(9,2501) ANG(I),HREF3*H(I,1),HREF3*
     C H(I,INT(NR/2.D0)+1),HREF3*H(I,NR),HREF3*H(I,3),
     C HREF3*H(I,8)
      DO 351 J=1,NR
      IF (I.EQ.INT(NT/2.D0)+1) WRITE(12,2502) R(J)*RI,
     C HREF3*H(I,J)
```

```
      WRITE(15,2500) ANG(I),R(J)*RI,HTNEW(I,J)*MU*
     C OMEGA**2.D0/HREF/32.2D0/12.D0**3.D0/778.D0*
     C 3600.D0*RI**4.D0
      WRITE(11,2500) ANG(I),R(J)*RI,F(I,J)
      WRITE(13,2500) ANG(I),R(J)*RI,H(I,J)*HREF3
351   WRITE(8,2500) ANG(I),R(J)*RI,P(I,J)
2501  FORMAT(F5.2,',',5(E13.8,','))
2500  FORMAT(F5.2,',',F6.4,',',E13.8)
2502  FORMAT(F6.4,',',E13.8)
      RETURN
      END
      SUBROUTINE HK(NT,NR,K,H,R)
*
*     SUBROUTINE FOR SETTING FILM THICKNESS
*
      IMPLICIT DOUBLE PRECISION (A-H,O-Z,K)
      DIMENSION K(41,11),H(41,11),R(11)
      DO 50 I=1,NT
      DO 50 J=1,NR
50    K(I,J) = R(J)*H(I,J)**3.D0
      RETURN
      END
      SUBROUTINE FINIT(F,NT,NR)
*
*     SUBROUTINE FOR INITIALIZING F VALUES
*
      IMPLICIT DOUBLE PRECISION (A-H,O-Z)
      DIMENSION F(41,11)
      DO 20 I=1,NT
      DO 20 J=1,NR
20    F(I,J) = 1.D0
      RETURN
      END
      SUBROUTINE PHIIN(NR,NT,PHI,PHII,NRD,NTD)
*
*     SUBROUTINE FOR INITIALIZING PHI VALUES
*
      IMPLICIT DOUBLE PRECISION (A-H,O-Z)
      DIMENSION PHI(41,11)
      DO 10 I=1,NT
      PHI(I,NR)=PHII
      PHI(I,1)=1.D0
      DO 10 J=2,NR-1
10    PHI(I,J)=1.D0 - DBLE(J-1)/DBLE(NR-1)
      DO 30 I=1,NTD
      DO 20 J=2,NRD
      PHI(NT-I+1,J) = 1.D0
20    PHI(I,J)=1.D0
      DO 30 J=NRD+1,NR
      PHI(NT-I+1,J) = 1.D0 - DBLE(J-NRD)/DBLE(NR-NRD)
30    PHI(I,J) = 1.D0 - DBLE(J-NRD)/DBLE(NR-NRD)
      RETURN
```

```
      END
      SUBROUTINE TDMA2(J,NT,A,B,C,D,PHITEM)
*
*     CALCULATE PHITEM IN THE JTH ROW USING TDMA ALGORITHM
*
      IMPLICIT DOUBLE PRECISION (A-H,O-Z)
      DIMENSION A(41),B(41),C(41),D(41),PHITEM(41,11)
      DO 5 I=2,NT
      Q = A(I)/B(I-1)
      B(I) = B(I)-C(I-1)*Q
5     D(I) = D(I) - D(I-1)*Q
*
*     BACK SUBSTITUTION
*
      PHITEM(NT,J) = D(NT)/B(NT)
      DO 6 I=1,NT-1
      K=NT-I
6     PHITEM(K,J) = (D(K)-C(K)*PHITEM(K+1,J))/B(K)
      RETURN
      END
      SUBROUTINE TDMA(I,NR,A,B,C,D,PHITEM)
*
*     CALCULATE PHITEM IN THE ITH COLUMN USING TDMA
*     ALGORITHM
*
      IMPLICIT DOUBLE PRECISION (A-H,O-Z)
      DIMENSION A(41),B(41),C(41),D(41),PHITEM(41,11)
      DO 5 J=2,NR
      Q = A(J)/B(J-1)
      B(J) =B(J)-C(J-1)*Q
5     D(J)=D(J)-D(J-1)*Q
*
*     BACK SUBSTITUTION
*
      PHITEM(I,NR)=D(NR)/B(NR)
      DO 6 J=1,NR-1
      K=NR-J
6     PHITEM(I,K)=(D(K)-C(K)*PHITEM(I,K+1))/B(K)
      RETURN
      END
      SUBROUTINE CTDMA(J,NT,A,B,C,D,PHITEM)
*
*     CALCULATE PHITEM IN THE JTH ROW USING CTDMA ALGORITHM
*
      IMPLICIT DOUBLE PRECISION (A-H,O-Z)
      DIMENSION PHITEM(41,11),A(41),B(41),C(41),D(41),E(41),
     C F(41),G(41),P(41),Q(41),R(41)
*
*     DECOMPOSITION AND FORWARD SUBSTITUTION
*
      E(1)=B(1)/A(1)
      F(1)=C(1)/A(1)
```

```
      G(1)=D(1)/A(1)
      DO 5 I=2,NT-2
        E(I)=B(I)/(A(I)-C(I)*E(I-1))
        F(I)=C(I)*F(I-1)/(A(I)-C(I)*E(I-1))
        G(I)=(D(I)+C(I)*G(I-1))/(A(I)-C(I)*E(I-1))
5     CONTINUE
      P(1)=A(NT-1)
      Q(1)=B(NT-1)
      R(1)=D(NT-1)
      DO 10 I=2,NT
        P(I)=P(I-1)-Q(I-1)*F(I-1)
        Q(I)=Q(I-1)*E(I-1)
        R(I)=R(I-1)+Q(I-1)*G(I-1)
10    CONTINUE
*
*     BACKWARD SUBSTITUTION
*
      PHITEM(NT-1,J)=((Q(NT-2)+C(NT-1))*G(NT-2)+
     C R(NT-2))/(P(NT-2)-(Q(NT-2)+C(NT-1))*
     C (E(NT-2)+F(NT-2)))
      DO 30 I=NT-2,1,-1
        PHITEM(I,J)=E(I)*PHITEM(I+1,J)+F(I)*
     C PHITEM(NT-1,J)+G(I)
30    CONTINUE
      PHITEM(NT,J)=PHITEM(1,J)
      RETURN
      END
      SUBROUTINE Q(K,PHI,NT,NR,QIN,QOUT,DT,DR,NRD)
      IMPLICIT DOUBLE PRECISION (A-H,O-Z,K)
      DIMENSION PHI(41,11),K(41,11)
      QIN = 0.D0
      DO 100 I=1,NT-1
      J=NRD
      IF (PHI(I,J+1).GE.-1.D-06.AND.PHI(I,J).GE.-1.D-06)
     C   THEN
         KN = K(I,J)
         KP = K(I,J+1)
         PHIN = PHI(I,J)
         PHIP = PHI(I,J+1)
         KNB = 2.0D0*KP*KN/(KN+KP)
         DQIN = KNB*(PHIN-PHIP)*DT/DR
      ELSE
         DQIN = 0.D0
      ENDIF
      QIN = QIN + DQIN
100   CONTINUE
      QOUT = 0.D0
      DO 110 I=1,NT-1
      IF (PHI(I,NR-1).GE.-1.D-06.AND.PHI(I,NR).GE.-1.D-06)
     C   THEN
         KS = K(I,NR)
         KP = K(I,NR-1)
```

```
            PHIS = PHI(I,NR)
            PHIP = PHI(I,NR-1)
            KSB = 2.D0*KP*KS/(KP+KS)
            DQOUT = KSB*(PHIP-PHIS)*DT/DR
         ELSE
            DQOUT = 0.D0
         ENDIF
         QOUT = QOUT + DQOUT
110      CONTINUE
         RETURN
         END
         SUBROUTINE HINIT(H,NT,NR,HREF,NRD,NTD,R,ANG,RI,RO,
        C DT,DEPTH)
         IMPLICIT DOUBLE PRECISION (A-H,O-Z)
         DIMENSION H(41,11),R(11),ANG(41)
         PI = 3.14159
         DO 10 I=1,NT
         DO 10 J=1,NR
         R(J)=(RI+(RO-RI)*DBLE(NR-J)/DBLE(NR-1))/RI
         ANG(I) = DBLE(I-1)*DT*180.0/PI
10       H(I,J) = 1.0D0
         DO 20 I=1,NTD-1
         DO 20 J=1,NRD
         H(NT+1-I,J) = 1.0D0 + DEPTH/HREF
20       H(I,J) = 1.0D0 + DEPTH/HREF
         RETURN
         END
         SUBROUTINE INA(NT,NR,A1,A2,A3,A4,PS1,SP)
         IMPLICIT DOUBLE PRECISION (A-H,O-Z)
         DIMENSION A1(21,11,21,11),A2(21,11,21,11),
        C A3(21,11,21,11),A4(21,11,21,11),PS1(21,11),SP(21,11)
         OPEN(UNIT=7,FILE='ROTORM.DAT')
         OPEN(UNIT=8,FILE='ROTORT.DAT')
         OPEN(UNIT=9,FILE='STATORM.DAT')
         OPEN(UNIT=5,FILE='STATORT.DAT')
         OPEN(UNIT=14,FILE='BCOND.DAT')
         OPEN(UNIT=13,FILE='SEALEDP.DAT')
         DO 10 I=1,21
         DO 10 J=1,NR
         READ(13,1000) PS1(I,J)
         READ(14,1000) SP(I,J)
         DO 10 K=1,21
         DO 10 L=1,NR
         READ(7,1000) A1(I,J,K,L)
         READ(8,1000) A2(I,J,K,L)
         READ(9,1000) A3(I,J,K,L)
10       READ(5,1000) A4(I,J,K,L)
1000     FORMAT(E15.8)
         RETURN
         END
         SUBROUTINE HEAT(HTNEW,NT,NR,DT,DR,H,HREF,R,F,PHI)
         IMPLICIT DOUBLE PRECISION (A-H,O-Z,M)
```

```
      DIMENSION HTNEW(41,11),H(41,11),R(11),F(41,11),
     C PHI(41,11)
      DO 10 I=1,NT
      DO 10 J=1,NR
      HF = 1.D0
      IF (J.EQ.NR.OR.J.EQ.1) HF=0.5D0
      HTNEW(I,J)=R(J)**3.D0*DR*DT*HF*
     C (1.D0+(1.D0-F(I,J))*PHI(I,J))/H(I,J)
10    CONTINUE
      RETURN
      END
      SUBROUTINE DEFORM(P,NT,NR,HTNEW,HREF,H,A1,A2,A3,A4,
     C R,RI,DR,DT,FLAG2,PS1,PS,SP,NTD,NRD,MU,OMEGA)
      IMPLICIT DOUBLE PRECISION (A-H,O-Z,M)
      INTEGER FLAG2
      DIMENSION P(41,11),HTNEW(41,11),H(41,11),
     C A1(21,11,21,11),A2(21,11,21,11),A3(21,11,21,11),
     C F(41,11),R(11),D1(41,11),D2(41,11),D3(41,11),
     C D4(41,11),PS1(21,11),A4(21,11,21,11),SP(21,11)
      DO 5 I=1,NT,2
      DO 5 J=1,NR
      D1(I,J) = 0.D0
      D2(I,J) = 0.D0
      D3(I,J) = 0.D0
      D4(I,J) = 0.D0
5     F(I,J) = 2.D0*R(J)*DR*DT*RI**2.D0*(P(I,J)+
     C P(I-1,J)+P(I+1,J))/3.D0
      DO 7 I=1,NT,2
      F(I,1) = F(I,1)/2.D0
7     F(I,NR)= F(I,NR)/2.D0
      DO 10 I=1,NT,2
      DO 10 J=1,NR
      DO 10 K=1,NT,2
      M = K/2 + 1
      DO 10 L=1,NR
      D1(I,J) = D1(I,J) + F(K,L)*A1(I/2+1,J,M,L)
      D2(I,J) = D2(I,J) + HTNEW(K,L)*A2(I/2+1,J,M,L)*
     C MU*OMEGA**2.D0/HREF/32.2D0/12.D0**3.D0/
     C 778.D0*3600.D0*RI**4.D0
      D3(I,J) = D3(I,J) + F(K,L)*A3(I/2+1,J,M,L)
      D4(I,J) = D4(I,J) + HTNEW(K,L)*A4(I/2+1,J,M,L)*
     C MU*OMEGA**2.D0/HREF/32.2D0/12.D0**3.D0/778.D0
     C *3600.D0*RI**4.D0
10    CONTINUE
      HO=(D1(1,NR) + D2(1,NR) + D3(1,NR) + D4(1,NR)
     C  + PS1(1,NR)*PS + SP(1,NR))/HREF
      DO 40 I=1,NT,2
      DO 40 J=1,NR
      M = I/2 + 1
      H(I,J) = H(I,J) + (D1(I,J)+D3(I,J)+D2(I,J)+
     C D4(I,J))/HREF + PS1(M,J)*PS/HREF + SP(M,J)/HREF - HO
      IF (H(I,J).LT.0) THEN
```

```
            H(I,J) = 0.D0
         ENDIF
40       CONTINUE
         DO 41 J=1,NR
41       H(NT,J) = H(1,J)
         DO 20 I=2,NT,2
         DO 20 J=1,NR
            IF (I.GE.NT/2) THEN
               II1 = I-3
               II2 = I-1
               II3 = I+1
            ELSE
               II1 = I-1
               II2 = I+1
               II3 = I+3
            ENDIF
            X1 = DBLE(II1)
            X2 = DBLE(II2)
            X3 = DBLE(II3)
            Y1 = H(II1,J)
            Y2 = H(II2,J)
            Y3 = H(II3,J)
            X  = DBLE(I)
            CALL FINTLG(X1,Y1,X2,Y2,X3,Y3,X,Y)
            H(I,J) = Y
            IF (H(I,J).LT.0) H(I,J) = 0.D0
            IF (I.LE.NTD-1) THEN
               DO 17 L=1,NRD
17             H(I,L) = H(I-1,L)
            ENDIF
            IF (I.GE.NT-NTD+2) THEN
               DO 18 L=1,NRD
18             H(I,L) = H(I+1,L)
            ENDIF
20       CONTINUE
         RETURN
         END
         SUBROUTINE INDAT(NB,PS,PA,PC,OMEGA,MU2,RI,RO,NW,NR,NT,
        C   NTD,NRD,HREF,NFIL,RELAX1,DEPTH,MAXIT2,START)
         IMPLICIT DOUBLE PRECISION (A-H,O-Z)
         DOUBLE PRECISION NB,MU2,NW
         INTEGER START
         CHARACTER*12 NFIL
         OPEN(UNIT=12,FILE='INPUT.FIL')
         READ(12,100) NB
100      FORMAT(44X,F7.5)
         READ(12,110) PS
110      FORMAT(44X,F8.2)
         READ(12,120) PA
120      FORMAT(44X,F8.2)
         READ(12,130) PC
130      FORMAT(44X,F8.2)
```

```
      READ(12,140) NW
140   FORMAT(44X,F4.1)
      READ(12,150) NT
150   FORMAT(44X,I2)
      READ(12,160) NR
160   FORMAT(44X,I2)
      READ(12,170) OMEGA
170   FORMAT(44X,F6.1)
      READ(12,180) MU2
180   FORMAT(44X,E10.4)
      READ(12,190) NTD
190   FORMAT(44X,I2)
      READ(12,200) NRD
200   FORMAT(44X,I2)
      READ(12,210) RI
210   FORMAT(44X,F8.5)
      READ(12,210) RO
      READ(12,220) NFIL
220   FORMAT(44X,A12)
      READ(12,230) HREF
230   FORMAT(44X,E13.7)
      READ(12,240) RELAX1
240   FORMAT(44X,F4.2)
      READ(12,250) DEPTH
250   FORMAT(44X,F9.6)
      READ(12,260) MAXIT2
260   FORMAT(44X,I3)
      READ(12,270) START
270   FORMAT(44X,I1)
      RETURN
      END
      SUBROUTINE HVAL(NR,NT,H,HMIN,HAVE,NRD,NTD,HAVERI)
      IMPLICIT DOUBLE PRECISION (A-H,O-Z)
      DIMENSION H(41,11)
      HAVE = 0.D0
      HAVERI = 0.D0
      HMIN = 1.D10
      DO 10 I=1,NT
      DO 10 J=1,NR
      IF (I.GE.NTD.AND.I.LE.NT-NTD+1.OR.J.GT.NRD) HAVE =
     C HAVE + H(I,J)
      IF (J.EQ.NR) HAVERI = HAVERI + H(I,J)
      IF (H(I,J).LT.HMIN) HMIN = H(I,J)
10    CONTINUE
      HAVERI = HAVERI / NT
      HAVE = HAVE / DBLE((NR-NRD-1)*NT+(NT-2*(NTD-1)*NRD))
      RETURN
      END
      SUBROUTINE FINTLG(X1,Y1,X2,Y2,X3,Y3,X,Y)
      IMPLICIT DOUBLE PRECISION (A-Z)
      C1 = Y1/((X1-X2)*(X1-X3))
      C2 = Y2/((X2-X1)*(X2-X3))
```

```
      C3 = Y3/((X3-X1)*(X3-X2))
      Y = C1*(X-X2)*(X-X3)+C2*(X-X1)*(X-X3)+C3*(X-X1)*(X-X2)
      RETURN
      END
      SUBROUTINE RESTART(NT,NR,P,PHI,H,F,PS,PC)
      IMPLICIT DOUBLE PRECISION (A-H,O-Z)
      DIMENSION P(41,11),PHI(41,11),H(41,11),F(41,11)
      OPEN(UNIT=15,FILE='RESTART.INP')
      DO 10 I=1,NT
      DO 10 J=1,NR
      READ(15,1000) PHI(I,J)
      READ(15,1000) H(I,J)
      READ(15,1000) F(I,J)
      IF (PHI(I,J).GT.0) THEN
         P(I,J) = PHI(I,J)*(PS-PC) + PC
      ELSE
         P(I,J) = PC
      ENDIF
10    CONTINUE
1000  FORMAT(E15.8)
      RETURN
      END
```

APPENDIX E

INSTRUCTIONS FOR COMPUTER PROGRAM

The computer code in appendix D requires several input files. These files and their contents are given in Table 2. The format for all the influence coefficient files is given in appendix G. The method for determining the coefficient is outlined in chapter III under the deformation analysis section.

The file INPUT.FIL, shown below, contains the operating conditions at which the seal design is to be analyzed and defines the seal geometry.

```
BALANCE RATIO                                = #.#####
SEAL PRESSURE (psig)                         = #####.##
AMBIENT PRESSURE (psig)                      = #####.##
CAVITATION PRESSURE (psig)                   = #####.##
NUMBER OF HYDROPADS                          = #.#
NUMBER THETA NODES                           = ##
NUMBER OF RADIAL NODES                       = ##
SHAFT SPEED (rad/s)                          = ####.#
ABSOLUTE VISCOSITY (reyn)                    = #.####E-##
THETA NODE # OF HYDROPAD                     = ##
RADIAL NODE # OF HYDROPAD                    = ##
INNER RADIUS (in)                            = ##.#####
OUTER RADIUS (in)                            = ##.#####
NAME OF OUTPUT FILE                          = ##########
INITIAL GUESS OF H(REFERENCE) (in)           = #.#######E-##
RELAXATION ON FILM THICKNESS                 = #.##
DEPTH OF HYDROPAD (in)                       = ##.######
MAXIMUM # OF ITERATIONS OF ADJUSTING HREF    = ##
RESTART FROM EXISTING FILE (1=YES,0=NO)      = #
```

On the left is the required information. The right

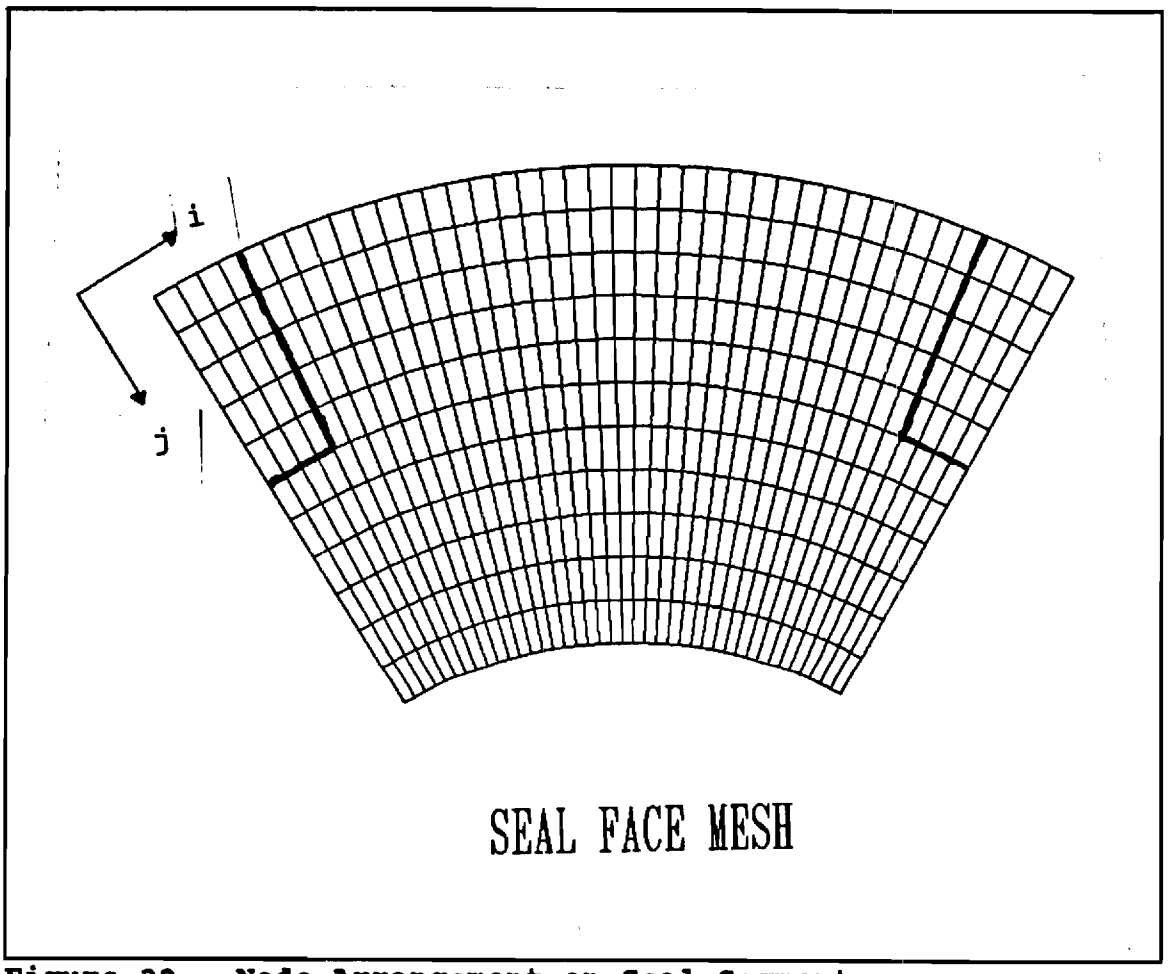

Figure 32. Node Arrangement on Seal Segment.

contains the format required for input into the program. It is important that the format given for this file be followed for the information to be read correctly into the computer program. Most of the information required is easily understood, but some items might require greater explanation. The balance ratio, number of hydropads, depth of hydropads, inner radius, and outer radius are set by the geometry of the seal design. The number of circumferential nodes (theta nodes) and the number radial nodes for the mesh

is set here. The theta node number and radial node number of the hydropad define the size and location of the hydropads on the seal segment. Figure 32 shows the seal segment with the numbering scheme used by the computer program. The location of the hydropad in the figure is defined by theta node number of 5 and a radial node number of 6.

The sealed pressure, cavitation pressure, ambient pressure, shaft speed, and viscosity define the operating conditions at which the seal design is analyzed.

The output file is simply the name of the file that the general information from the analysis such as convergence criterion, leakage rate, reference film thickness, etc. is written. An example one is given in appendix F. Several other output files with preset names are written to provide plot files for the pressure, film thickness, cavitation index, and heat generation distributions. The names of these files are given in Table 3.

The initial guess of the h_{rcf} is the assumed film thickness at the inner radius at θ=0°. It is necessary to start at some guess on the reference film thickness in the solution procedure. The value of this parameter is chosen by the user based on experience in analyzing similar designs. As a guideline, it is better to start with an initial film thickness that is high because a very low guess can lead to convergence problems.

The user is allowed to set the relaxation factor on the film thickness. In the cases analyzed in this study, a relaxation factor of 0.5 is found to work well, but in analyzing various seal designs it may be necessary to adjust this factor if convergence problems are encountered.

The user can set the maximum number of iterations on the reference film thickness. The program will automatically stop once it converges on a steady-state solution, but if the seal design does not have positive stiffness or there is convergence problems the program could iterate continuously unless a limit is placed on the number of iterations. Therefore, this parameter is input by the user. For the cases in this study the number of iterations on h_{ref} is usually less than 20 so a number around this magnitude is probably sufficient.

Finally, the last input in the file allows the user to restart an analysis from a previous one. This is a simple yes or no option which is set by input 1 to restart from a previous file or 0 to not.

Table 2. Input files.

INPUT FILES	FILE DESCRIPTION
INPUT.FIL	Input file that contains operating conditions and geometry of seal design
ROTOTRM.DAT	Mechanical influence coefficients for rotor
ROTORT.DAT	Thermal influence coefficients for rotor
STATORM.DAT	Mechanical influence coefficients for stator
STATORT.DAT	Thermal influence coefficients for stator
SEALEDP.DAT	Influence coefficients for sealed pressure on rotor
BCOND.DAT	Influence coefficients that account for boundary conditions on mesh
RESTART.INP	(Optional) Restart file needed only when restarting an analysis from a previous run

Table 3. Output files.

FILE NAME	CONTENTS
OUTPUT.FIL	General output file - contains general information about operating conditions Name of file set by user in INPUT.FIL
PLOTF.FIL	Contains cavitation index F distribution for plotting
PLOTH.FIL	Contains film thickness distribution for plotting
PLOTP.FIL	Contains pressure distribution for plotting
PLOTHT.FIL	Contains film thickness at 5 different radii as a function of θ
PLOTHR.FIL	Contains film thickness as functions of radius
HTGEN.FIL	Contains heat generation rate distribution
RESTART.FIL	File to be used for a restart from this analysis

APPENDIX F

SAMPLE OUTPUT FILE

```
          SOLUTION OF PRESSURE FIELD IN RADIAL SEAL

BALANCE RATIO = 0.72212
SEAL PRESSURE =  150.0000 PSI
AMBIENT PRESSURE =    0.0000 PSI
CAVITATION PRESSURE =    0.0000 PSI
NUMBER OF ITERATIONS IN REYNOLD"S EQT. =    1
CONVERGENCE FOR REYNOLD"S EQT. = 0.62E-04
RELAXATION FACTOR FOR F = 0.01
RELAXATION FACTOR FOR PHI = 0.20
RELAXATION FACTOR ON FILM THICKNESS = 0.50
# RADIAL NODES = 11          # OF THETA NODES = 41
MAXIMUM DIFFERENCE IN PHI = 0.3806E-04          IN F = 0.2109E-14
GAMMA =  0.69282473E+02
VISCOSITY = 0.1460E-06 REYN
ROTATIONAL SPEED =   100.000 RAD/S
INNER RADIUS =  1.8750 IN
OUTER RADIUS =  2.3165 IN
QIN =  0.44014930E+01
QOUT =  0.44023147E+01
LEAKAGE RATE =  0.11343052E+02 CM^3/MIN
OPENING FORCE =  0.62842973E+03 LBF
CLOSING FORCE =  0.62972410E+03 LBF
HREF =  0.17214563E-03 IN
HREF =  0.43724990E+01 10^-6 METERS
HMIN =  0.13870809E+01 10^-6 METERS
HAVE =  0.78677746E+01 10^-6 METERS
HAVE @ RI =  0.38842655E+01 10^-6 METERS
NUMBER OF ITERATIONS OF DEFORMATION ANALYSIS =  22
MAXIMUM DIFFERENCE IN PHI BETWEEN DEFORMATION ANAL. =  0.58297612E-04
MAXIMUM DIFFERENCE IN HT BETWEEN DEFORMATION ANAL. =  0.81173548E-07
MAXIMUM DIFFERENCE IN H BETWEEN DEFORMATION ANAL. =  0.11692215E-04
# OF ITERATIONS OF ADJUSTING HREF =   3

          DIMENSIONLESS FILM THICKNESS

RADIUS       0.00              1.50              3.00              4.50

1.2355  0.72684970E+03    0.72684970E+03    0.72680840E+03    0.72680840E+03
1.2119  0.72688848E+03    0.72688848E+03    0.72684233E+03    0.72684233E+03
1.1884  0.72692689E+03    0.72692689E+03    0.72688064E+03    0.72688064E+03
1.1648  0.72696903E+03    0.72696903E+03    0.72692567E+03    0.72692567E+03
1.1413  0.72701146E+03    0.72701146E+03    0.72697568E+03    0.72697568E+03
1.1177  0.72788197E+03    0.72788197E+03    0.72704032E+03    0.72704032E+03
1.0942  0.93719801E+00    0.91108058E+00    0.89236892E+00    0.88691095E+00
1.0706  0.95573824E+00    0.94055481E+00    0.92825759E+00    0.92170443E+00
```

1.0471	0.95837770E+00	0.95096701E+00	0.94372937E+00	0.93786707E+00
1.0235	0.98107069E+00	0.97837898E+00	0.97428678E+00	0.96906910E+00
1.0000	0.10000000E+01	0.99938484E+00	0.99708544E+00	0.99322862E+00
RADIUS	6.00	7.50	9.00	10.50
1.2355	0.81665714E+00	0.67312815E+00	0.58635605E+00	0.58640742E+00
1.2119	0.88130674E+00	0.73767573E+00	0.64766865E+00	0.63849610E+00
1.1884	0.92051371E+00	0.78243410E+00	0.69473019E+00	0.68273155E+00
1.1648	0.94386840E+00	0.81729978E+00	0.73621224E+00	0.72350476E+00
1.1413	0.94207487E+00	0.84158899E+00	0.77581880E+00	0.76216324E+00
1.1177	0.88902669E+00	0.84939867E+00	0.81883438E+00	0.80100268E+00
1.0942	0.87716298E+00	0.86085310E+00	0.84479706E+00	0.82831709E+00
1.0706	0.91232183E+00	0.89890595E+00	0.88506832E+00	0.87007865E+00
1.0471	0.92977319E+00	0.91856974E+00	0.90689072E+00	0.89413102E+00
1.0235	0.96190093E+00	0.95205105E+00	0.94171310E+00	0.93036449E+00
1.0000	0.98743388E+00	0.97896150E+00	0.97003068E+00	0.96014930E+00
RADIUS	12.00	13.50	15.00	16.50
1.2355	0.58308251E+00	0.57490247E+00	0.56630381E+00	0.55744080E+00
1.2119	0.62852628E+00	0.61699872E+00	0.60619486E+00	0.59669291E+00
1.1884	0.67044947E+00	0.65712238E+00	0.64503501E+00	0.63490308E+00
1.1648	0.71048041E+00	0.69628937E+00	0.68348106E+00	0.67272461E+00
1.1413	0.74842543E+00	0.73387540E+00	0.72070300E+00	0.70947753E+00
1.1177	0.78489700E+00	0.77085461E+00	0.75786366E+00	0.74626693E+00
1.0942	0.81344643E+00	0.80052342E+00	0.78853299E+00	0.77772772E+00
1.0706	0.85612780E+00	0.84336352E+00	0.83134257E+00	0.82019376E+00
1.0471	0.88210601E+00	0.87085538E+00	0.86026000E+00	0.85042213E+00
1.0235	0.91957296E+00	0.90933902E+00	0.89966114E+00	0.89062905E+00
1.0000	0.95079369E+00	0.94201562E+00	0.93365978E+00	0.92581577E+00
RADIUS	18.00	19.50	21.00	22.50
1.2355	0.54785058E+00	0.53714429E+00	0.52648855E+00	0.51581537E+00
1.2119	0.58675824E+00	0.57610877E+00	0.56559070E+00	0.55516772E+00
1.1884	0.62457943E+00	0.61386278E+00	0.60335703E+00	0.59305126E+00
1.1648	0.66201266E+00	0.65122835E+00	0.64072229E+00	0.63050339E+00
1.1413	0.69849102E+00	0.68769695E+00	0.67723491E+00	0.66712590E+00
1.1177	0.73503610E+00	0.72416747E+00	0.71367216E+00	0.70357878E+00
1.0942	0.76734986E+00	0.75743513E+00	0.74787638E+00	0.73870891E+00
1.0706	0.80953064E+00	0.79940596E+00	0.78966154E+00	0.78033017E+00
1.0471	0.84103500E+00	0.83216360E+00	0.82361300E+00	0.81541862E+00
1.0235	0.88197357E+00	0.87374791E+00	0.86579244E+00	0.85813201E+00
1.0000	0.91821480E+00	0.91088333E+00	0.90374200E+00	0.89679761E+00
RADIUS	24.00	25.50	27.00	28.50
1.2355	0.50532879E+00	0.49497121E+00	0.48491541E+00	0.47516138E+00
1.2119	0.54494875E+00	0.53488938E+00	0.52512282E+00	0.51564904E+00
1.1884	0.58297822E+00	0.57310700E+00	0.56353030E+00	0.55424814E+00
1.1648	0.62054494E+00	0.61082826E+00	0.60140939E+00	0.59228834E+00
1.1413	0.65730693E+00	0.64777379E+00	0.63853911E+00	0.62960288E+00
1.1177	0.69380150E+00	0.68434441E+00	0.67519526E+00	0.66635403E+00
1.0942	0.72982681E+00	0.72124420E+00	0.71291871E+00	0.70485034E+00
1.0706	0.77131351E+00	0.76262830E+00	0.75422431E+00	0.74610155E+00
1.0471	0.80747420E+00	0.79979724E+00	0.79233529E+00	0.78508836E+00
1.0235	0.85069208E+00	0.84348665E+00	0.83647378E+00	0.82965347E+00
1.0000	0.89002979E+00	0.88344792E+00	0.87702383E+00	0.87075752E+00
RADIUS	30.00	31.50	33.00	34.50

1.2355	0.46570912E+00	0.45646149E+00	0.44745088E+00	0.43893993E+00
1.2119	0.50646806E+00	0.49745681E+00	0.48865630E+00	0.48032008E+00
1.1884	0.54526051E+00	0.53642713E+00	0.52779476E+00	0.51961114E+00
1.1648	0.58346509E+00	0.57478257E+00	0.56629312E+00	0.55824238E+00
1.1413	0.62096512E+00	0.61246038E+00	0.60414382E+00	0.59625539E+00
1.1177	0.65782072E+00	0.64942506E+00	0.64122379E+00	0.63345806E+00
1.0942	0.69703910E+00	0.68930856E+00	0.68171752E+00	0.67449806E+00
1.0706	0.73826002E+00	0.73053349E+00	0.72297738E+00	0.71583706E+00
1.0471	0.77805645E+00	0.77107458E+00	0.76419774E+00	0.75767008E+00
1.0235	0.82302572E+00	0.81643915E+00	0.80994422E+00	0.80379625E+00
1.0000	0.86464900E+00	0.85855630E+00	0.85252675E+00	0.84682990E+00

RADIUS	36.00	37.50	39.00	40.50
1.2355	0.43084109E+00	0.42291444E+00	0.41523994E+00	0.40749671E+00
1.2119	0.47236364E+00	0.46459214E+00	0.45707054E+00	0.44966396E+00
1.1884	0.51179369E+00	0.50418728E+00	0.49684361E+00	0.48968732E+00
1.1648	0.55054848E+00	0.54307133E+00	0.53585762E+00	0.52881809E+00
1.1413	0.58871512E+00	0.58139841E+00	0.57434680E+00	0.56744372E+00
1.1177	0.62604747E+00	0.61887416E+00	0.61197741E+00	0.60524058E+00
1.0942	0.66757281E+00	0.66082534E+00	0.65429448E+00	0.64788019E+00
1.0706	0.70903073E+00	0.70246762E+00	0.69617799E+00	0.69011594E+00
1.0471	0.75141021E+00	0.74532647E+00	0.73944942E+00	0.73378747E+00
1.0235	0.79791012E+00	0.79220478E+00	0.78670726E+00	0.78145681E+00
1.0000	0.84137590E+00	0.83609123E+00	0.83100041E+00	0.82614408E+00

RADIUS	42.00	43.50	45.00	46.50
1.2355	0.39979172E+00	0.39021839E+00	0.37941224E+00	0.36748307E+00
1.2119	0.44241736E+00	0.43352637E+00	0.42359246E+00	0.41394976E+00
1.1884	0.48274353E+00	0.47440429E+00	0.46520559E+00	0.45650726E+00
1.1648	0.52198249E+00	0.51402953E+00	0.50539964E+00	0.49723356E+00
1.1413	0.56072804E+00	0.55321868E+00	0.54524267E+00	0.53784531E+00
1.1177	0.59870257E+00	0.59172447E+00	0.58451925E+00	0.57786260E+00
1.0942	0.64161583E+00	0.63518452E+00	0.62869189E+00	0.62307924E+00
1.0706	0.68429676E+00	0.67867906E+00	0.67327663E+00	0.66898770E+00
1.0471	0.72833782E+00	0.72326338E+00	0.71850984E+00	0.71504215E+00
1.0235	0.77644034E+00	0.77191088E+00	0.76778408E+00	0.76501304E+00
1.0000	0.82150868E+00	0.81735010E+00	0.81358305E+00	0.81112515E+00

RADIUS	48.00	49.50	51.00	52.50
1.2355	0.35439428E+00	0.33732983E+00	0.31722841E+00	0.38904447E+00
1.2119	0.40415356E+00	0.38848594E+00	0.36885288E+00	0.44448600E+00
1.1884	0.44785604E+00	0.43418887E+00	0.41719344E+00	0.49214967E+00
1.1648	0.48915104E+00	0.47809270E+00	0.46507833E+00	0.53497005E+00
1.1413	0.53067816E+00	0.52333972E+00	0.51596382E+00	0.57260732E+00
1.1177	0.57149596E+00	0.56951027E+00	0.57054189E+00	0.59557109E+00
1.0942	0.61803281E+00	0.61776479E+00	0.62087111E+00	0.63222578E+00
1.0706	0.66551287E+00	0.66605186E+00	0.66953809E+00	0.67738520E+00
1.0471	0.71253867E+00	0.71323487E+00	0.71638558E+00	0.72199846E+00
1.0235	0.76328007E+00	0.76412277E+00	0.76702862E+00	0.77136382E+00
1.0000	0.80967051E+00	0.81044047E+00	0.81302790E+00	0.81641988E+00

RADIUS	54.00	55.50	57.00	58.50
1.2355	0.52112652E+00	0.72655186E+03	0.72655186E+03	0.72684970E+03
1.2119	0.58230810E+00	0.72659019E+03	0.72659019E+03	0.72688848E+03
1.1884	0.62729761E+00	0.72663409E+03	0.72663409E+03	0.72692689E+03
1.1648	0.65948048E+00	0.72668512E+03	0.72668512E+03	0.72696903E+03
1.1413	0.67191794E+00	0.72673955E+03	0.72673955E+03	0.72701146E+03
1.1177	0.63760447E+00	0.72678920E+03	0.72678920E+03	0.72788197E+03

1.0942	0.65020413E+00	0.66023373E+00	0.66717205E+00	0.77055278E+00
1.0706	0.68912196E+00	0.69672001E+00	0.70285545E+00	0.79940318E+00
1.0471	0.73007095E+00	0.73555230E+00	0.74012608E+00	0.82322733E+00
1.0235	0.77733963E+00	0.78151720E+00	0.78504282E+00	0.85951617E+00
1.0000	0.82095406E+00	0.82375063E+00	0.82576953E+00	0.89170789E+00

DIMENSIONLESS PHI VALUES

RADIUS	0.00	1.50	3.00	4.50
1.2355	0.10000000E+01	0.10000000E+01	0.10000000E+01	0.10000000E+01
1.2119	0.10000000E+01	0.10000000E+01	0.10000000E+01	0.10000000E+01
1.1884	0.10000000E+01	0.10000000E+01	0.10000000E+01	0.10000000E+01
1.1648	0.10000000E+01	0.10000000E+01	0.10000000E+01	0.10000000E+01
1.1413	0.10000000E+01	0.10000000E+01	0.10000000E+01	0.10000000E+01
1.1177	0.10000000E+01	0.10000000E+01	0.10000000E+01	0.10000000E+01
1.0942	0.75686593E+00	0.84623964E+00	0.87039843E+00	0.87356498E+00
1.0706	0.40477202E+00	0.55316058E+00	0.61335403E+00	0.63648065E+00
1.0471	0.16721857E+00	0.31353620E+00	0.38175964E+00	0.41233935E+00
1.0235	0.81354380E-02	0.12794728E+00	0.17788751E+00	0.20003302E+00
1.0000	-0.37357583E-13	0.00000000E+00	0.00000000E+00	0.00000000E+00

RADIUS	6.00	7.50	9.00	10.50
1.2355	0.10000000E+01	0.10000000E+01	0.10000000E+01	0.10000000E+01
1.2119	0.10000000E+01	0.13133605E+01	0.13248345E+01	0.12023802E+01
1.1884	0.10000000E+01	0.13680878E+01	0.14029106E+01	0.12761536E+01
1.1648	0.10000000E+01	0.13201870E+01	0.13533982E+01	0.12493881E+01
1.1413	0.10000000E+01	0.12142287E+01	0.12271404E+01	0.11526362E+01
1.1177	0.10000000E+01	0.10560626E+01	0.10511494E+01	0.10092253E+01
1.0942	0.84570200E+00	0.85807089E+00	0.85294948E+00	0.83030019E+00
1.0706	0.64091027E+00	0.64802485E+00	0.64583090E+00	0.63314587E+00
1.0471	0.42592196E+00	0.43302518E+00	0.43296650E+00	0.42607787E+00
1.0235	0.21057401E+00	0.21554072E+00	0.21619195E+00	0.21322609E+00
1.0000	0.00000000E+00	0.00000000E+00	0.00000000E+00	0.00000000E+00

RADIUS	12.00	13.50	15.00	16.50
1.2355	0.10000000E+01	0.10000000E+01	0.10000000E+01	0.10000000E+01
1.2119	0.11564966E+01	0.11348300E+01	0.11192193E+01	0.11109180E+01
1.1884	0.12141568E+01	0.11793139E+01	0.11533809E+01	0.11376866E+01
1.1648	0.11892735E+01	0.11504444E+01	0.11200495E+01	0.10998922E+01
1.1413	0.11021785E+01	0.10647712E+01	0.10342000E+01	0.10124502E+01
1.1177	0.96990417E+00	0.93621600E+00	0.90835453E+00	0.88739193E+00
1.0942	0.80214315E+00	0.77509285E+00	0.75166316E+00	0.73304751E+00
1.0706	0.61435419E+00	0.59464857E+00	0.57661486E+00	0.56153595E+00
1.0471	0.41443606E+00	0.40141077E+00	0.38891387E+00	0.37804436E+00
1.0235	0.20759293E+00	0.20102538E+00	0.19453834E+00	0.18877727E+00
1.0000	0.00000000E+00	0.00000000E+00	0.00000000E+00	0.00000000E+00

RADIUS	18.00	19.50	21.00	22.50
1.2355	0.10000000E+01	0.10000000E+01	0.10000000E+01	0.10000000E+01
1.2119	0.11107636E+01	0.11135019E+01	0.11164709E+01	0.11198761E+01
1.1884	0.11330688E+01	0.11332884E+01	0.11349488E+01	0.11376455E+01
1.1648	0.10906245E+01	0.10869533E+01	0.10857507E+01	0.10861360E+01
1.1413	0.99996326E+00	0.99290487E+00	0.98881609E+00	0.98664699E+00
1.1177	0.87348667E+00	0.86426433E+00	0.85800697E+00	0.85374315E+00
1.0942	0.71947120E+00	0.70961462E+00	0.70239512E+00	0.69702471E+00
1.0706	0.54974595E+00	0.54067450E+00	0.53371078E+00	0.52828009E+00

1.0471	0.36916986E+00	0.36209028E+00	0.35649157E+00	0.35200048E+00
1.0235	0.18398127E+00	0.18009026E+00	0.17696710E+00	0.17442513E+00
1.0000	0.00000000E+00	0.00000000E+00	0.00000000E+00	0.00000000E+00

RADIUS	24.00	25.50	27.00	28.50
1.2355	0.10000000E+01	0.10000000E+01	0.10000000E+01	0.10000000E+01
1.2119	0.11235306E+01	0.11271343E+01	0.11304327E+01	0.11336756E+01
1.1884	0.11409690E+01	0.11444109E+01	0.11476431E+01	0.11508334E+01
1.1648	0.10875121E+01	0.10892588E+01	0.10910160E+01	0.10928046E+01
1.1413	0.98571444E+00	0.98538490E+00	0.98529411E+00	0.98533223E+00
1.1177	0.85081550E+00	0.84863743E+00	0.84686250E+00	0.84530670E+00
1.0942	0.69294170E+00	0.68965193E+00	0.68685232E+00	0.68433093E+00
1.0706	0.52395001E+00	0.52034084E+00	0.51720815E+00	0.51435900E+00
1.0471	0.34832633E+00	0.34520762E+00	0.34247378E+00	0.33998264E+00
1.0235	0.17231421E+00	0.17050288E+00	0.16890434E+00	0.16744501E+00
1.0000	0.00000000E+00	0.00000000E+00	0.00000000E+00	0.00000000E+00

RADIUS	30.00	31.50	33.00	34.50
1.2355	0.10000000E+01	0.10000000E+01	0.10000000E+01	0.10000000E+01
1.2119	0.11371438E+01	0.11404138E+01	0.11421444E+01	0.11426075E+01
1.1884	0.11542364E+01	0.11572485E+01	0.11583139E+01	0.11577474E+01
1.1648	0.10947760E+01	0.10962772E+01	0.10958474E+01	0.10937422E+01
1.1413	0.98554601E+00	0.98529628E+00	0.98329670E+00	0.97970883E+00
1.1177	0.84394343E+00	0.84218146E+00	0.83891200E+00	0.83421005E+00
1.0942	0.68202418E+00	0.67941024E+00	0.67555977E+00	0.67048477E+00
1.0706	0.51172186E+00	0.50886610E+00	0.50503564E+00	0.50021025E+00
1.0471	0.33768882E+00	0.33527573E+00	0.33217448E+00	0.32836901E+00
1.0235	0.16611484E+00	0.16473830E+00	0.16297207E+00	0.16081785E+00
1.0000	0.00000000E+00	0.00000000E+00	0.00000000E+00	0.00000000E+00

RADIUS	36.00	37.50	39.00	40.50
1.2355	0.10000000E+01	0.10000000E+01	0.10000000E+01	0.10000000E+01
1.2119	0.11435472E+01	0.11453241E+01	0.11483433E+01	0.11543503E+01
1.1884	0.11574188E+01	0.11578429E+01	0.11594673E+01	0.11638991E+01
1.1648	0.10915426E+01	0.10896918E+01	0.10884464E+01	0.10885178E+01
1.1413	0.97573743E+00	0.97163831E+00	0.96736385E+00	0.96268285E+00
1.1177	0.82894511E+00	0.82316297E+00	0.81650161E+00	0.80807020E+00
1.0942	0.66478215E+00	0.65833396E+00	0.65056854E+00	0.64029707E+00
1.0706	0.49479404E+00	0.48858902E+00	0.48096620E+00	0.47076791E+00
1.0471	0.32414364E+00	0.31930614E+00	0.31331598E+00	0.30529314E+00
1.0235	0.15845948E+00	0.15577624E+00	0.15245203E+00	0.14802570E+00
1.0000	0.00000000E+00	0.00000000E+00	0.00000000E+00	0.00000000E+00

RADIUS	42.00	43.50	45.00	46.50
1.2355	0.10000000E+01	0.10000000E+01	0.10000000E+01	0.10000000E+01
1.2119	0.11687576E+01	0.11860941E+01	0.11871192E+01	0.11660628E+01
1.1884	0.11751305E+01	0.11848463E+01	0.11704397E+01	0.11206337E+01
1.1648	0.10912570E+01	0.10877146E+01	0.10576468E+01	0.98786926E+00
1.1413	0.95684357E+00	0.94158558E+00	0.90066693E+00	0.82211875E+00
1.1177	0.79595051E+00	0.77329077E+00	0.72825136E+00	0.65164480E+00
1.0942	0.62522622E+00	0.60013545E+00	0.55690564E+00	0.48996248E+00
1.0706	0.45590814E+00	0.43276633E+00	0.39629165E+00	0.34381214E+00
1.0471	0.29369798E+00	0.27631749E+00	0.25026848E+00	0.21456941E+00
1.0235	0.14168161E+00	0.13239669E+00	0.11882922E+00	0.10074674E+00
1.0000	0.00000000E+00	0.00000000E+00	0.00000000E+00	0.52102900E-15

RADIUS	48.00	49.50	51.00	52.50

1.2355	0.10000000E+01	0.10000000E+01	0.10000000E+01	0.10000000E+01
1.2119	0.11226094E+01	0.93982505E+00	0.16911980E+00	-0.16400037E-01
1.1884	0.10237067E+01	0.76253195E+00	0.20680875E-01	-0.70951683E-01
1.1648	0.86197366E+00	0.60240249E+00	0.44134865E-01	0.20158028E-01
1.1413	0.69149775E+00	0.47669930E+00	0.13597125E+00	0.18144957E+00
1.1177	0.53259207E+00	0.37408224E+00	0.21738215E+00	0.32600691E+00
1.0942	0.39509536E+00	0.28762285E+00	0.21453168E+00	0.28450742E+00
1.0706	0.27528555E+00	0.20499664E+00	0.16384018E+00	0.19243831E+00
1.0471	0.17053511E+00	0.12750958E+00	0.10216677E+00	0.10833928E+00
1.0235	0.79120821E-01	0.58311474E-01	0.45470941E-01	0.44521543E-01
1.0000	0.30837398E-15	-0.16327238E-15	-0.54858829E-15	-0.71918039E-15

RADIUS	54.00	55.50	57.00	58.50
1.2355	0.10000000E+01	0.10000000E+01	0.10000000E+01	0.10000000E+01
1.2119	0.10000000E+01	0.10000000E+01	0.10000000E+01	0.10000000E+01
1.1884	0.10000000E+01	0.10000000E+01	0.10000000E+01	0.10000000E+01
1.1648	0.10000000E+01	0.10000000E+01	0.10000000E+01	0.10000000E+01
1.1413	0.10000000E+01	0.10000000E+01	0.10000000E+01	0.10000000E+01
1.1177	0.10000000E+01	0.10000000E+01	0.10000000E+01	0.10000000E+01
1.0942	0.55922359E+00	0.71149821E+00	0.65591806E+00	0.63200117E+00
1.0706	0.29415387E+00	0.34211820E+00	0.25007247E+00	0.22567923E+00
1.0471	0.13973673E+00	0.14140317E+00	0.57493254E-01	0.33311509E-01
1.0235	0.51311652E-01	0.44646383E-01	-0.12398363E-01	-0.99180585E-01
1.0000	-0.96134709E-15	-0.59293227E-15	-0.24445214E-02	-0.76187307E-01

VALUES FOR F

RADIUS	0.00	1.50	3.00	4.50
1.2355	1.0000	1.0000	1.0000	1.0000
1.2119	1.0000	1.0000	1.0000	1.0000
1.1884	1.0000	1.0000	1.0000	1.0000
1.1648	1.0000	1.0000	1.0000	1.0000
1.1413	1.0000	1.0000	1.0000	1.0000
1.1177	1.0000	1.0000	1.0000	1.0000
1.0942	1.0000	1.0000	1.0000	1.0000
1.0706	1.0000	1.0000	1.0000	1.0000
1.0471	1.0000	1.0000	1.0000	1.0000
1.0235	1.0000	1.0000	1.0000	1.0000
1.0000	0.0000	1.0000	1.0000	1.0000

RADIUS	6.00	7.50	9.00	10.50
1.2355	1.0000	1.0000	1.0000	1.0000
1.2119	1.0000	1.0000	1.0000	1.0000
1.1884	1.0000	1.0000	1.0000	1.0000
1.1648	1.0000	1.0000	1.0000	1.0000
1.1413	1.0000	1.0000	1.0000	1.0000
1.1177	1.0000	1.0000	1.0000	1.0000
1.0942	1.0000	1.0000	1.0000	1.0000
1.0706	1.0000	1.0000	1.0000	1.0000
1.0471	1.0000	1.0000	1.0000	1.0000
1.0235	1.0000	1.0000	1.0000	1.0000
1.0000	1.0000	1.0000	1.0000	1.0000

RADIUS	12.00	13.50	15.00	16.50
1.2355	1.0000	1.0000	1.0000	1.0000
1.2119	1.0000	1.0000	1.0000	1.0000
1.1884	1.0000	1.0000	1.0000	1.0000

1.1648	1.0000	1.0000	1.0000	1.0000
1.1413	1.0000	1.0000	1.0000	1.0000
1.1177	1.0000	1.0000	1.0000	1.0000
1.0942	1.0000	1.0000	1.0000	1.0000
1.0706	1.0000	1.0000	1.0000	1.0000
1.0471	1.0000	1.0000	1.0000	1.0000
1.0235	1.0000	1.0000	1.0000	1.0000
1.0000	1.0000	1.0000	1.0000	1.0000

RADIUS	18.00	19.50	21.00	22.50
1.2355	1.0000	1.0000	1.0000	1.0000
1.2119	1.0000	1.0000	1.0000	1.0000
1.1884	1.0000	1.0000	1.0000	1.0000
1.1648	1.0000	1.0000	1.0000	1.0000
1.1413	1.0000	1.0000	1.0000	1.0000
1.1177	1.0000	1.0000	1.0000	1.0000
1.0942	1.0000	1.0000	1.0000	1.0000
1.0706	1.0000	1.0000	1.0000	1.0000
1.0471	1.0000	1.0000	1.0000	1.0000
1.0235	1.0000	1.0000	1.0000	1.0000
1.0000	1.0000	1.0000	1.0000	1.0000

RADIUS	24.00	25.50	27.00	28.50
1.2355	1.0000	1.0000	1.0000	1.0000
1.2119	1.0000	1.0000	1.0000	1.0000
1.1884	1.0000	1.0000	1.0000	1.0000
1.1648	1.0000	1.0000	1.0000	1.0000
1.1413	1.0000	1.0000	1.0000	1.0000
1.1177	1.0000	1.0000	1.0000	1.0000
1.0942	1.0000	1.0000	1.0000	1.0000
1.0706	1.0000	1.0000	1.0000	1.0000
1.0471	1.0000	1.0000	1.0000	1.0000
1.0235	1.0000	1.0000	1.0000	1.0000
1.0000	1.0000	1.0000	1.0000	1.0000

RADIUS	30.00	31.50	33.00	34.50
1.2355	1.0000	1.0000	1.0000	1.0000
1.2119	1.0000	1.0000	1.0000	1.0000
1.1884	1.0000	1.0000	1.0000	1.0000
1.1648	1.0000	1.0000	1.0000	1.0000
1.1413	1.0000	1.0000	1.0000	1.0000
1.1177	1.0000	1.0000	1.0000	1.0000
1.0942	1.0000	1.0000	1.0000	1.0000
1.0706	1.0000	1.0000	1.0000	1.0000
1.0471	1.0000	1.0000	1.0000	1.0000
1.0235	1.0000	1.0000	1.0000	1.0000
1.0000	1.0000	1.0000	1.0000	1.0000

RADIUS	36.00	37.50	39.00	40.50
1.2355	1.0000	1.0000	1.0000	1.0000
1.2119	1.0000	1.0000	1.0000	1.0000
1.1884	1.0000	1.0000	1.0000	1.0000
1.1648	1.0000	1.0000	1.0000	1.0000
1.1413	1.0000	1.0000	1.0000	1.0000
1.1177	1.0000	1.0000	1.0000	1.0000
1.0942	1.0000	1.0000	1.0000	1.0000
1.0706	1.0000	1.0000	1.0000	1.0000
1.0471	1.0000	1.0000	1.0000	1.0000

1.0235	1.0000	1.0000	1.0000	1.0000
1.0000	1.0000	1.0000	1.0000	1.0000
RADIUS	42.00	43.50	45.00	46.50
1.2355	1.0000	1.0000	1.0000	1.0000
1.2119	1.0000	1.0000	1.0000	1.0000
1.1884	1.0000	1.0000	1.0000	1.0000
1.1648	1.0000	1.0000	1.0000	1.0000
1.1413	1.0000	1.0000	1.0000	1.0000
1.1177	1.0000	1.0000	1.0000	1.0000
1.0942	1.0000	1.0000	1.0000	1.0000
1.0706	1.0000	1.0000	1.0000	1.0000
1.0471	1.0000	1.0000	1.0000	1.0000
1.0235	1.0000	1.0000	1.0000	1.0000
1.0000	1.0000	1.0000	1.0000	1.0000
RADIUS	48.00	49.50	51.00	52.50
1.2355	1.0000	1.0000	1.0000	1.0000
1.2119	1.0000	1.0000	1.0000	0.0000
1.1884	1.0000	1.0000	1.0000	0.0000
1.1648	1.0000	1.0000	1.0000	1.0000
1.1413	1.0000	1.0000	1.0000	1.0000
1.1177	1.0000	1.0000	1.0000	1.0000
1.0942	1.0000	1.0000	1.0000	1.0000
1.0706	1.0000	1.0000	1.0000	1.0000
1.0471	1.0000	1.0000	1.0000	1.0000
1.0235	1.0000	1.0000	1.0000	1.0000
1.0000	1.0000	0.0000	0.0000	0.0000
RADIUS	54.00	55.50	57.00	58.50
1.2355	1.0000	1.0000	1.0000	1.0000
1.2119	1.0000	1.0000	1.0000	1.0000
1.1884	1.0000	1.0000	1.0000	1.0000
1.1648	1.0000	1.0000	1.0000	1.0000
1.1413	1.0000	1.0000	1.0000	1.0000
1.1177	1.0000	1.0000	1.0000	1.0000
1.0942	1.0000	1.0000	1.0000	1.0000
1.0706	1.0000	1.0000	1.0000	1.0000
1.0471	1.0000	1.0000	1.0000	1.0000
1.0235	1.0000	1.0000	0.0000	0.0000
1.0000	0.0000	0.0000	0.0000	0.0000

VALUES FOR P IN psig

RADIUS	0.00	1.50	3.00	4.50
1.2355	0.15000000E+03	0.15000000E+03	0.15000000E+03	0.15000000E+03
1.2119	0.15000000E+03	0.15000000E+03	0.15000000E+03	0.15000000E+03
1.1884	0.15000000E+03	0.15000000E+03	0.15000000E+03	0.15000000E+03
1.1648	0.15000000E+03	0.15000000E+03	0.15000000E+03	0.15000000E+03
1.1413	0.15000000E+03	0.15000000E+03	0.15000000E+03	0.15000000E+03
1.1177	0.15000000E+03	0.15000000E+03	0.15000000E+03	0.15000000E+03
1.0942	0.11352989E+03	0.12693595E+03	0.13055976E+03	0.13103475E+03
1.0706	0.60715804E+02	0.82974087E+02	0.92003104E+02	0.95472098E+02
1.0471	0.25082786E+02	0.47030430E+02	0.57263945E+02	0.61850903E+02
1.0235	0.12203157E+01	0.19192092E+02	0.26683127E+02	0.30004953E+02
1.0000	0.00000000E+00	0.00000000E+00	0.00000000E+00	0.00000000E+00
RADIUS	6.00	7.50	9.00	10.50

1.2355	0.15000000E+03	0.15000000E+03	0.15000000E+03	0.15000000E+03
1.2119	0.15000000E+03	0.19700407E+03	0.19872517E+03	0.18035703E+03
1.1884	0.15000000E+03	0.20521317E+03	0.21043660E+03	0.19142304E+03
1.1648	0.15000000E+03	0.19802805E+03	0.20300973E+03	0.18740821E+03
1.1413	0.15000000E+03	0.18213430E+03	0.18407106E+03	0.17289543E+03
1.1177	0.15000000E+03	0.15840939E+03	0.15767241E+03	0.15138380E+03
1.0942	0.12685530E+03	0.12871063E+03	0.12794242E+03	0.12454503E+03
1.0706	0.96136541E+02	0.97203728E+02	0.96874635E+02	0.94971881E+02
1.0471	0.63888294E+02	0.64953777E+02	0.64944974E+02	0.63911680E+02
1.0235	0.31586101E+02	0.32331108E+02	0.32428792E+02	0.31983913E+02
1.0000	0.00000000E+00	0.00000000E+00	0.00000000E+00	0.00000000E+00

RADIUS	12.00	13.50	15.00	16.50
1.2355	0.15000000E+03	0.15000000E+03	0.15000000E+03	0.15000000E+03
1.2119	0.17347449E+03	0.17022450E+03	0.16788290E+03	0.16663770E+03
1.1884	0.18212352E+03	0.17689708E+03	0.17300714E+03	0.17065299E+03
1.1648	0.17839102E+03	0.17256665E+03	0.16800743E+03	0.16498383E+03
1.1413	0.16532677E+03	0.15971567E+03	0.15513000E+03	0.15186754E+03
1.1177	0.14548562E+03	0.14043240E+03	0.13625318E+03	0.13310879E+03
1.0942	0.12032147E+03	0.11626393E+03	0.11274947E+03	0.10995713E+03
1.0706	0.92153129E+02	0.89197285E+02	0.86492229E+02	0.84230392E+02
1.0471	0.62165409E+02	0.60211616E+02	0.58337080E+02	0.56706654E+02
1.0235	0.31138940E+02	0.30153807E+02	0.29180752E+02	0.28316590E+02
1.0000	0.00000000E+00	0.00000000E+00	0.00000000E+00	0.00000000E+00

RADIUS	18.00	19.50	21.00	22.50
1.2355	0.15000000E+03	0.15000000E+03	0.15000000E+03	0.15000000E+03
1.2119	0.16661454E+03	0.16702529E+03	0.16747064E+03	0.16798142E+03
1.1884	0.16996032E+03	0.16999326E+03	0.17024232E+03	0.17064683E+03
1.1648	0.16359368E+03	0.16304299E+03	0.16286260E+03	0.16292040E+03
1.1413	0.14999449E+03	0.14893573E+03	0.14832241E+03	0.14799705E+03
1.1177	0.13102300E+03	0.12963965E+03	0.12870105E+03	0.12806147E+03
1.0942	0.10792068E+03	0.10644219E+03	0.10535927E+03	0.10455371E+03
1.0706	0.82461892E+02	0.81101176E+02	0.80056618E+02	0.79242013E+02
1.0471	0.55375479E+02	0.54313543E+02	0.53473736E+02	0.52800073E+02
1.0235	0.27597191E+02	0.27013540E+02	0.26545065E+02	0.26163770E+02
1.0000	0.00000000E+00	0.00000000E+00	0.00000000E+00	0.00000000E+00

RADIUS	24.00	25.50	27.00	28.50
1.2355	0.15000000E+03	0.15000000E+03	0.15000000E+03	0.15000000E+03
1.2119	0.16852959E+03	0.16907015E+03	0.16956490E+03	0.17005135E+03
1.1884	0.17114535E+03	0.17166164E+03	0.17214646E+03	0.17262501E+03
1.1648	0.16312681E+03	0.16338882E+03	0.16365241E+03	0.16392069E+03
1.1413	0.14785717E+03	0.14780773E+03	0.14779412E+03	0.14779983E+03
1.1177	0.12762232E+03	0.12729561E+03	0.12702938E+03	0.12679601E+03
1.0942	0.10394126E+03	0.10344779E+03	0.10302785E+03	0.10264964E+03
1.0706	0.78592502E+02	0.78051127E+02	0.77581222E+02	0.77153850E+02
1.0471	0.52248949E+02	0.51781143E+02	0.51371067E+02	0.50997395E+02
1.0235	0.25847131E+02	0.25575432E+02	0.25335651E+02	0.25116752E+02
1.0000	0.00000000E+00	0.00000000E+00	0.00000000E+00	0.00000000E+00

RADIUS	30.00	31.50	33.00	34.50
1.2355	0.15000000E+03	0.15000000E+03	0.15000000E+03	0.15000000E+03
1.2119	0.17057157E+03	0.17106207E+03	0.17132167E+03	0.17139112E+03
1.1884	0.17313546E+03	0.17358727E+03	0.17374708E+03	0.17366211E+03
1.1648	0.16421640E+03	0.16444158E+03	0.16437711E+03	0.16406133E+03
1.1413	0.14783190E+03	0.14779444E+03	0.14749451E+03	0.14695632E+03
1.1177	0.12659152E+03	0.12632722E+03	0.12583680E+03	0.12513151E+03

1.0942	0.10230363E+03	0.10191154E+03	0.10133397E+03	0.10057272E+03
1.0706	0.76758280E+02	0.76329915E+02	0.75755347E+02	0.75031538E+02
1.0471	0.50653322E+02	0.50291359E+02	0.49826172E+02	0.49255352E+02
1.0235	0.24917227E+02	0.24710745E+02	0.24445810E+02	0.24122677E+02
1.0000	0.00000000E+00	0.00000000E+00	0.00000000E+00	0.00000000E+00

RADIUS	36.00	37.50	39.00	40.50
1.2355	0.15000000E+03	0.15000000E+03	0.15000000E+03	0.15000000E+03
1.2119	0.17153208E+03	0.17179861E+03	0.17225150E+03	0.17315255E+03
1.1884	0.17361282E+03	0.17367643E+03	0.17392009E+03	0.17458487E+03
1.1648	0.16373139E+03	0.16345377E+03	0.16326695E+03	0.16327767E+03
1.1413	0.14636061E+03	0.14574575E+03	0.14510458E+03	0.14440243E+03
1.1177	0.12434177E+03	0.12347445E+03	0.12247524E+03	0.12121053E+03
1.0942	0.99717323E+02	0.98750094E+02	0.97585281E+02	0.96044560E+02
1.0706	0.74219106E+02	0.73288352E+02	0.72144930E+02	0.70615187E+02
1.0471	0.48621547E+02	0.47895922E+02	0.46997396E+02	0.45793971E+02
1.0235	0.23768922E+02	0.23366437E+02	0.22867805E+02	0.22203855E+02
1.0000	0.00000000E+00	0.00000000E+00	0.00000000E+00	0.00000000E+00

RADIUS	42.00	43.50	45.00	46.50
1.2355	0.15000000E+03	0.15000000E+03	0.15000000E+03	0.15000000E+03
1.2119	0.17531364E+03	0.17791411E+03	0.17806788E+03	0.17490942E+03
1.1884	0.17626957E+03	0.17772695E+03	0.17556596E+03	0.16809505E+03
1.1648	0.16368855E+03	0.16315719E+03	0.15864702E+03	0.14818039E+03
1.1413	0.14352654E+03	0.14123784E+03	0.13510004E+03	0.12331781E+03
1.1177	0.11939258E+03	0.11599362E+03	0.10923770E+03	0.97746719E+02
1.0942	0.93783933E+02	0.90020318E+02	0.83535845E+02	0.73494373E+02
1.0706	0.68386221E+02	0.64914949E+02	0.59443747E+02	0.51571820E+02
1.0471	0.44054697E+02	0.41447624E+02	0.37540272E+02	0.32185412E+02
1.0235	0.21252242E+02	0.19859503E+02	0.17824384E+02	0.15112011E+02
1.0000	0.00000000E+00	0.00000000E+00	0.00000000E+00	0.78154350E-13

RADIUS	48.00	49.50	51.00	52.50
1.2355	0.15000000E+03	0.15000000E+03	0.15000000E+03	0.15000000E+03
1.2119	0.16839142E+03	0.14097376E+03	0.25367970E+02	0.00000000E+00
1.1884	0.15355600E+03	0.11437979E+03	0.31021313E+01	0.00000000E+00
1.1648	0.12929605E+03	0.90360373E+02	0.66202297E+01	0.30237042E+01
1.1413	0.10372466E+03	0.71504895E+02	0.20395687E+02	0.27217435E+02
1.1177	0.79888810E+02	0.56112336E+02	0.32607323E+02	0.48901037E+02
1.0942	0.59264305E+02	0.43143427E+02	0.32179752E+02	0.42676114E+02
1.0706	0.41292832E+02	0.30749496E+02	0.24576028E+02	0.28865747E+02
1.0471	0.25580266E+02	0.19126437E+02	0.15325015E+02	0.16250893E+02
1.0235	0.11868123E+02	0.87467211E+01	0.68206412E+01	0.66782314E+01
1.0000	0.46256097E-13	0.00000000E+00	0.00000000E+00	0.00000000E+00

RADIUS	54.00	55.50	57.00	58.50
1.2355	0.15000000E+03	0.15000000E+03	0.15000000E+03	0.15000000E+03
1.2119	0.15000000E+03	0.15000000E+03	0.15000000E+03	0.15000000E+03
1.1884	0.15000000E+03	0.15000000E+03	0.15000000E+03	0.15000000E+03
1.1648	0.15000000E+03	0.15000000E+03	0.15000000E+03	0.15000000E+03
1.1413	0.15000000E+03	0.15000000E+03	0.15000000E+03	0.15000000E+03
1.1177	0.15000000E+03	0.15000000E+03	0.15000000E+03	0.15000000E+03
1.0942	0.83883538E+02	0.10672473E+03	0.98387709E+02	0.94800176E+02
1.0706	0.44123081E+02	0.51317730E+02	0.37510871E+02	0.33851884E+02
1.0471	0.20960510E+02	0.21210475E+02	0.86239881E+01	0.49967263E+01
1.0235	0.76967478E+01	0.66969575E+01	0.00000000E+00	0.00000000E+00
1.0000	0.00000000E+00	0.00000000E+00	0.00000000E+00	0.00000000E+00

APPENDIX G

INFLUENCE COEFFICIENT FILES

The method for finding the influence coefficients is described in chapter III. These files are input into the computer program through six different files. Each file is read one influence coefficient at a time by a FORTRAN E15.8 format. It is important that the influence coefficients are arranged in a particular pattern for them to be read in correctly. Figure 33 shows how the nodes are numbered in the computer program. For the mechanical and thermal influence coefficients the program starts at node i=1 and j=1. At this node it reads in all of the influence coefficients for a unit force (or heat flux) applied at that node. These influence coefficients are read starting at node (1,1). The radial columns are read consecutively until node (n,m) is reached. Now, the influence coefficients for the next node (1,2) are read in the same manner. This process is continued reading the influence coefficients for each node starting at the outer radius going to the inner radius and then proceeding to the next radial column until the entire influence coefficient array is inputted.

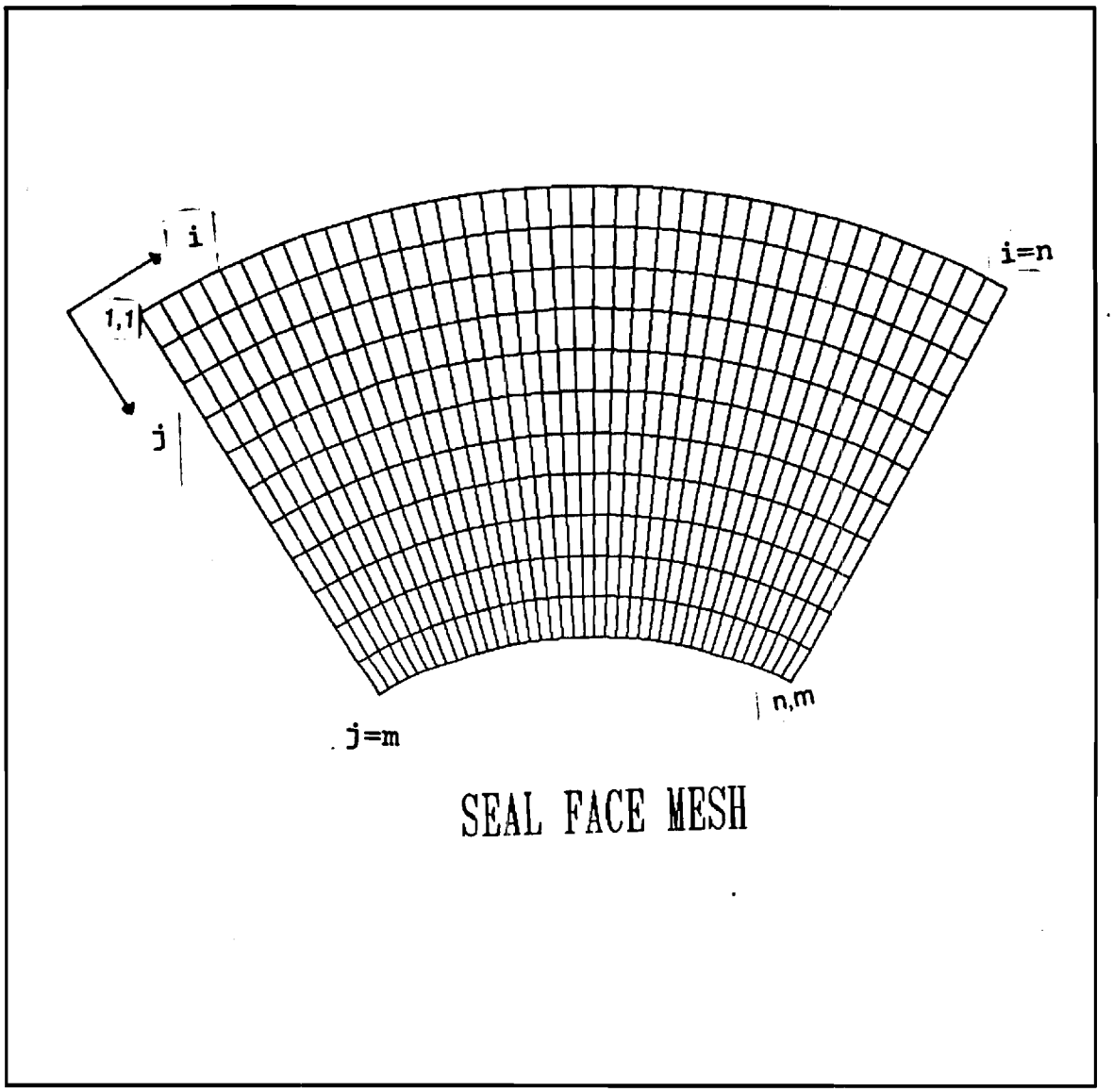

Figure 33. Arrangement of Influence Coefficients.

The influence coefficients for the sealed pressure and the boundary conditions are organized in a similar manner. Since each is a matrix, it is only necessary to organize the coefficients in the pattern starting with node (1,1) and proceeding to the inner radius, and then advancing one radial column at a time.

It is also important that the influence coefficients have the proper units. The mechanical coefficients have units of in/lbf. The thermal coefficients have units in/(Btu/hr). The sealed pressure coefficients have units of in/psi. The boundary condition coefficients have units of inches.

The influence coefficients must also have the proper sign. All of the mechanical and thermal coefficients should produce a positive displacement for a positive force or heat input. A positive displacement is considered one that increases the film thickness. In other words, a positive displacement is one that causes an indentation on the seal face. For the sealed pressure and boundary condition coefficients, the sealed pressure should produce a negative displacement for a positive sealed pressure since it is acting on the back side of the floating seal.

APPENDIX H

EXAMPLE ANSYS INPUT FILES AND PROGRAMS FOR GENERATION OF INFLUENCE COEFFICIENTS

The procedure for finding the influence coefficients is outlined in the chapter III. This appendix contains some example input files and programs that can automate the process of finding the entire set of influence coefficients of a seal face. These examples are for finding the mechanical influence coefficients for the floating seal face. The first program, shown below, is a DOS batch file that automates the process of performing a finite element analysis on each node of the seal face for a unit force applied at that node.

```
CALL C:\ANSYS -I SEAL.FIL
:START
MKFIL2.EXE
CALL C:\ANSYS -I SEAL1.FIL
CHECK.EXE
IF ERRORLEVEL 1 GOTO FINISH
COPY NEW.CNT NODE.CNT
GOTO START
:FINISH
```

The first line performs an initial finite element analysis of the seal face to form the stiffness matrix for the structure. Then an iterative loop is entered. This

loop uses a restart procedure available in ANSYS to find the deformations of all the nodes on the seal face for a unit force applied at each node on the face. The ANSYS input file SEAL.FIL is given below,

```
/PREP7
/TITLE,SIMPLE SEAL-ROTATING FACE MECH. COEFFS.
KAN,0
ET,1,45
ET,2,14,,0,0
R,1,19.14
MP,EX,1,3.19E06
MP,EY,1,3.19E06
MP,EZ,1,3.19E06
MP,NUXY,1,.3
MP,NUYZ,1,.3
MP,NUXZ,1,.3
CSYS,1
N,1,2.3165,0,0
N,11,1.875,0,0
FILL
NGEN,21,11,1,11,1,0,-3.0
NGEN,2,231,1,231,1,0,0,.125
E,6,7,18,17,237,238,249,248
EGEN,5,1,1
EGEN,2,11,1,5
EGEN,2,6,6,10
EGEN,2,5,11,15
EGEN,16,11,11,20
EGEN,3,11,166,170
NGEN,2,231,232,462,1,0,0,0.5
E,232,233,244,243,463,464,475,474
EGEN,10,1,181
EGEN,20,11,181,190
NGEN,2,231,463,693,1,0,0,0.375
E,463,464,475,474,694,695,706,705
EGEN,7,1,381
EGEN,20,11,381,387
NGEN,2,231,694,921,1,0,0,0.375
EGEN,2,231,381,520
NDELE,1,5,1
NDELE,12,16,1
NDELE,210,214,1
NDELE,221,225,1
NDELE,702,922,11
NDELE,703,923,11
NDELE,704,924,11
NDELE,933,1153,11
```

```
NDELE,934,1154,11
NDELE,935,1155,11
N,2253,1.0,0,1.0
N,2473,1.0,-60,1.0
FILL,2253,2473,19,2264,11
TYPE,2
E,701,2253
EGEN,21,11,701
NROTAT,ALL
D,2253,ALL,0,,2473,11
D,701,UZ,0,,921,11
SYMBC,1,2,0,0.01
SYMBC,1,2,-60,0,0.01
F,6,FZ,1
WSORT,Y
AFWRITE
FINISH
/INPUT,27
FINISH
/POST1
SET
NSEL,NODE,6,11
NASEL,NODE,17,209
NASEL,NODE,215,220
NASEL,NODE,226,236
NASEL,NODE,243,247
NASEL,NODE,441,445
NASEL,NODE,452,456
/OUTPUT,TEST1,DAT
PRDISP
FINISH
/EOF
```

MKFIL2.EXE is an executable fortran program, given below, that creates the restart ANSYS input file SEAL1.FIL.

```
      OPEN(UNIT=7,FILE='SEAL1.FIL')
      OPEN(UNIT=5,FILE='NODE.CNT')
      READ(5,5000) NODE
5000  FORMAT(I3)
      WRITE(7,91)
      WRITE(7,92)
      WRITE(7,93)
      WRITE(7,94)
      WRITE(7,95)
      WRITE(7,96)
      WRITE(7,97)
      WRITE(7,1080)
      WRITE(7,1081)
```

```
      WRITE(7,1090) NODE
      WRITE(7,1100)
      WRITE(7,1105)
      WRITE(7,1110)
      WRITE(7,1120)
      WRITE(7,1130)
      WRITE(7,1220) NODE
      WRITE(7,1260)
      WRITE(7,1120)
      WRITE(7,1250)
91    FORMAT('/PREP7')
92    FORMAT('RESUME')
93    FORMAT('ITER,1,0,1')
94    FORMAT('PRDISP,1,1,236,1')
95    FORMAT('PRDISP,1,243,247,1')
96    FORMAT('PRDISP,1,441,445,1')
97    FORMAT('PRDISP,1,452,456,1')
1080  FORMAT('F,1,FZ,0,,236,1')
1081  FORMAT('F,243,FZ,0,,247,1')
1090  FORMAT('F,',I3,',FZ,1')
1100  FORMAT('SLOAD,1')
1105  FORMAT('KUSE,1')
1110  FORMAT('AFWRITE')
1120  FORMAT('FINISH')
1130  FORMAT('/LOAD')
1220  FORMAT('/OUTPUT,COEF',I3,',DAT')
1250  FORMAT('/EOF')
1260  FORMAT('/INPUT,27')
      END
```

This program also updates a file called NODE.CNT so that the DOS batch file can be exited when all the coefficients for the seal face are calculated. The ANSYS restart file SEAL1.FIL, shown below, is now called.

```
/PREP7
RESUME
ITER,1,0,1
PRDISP,1,1,236,1
PRDISP,1,243,247,1
PRDISP,1,441,445,1
PRDISP,1,452,456,1
F,1,FZ,0,,236,1
F,243,FZ,0,,247,1
F,6,FZ,1
F,226,FZ,1
SLOAD,1
KUSE,1
```

```
AFWRITE
FINISH
/LOAD
/OUTPUT,COEF6,DAT
/INPUT,27
FINISH
/EOF
```

After the restart program is finished, an executable fortran program CHECK.EXE is called. This program, shown below, simply checks to see if the overall procedure has been repeated for each of the nodes on the entire seal face. If it has then it calls for an errorlevel to be set so that the DOS batch file can exit the iterative loop.

```
      OPEN(UNIT=7,FILE='NODE.CNT')
      OPEN(UNIT=8,FILE='NEW.CNT')
      READ(7,500) NODE
500   FORMAT(I3)
      WRITE(*,500) NODE
      IF (NODE.EQ.236) NODE=242
      IF (NODE.EQ.247) NODE=6
      IF (NODE.EQ.11) NODE=16
      IF (NODE.EQ.121) CALL EXIT(1)
      NODE=NODE+1
      WRITE(8,500) NODE
      END
```

Using programs similar to these the procedure for finding any of the influence coefficients for both seal faces is automated. These procedures provide output files of all the influence coefficients which then must be sorted according to the layout described in Appendix G.

BIBLIOGRAPHY

1. Key, W. E., Salant, R. F., Payvar, P., Gopalakrishnan, S., and Vaghasia, G., "Analysis of a Mechanical Seal With Deep Hydropads," STLE Preprint no. 88-TC-3C-3, 1988.

2. Metcalfe, R., "Performance Analysis of Axisymmetric Flat Face Mechanical Seals," Proc. 6th Intl. Conf. on Fluid Sealing, Paper D1, BHRA Fluid Eng., Cranfield, U.K. 1973.

3. Green, I., and Etsion, I., "Stability Threshold and Steady-State Response of Noncontacting Coned-Faced Seals," ASLE Transactions, Vol. 28, No. 4, pp. 449-460, 1985.

4. Cheng, H.S., Chow, C.Y., and Wilcock, D.F., "Behavior of Hydrostatic and Hydrodynamic Noncontacting Face Seals," Journal of Lubrication Technology, 90, 2, pp. 510-519, 1968.

5. Johnson, R.L. and Ludwig, L.P.,"Shaft Face Seal with Self-Acting Lift Augmentation for Advanced Gas Turbing Engines," Proc. 4th Intl. Conf. on Fluid Sealing, BHRA Fluid Eng., Cranfield, U.K. 1969.

6. Iny, E.H., "A Theory of Sealing wiht Radial Face Seals," Wear, 18, 1, pp.51-69, 1971.

7. Iny, E.H., "The Design of Hydrodynamically Lubricated Seals with Predictable Operating Characteristics," Proc. 5th Intl. Conf. on Fluid Sealing, Paper H1, BHRA Fluid Eng., Cranfield, U.K. 1971.

8. Stangham-Batch, B. and Iny, E.H., "A Hydrodynamic Theory of Radial Face Mechanical Seals," Journal of Mechanical Engineering Science, 15, 1, pp. 17-24, 1973.

9. Reynolds, O., "On the Theory of Lubrication and Its Application to Mr. Beachamp Tower's Experiments,", Phil. Trans. Royal Society, Vol. 177, pt. I, 1886, pp. 157-234.

10. Elrod, H.G., "A Cavitation Algorithm," Journal Lubrication Technology, 103, 3, pp. 350-354., 1981.

11. Payvar, P. and Salant, R.F., "A Computational Method for Cavitation in a Wavy Mechanical Seal," submitted to Journal of Tribology, 1990.

12. Huebner, K.H. and Thornton, E.A., The Finite Element Method for Engineers, John Wiley & Sons, New York, New York, 1982.

13. Cook, R.D., Malkus, P.S., and Plesha, M.E., Concepts and Applications of Finite Element Analysis, 3rd ed., John Wiley & Sons, New York, New York, 1989.

14. Gross, W.A., Fluid Film Lubrication, John Wiley & Sons, New York, New York, 1980.

15. Jakobsson, B. and Floberg, F., "The finite Journal Bearing, Considering Vaporization," Reeport No. 3, Institute of Machine Elements, Chalmers, U., Gothenberg, Sweden 1957.

16. DeSalvo, G.J. and Gorman, R.W., ANSYS - Engineering Analysis System - User's Manual, May, 1989.

17. Patankar, S.V., Numerical Heat Transfer and Fluid Flow, Hemisphere Publishing Corporation, New York, New York, 1980.

18. Green, I. and English, "Analysis of Elastomeric O-Ring Seals in Compression Using the Finite Element Method," to appear in STLE, Tribology Transaction.

19. Gazley, Jr., C., "Heat-Transfer Characteristics of the Rotational and Axial Flow Between Concentric Cylinders," Transactions ASME, Vol. 80, pt. 1, 1958, pp. 79-90.

20. Kreith, F., Taylor, J.H., and Chong, J.P., "Heat and Masss Transfer From a Rotating Disk," Journal of Heat Transfer, Vol. 81, 1959, pp. 95-105.